

CHARACTERIZING NOTCH1 SIGNALING REGULATION AND AMYLOID  
BETA CLEAVAGE

A Dissertation

Presented to the Faculty of the Weill Cornell Graduate School  
of Medical Sciences

in Partial fulfillment of the Requirements for the Degree of  
Doctor of Philosophy

by

David Alex Schachter

May 2019

© 2019 David Schachter

# Characterizing Notch1 Signaling Regulation and Amyloid Beta Cleavage

David Schachter, Ph.D.

Cornell University 2019

Gamma secretase cleaves numerous substrates that regulate a variety of cellular processes. The involvement of Gamma secretase in so many different signaling systems makes it a challenging enzyme to target without toxic side-effects. The two predominantly studied substrates are Notch and Amyloid precursor protein (APP). Dysregulated cleavage of the first can lead to cancer, while cleavage of the second results Amyloid Beta ( $A\beta$ ) production which contributes to Alzheimer's Disease (AD). Therefore, the development of substrate specific gamma secretase modulators is of primary importance.

To find a modulator of Notch signaling we screened a 20-amino acid displaying bacteriophage library for a peptide sequence that recognizes Notch1. Through this approach we identified a sequence that specifically binds to Notch1 and none of the other isoforms of Notch. The phage displaying this sequence co-localized and co-immunoprecipitated with Notch1 and was able to reduce Notch1 signaling in a Notch reporter system. Therefore, we have identified a novel sequence that can specifically modulate Notch1 signaling without interfering with cleavage of similar proteins.

The AD field has been primarily restricted to studying two  $A\beta$  species:  $A\beta$ -40 and  $A\beta$ -42, that are produced after gamma secretase cleavage of two sites on APP. While other cleavage sites have been reported, the ability to study and characterize them, especially in relation to Alzheimer's Disease, has been hampered due to the lack of tools specific to these alternate sites. To

address this issue, we generated, and characterized, monoclonal antibodies to these cleavage sites. We confirmed that these antibodies are selective for the alternative species, including A $\beta$ -43 and A $\beta$ -45, and utilized Alpha-LISA technology to quantify binding strength. We were also able to utilize some of these antibodies in immunohistochemistry and aggregation binding studies to further investigate difference in behavior of these amyloid species. The development of these antibodies will enable us to focus on alternative cleavage sites of A $\beta$  and study their contribution to AD.

## BIOGRAPHICAL SKETCH

David grew up in Edison, NJ. His interest in science began when he was seven as his mother went back to school for her Ph.D. in Organic Chemistry at Rutgers University. After leaving high school after eleventh grade, he was accepted early admissions to Yeshiva University. He matriculated two years later as Pre-Engineering major, after spending two years studying abroad in Israel. After two years, David switched to a dual major in Biology and Chemistry, realizing that the two majors would give him a very broad scientific background.

In the summer after his junior year at Yeshiva, David interned in the lab of Dr. Joachim Kohn at Rutgers University, analyzing the degradation of polyarylates that would be used as neural conduits to assist in neural growth. He returned to the lab after his senior year to continue work on degradation of polyarylates, this time used as craniofacial scaffolds to regrow critical defects in the craniofacial bones.

After he graduated from college, David took a year off to study towards Rabbinic Ordination. He then matriculated at Rutgers Biomedical Engineering in the MS to Ph.D. program. He worked in the Lab of Dr. Laura Fabris, studying the sources of cytotoxicity of the surfactants used to create gold nanorods and the ability of iodine to fine-tune the fabrication of the nanorods after formation. David received his MS from Rutgers after a year and half, while concurrently finishing his Rabbinic Ordination.

In July 2013 David matriculated at Weill Cornell in the Pharmacology department and rotated in the lab of Dr. Gavril Pasternak studying the binding of opioid drugs to the opioid receptors. In November of that year he rotated

and subsequently joined the lab of Dr. Yueming Li at Memorial Sloan Kettering Cancer Center for his thesis research. Over the past five years David studied ways to modulate substrate cleavage by Gamma secretase by focusing on the individual substrates instead of on the enzyme.

## DEDICATION

This thesis is dedicated to my children, which currently number three-Aharon, Moshe, and Naava. You are my source of inspiration and dedication for, and to, the work. The best feeling is when you ask a question and we have to go figure out the answer together -no matter what the subject. But the most important thing to realize is that there is an answer. No matter what the topic is, an answer does exist. Whether we understand or have access to the answer is another story (See Rav Aharon Lichtenstein in Leaves of Faith).

Most importantly you must realize that nothing happens in a vacuum. For example, Rav Akiva Eiger was born right before the American Revolution. Whether this influenced any of his writings is something to be looked into, but the fact is there. In חולין (57b) רב שמעון בן חלפתא was called the experimenter and he was able to prove that an animal that was thought to be כשר was טרף. He was called the experimenter because he experimented to see how the נמלות would interact with each other. Once he proved the פסוק (6:6) משלי in חסוק. There was no need for further experimentation since he was able to be סומך. אהימנותא דשלמה.

When you learn something new see how it fits in with everything else you learned, because everything is interconnected. You can learn about גניבה and end up discussing טמא and טהרה and then נחלת הבכור. Build on your inquisitiveness, because you will only grow from it.

## ACKNOWLEDGEMENT

I could not have completed this without the help of so many people both at work and at home, from colleagues to friends and family.

To start, the person who dragged this thesis over the finish line was my mentor, Dr. Yueming Li. His ability to motivate me when I had given up hope on the project was how this thesis can to fruition. He cares about us, his students, not only as scientists, but as people. Through the highs-and-lows of lab he was there to coach me along. I am grateful for the added understanding he has of my commitments and his respect for them.

I also would like to thank my committee members, Dr. David Scheinberg, Dr. Steve Gross, and Dr. Pengbo Zhou. Both the formal and informal meetings that we had shaped this thesis and I am a better scientist because of them.

Next, I want to thank the people of the Yueming Li lab, especially for dealing with all the shenanigans that happened on the curvy, bumpy, and hilly road on the way to a Ph.D. Most importantly I want to thank Georgia Frost for being there from the first classes we took together to the final practice presentation for having my back and acting as a sounding board for all my issues, ideas, and most importantly complaints.

Lastly, I need to thank my friends and family. For 13 years Rabbi Mo. La(e)ster has been putting up with me, swallowing the ideas that I have sent his way, and being a support system. To the Dr. Schachters three - my mother, sister-in-law Tova, and wife Miriam - who paved the way and showed me how to get a Ph.D. Most importantly to Miriam for rolling her eyes at every



stage of the Ph.D., especially about things that had nothing to do with the Ph.D. To the other friends and family that stepped in to help when responsibilities converged, and we couldn't do it all alone, thank you.

## TABLE OF CONTENTS

Biographical Sketch.....	iii
Dedication .....	v
Acknowledgement .....	vi
List of Figures.....	x
List of Tables .....	xii
List of Abbreviations .....	xiii
 Chapter 1: Introduction.....	 1
1. The Gamma-Secretase Complex and its Regulated Proteolysis .....	1
2. Notch Protein Cleavage and Function .....	3
a. Notch Therapeutic potential.....	8
3. Phage Display .....	9
a. Phage Screening.....	12
4. Amyloid precursor protein structure and cleavage.....	15
a. APP cleavage inhibition and mutations .....	17
5. Antibodies and their structure .....	18
a. Antibody uses.....	20
 Chapter 2: Discovery of Notch1 modulating peptides.....	 21
1. Introduction:.....	21
2. Results: .....	24
3. Conclusion:.....	36
4. Materials and Methods: .....	36
 Chapter 3: Development of antibodies to bind to multiple Amyloid Beta cleavage sites.....	 40
1. Amyloid beta cascade hypothesis and cleavage targets .....	40
2. Target development.....	43
a. First cohort A $\beta$ -37, A $\beta$ -38, A $\beta$ -40, A $\beta$ -42, A $\beta$ -43.....	44
b. Second cohort A $\beta$ -45, A $\beta$ -46, A $\beta$ -48, A $\beta$ -49 .....	52
3. Antibody characterization .....	55

a. Kd determination .....	59
b. Epitope specificity.....	60
c. Aggregated A $\beta$ -42 recognition.....	61
d. In vivo-immunohistochemical characterization .....	62
e. In vitro gamma secretase activity assay .....	64
f. Kd determination and characterization of second cohort of antibodies .....	67
4. Conclusion.....	72
5. Materials and Methods .....	74
Chapter 4: Conclusion and Implications of this Thesis .....	79
REFERENCES.....	82

## LIST OF FIGURES

### Chapter 1:

Figure 1: The four proteins that make up the Gamma-secretase complex: .....	2
Figure 2: General cleavage mechanism of aspartyl proteases: .....	3
Figure 3: The four mammalian Notch receptors: .....	5
Figure 4: The Notch signaling system: .....	6
Figure 5: Bacteriophage structure: .....	10
Figure 6: Phages displaying the two types of libraries: .....	12
Figure 7: Solid-phase phage display screening: .....	13
Figure 8: Liquid-phase phage screening: .....	14
Figure 9: Plaque formation caused by APP cleavage by Gamma-secretase: .....	16
Figure 10: The two possible pathways that Gamma-secretase can take to cleave APP .....	16
Figure 11: Structure of an IgG antibody .....	19

### Chapter 2:

Figure 12: M13 bacteriophage structure .....	24
Figure 13: Screening the phage library to discover peptides that recognize Notch1 .....	26
Figure 14: P1 phage binds to cells that upregulate Notch1: .....	28
Figure 15: P1 phage only recognizes Notch1: .....	30
Figure 16: Co-immunoprecipitation of Notch1 and P1 phage: .....	31
Figure 17: Notch signaling is partially inhibited by P1 phage: .....	32
Figure 18: Synthetic scheme to synthesize dVGG: .....	34
Figure 19: dVGG inhibits cells signaling: .....	35

### Chapter 3:

Figure 20: Amyloid Beta sequence and cleavage pathways: .....	42
Figure 21: Signal and cross-reactivity of inoculated mice first cohort: .....	46
Figure 22: ELISA results comparing the amidated and non amidated A $\beta$ -42 peptide for 15g11: .....	51
Figure 23: Signal and cross-reactivity for A $\beta$ -45 mice: .....	53
Figure 24: Signal and cross-reactivity for A $\beta$ -48 and A $\beta$ -49 mice: .....	54
Figure 25: MBP Amyloid beta protein construct: .....	56
Figure 26: AlphaLISA reaction: .....	57
Figure 27: Mechanism of AlphaLISA reaction: .....	58
Figure 28: K <sub>d</sub> for 15G11 and 10G3 .....	59
Figure 29: Aggregated biotinylated-A $\beta$ <sub>1-42</sub> : .....	62

Figure 30: 5xFAD brains and wild type brain incubated with A $\beta$ -42 antibodies:..	64
.....	
Figure 31: Alpha-LISA assay of Hela membrane cleaving CT6:.....	65
Figure 32: CT6 spike-in blocks 15G11 signal:.....	66
Figure 33: In vitro Alpha-LISA measuring the amount of A $\beta$ -40: .....	67
Figure 34: Alpha-LISA of two subclones from 32F09 screen:.....	68
Figure 35: The Alpha-LISA of 32F09 against MBP-A $\beta$ -45 and MBP-A $\beta$ -46:...	69
Figure 36: The Alpha-LISA of 05B01 against MBP-A $\beta$ -45 and MBP-A $\beta$ -46:. .	70
Figure 37:Alpha-LISA of HELA cleavage of CT6 detected by 32F09: .....	70
Figure 38: Screening 05B01 and 32F09 against the group of MBP-A $\beta$ proteins:	
.....	71

## LIST OF TABLES

### Chapter 1:

Table 1: Mutations in APP and PSEN1..	18
---------------------------------------	----

### Chapter 2:

Table 2: Sequences recovered.....	27
-----------------------------------	----

### Chapter 3:

Table 3: Pathologic Mutations in APP .....	43
Table 4: ELISA results of 18A05 .....	49
Table 5: ELISA results of 11G10 and 12F04 .....	49
Table 6: ELISA results of 13B08, 27G11, 29A11, 30A02, 32A06, and 15G11	50
Table 7: ELISA results of 20B11 .....	51
Table 8: ELISA results of 05B01 .....	55
Table 9: ELISA results of 32F09.....	55
Table 10: Kd values for antibodies .....	60
Table 11: Kd values for 15G11 and 10G3 against modified peptides.....	61
Table 12: Primers for MBP-A $\beta$ species.....	75

## LIST OF ABBREVIATIONS

A $\beta$ : Amyloid Beta  
AD: Alzheimer's disease  
ADAM: A disintegrin and metalloproteinase domain containing protein  
APH-1: Anterior pharynx defective - 1  
APP: Amyloid precursor protein  
BACE1:  $\beta$ -site APP Cleaving Enzyme 1, also known as:  $\beta$ -secretase  
CHAPSO: 3-[(3-Cholamidopropyl)dimethylammonio]-2-hydroxy-1-propanesulfonate  
terminal transactivation domain  
Cys: cysteine  
DLL: Delta-like ligand  
DMSO: Dimethyl sulfoxide  
E: Glutamic acid  
EDTA: Ethylenediaminetetraacetic Acid  
EGF: Epidermal growth factor  
GS:  $\gamma$ -secretase  
GSI:  $\gamma$ -secretase inhibitor  
HEPES: 4-(2-Hydroxyethyl)piperazine-1-ethanesulfonic acid  
HES: hairy/enhancer of split  
HEY: Hairy/enhancer-of-split related with YRPW motif protein  
HIF: hypoxia inducible factor  
IC<sub>50</sub>: Half maximal inhibitory concentration  
ICD: Intracellular domain  
L458: L-685,458  
MES: 2-(N-morpholino)ethanesulfonic acid  
Nct/NCT: Nicastrin  
NEXT: Notch Extracellular Truncation  
NICD: Notch intracellular domain  
NRR: Notch regulatory region  
PBS: Phosphate buffered saline  
PCR: Polymerase chain reaction  
PEN-2: Presenilin enhancer 2  
PEST: A peptide sequence which is rich in P, E, S, and T amino acids.  
PIPES: 1,4-piperazinediethanesulfonic acid  
P: Proline  
PS: Presenilin  
PS1-CTF: Presenilin1 C-terminal fragment  
PS1-NTF: Presenilin1 N-terminal fragment  
RIP: Regulated intramembrane proteolysis  
RIPA: Radioimmunoprecipitation assay buffer  
RT-PCR: Real-time Polymerase Chain Reaction  
S: Serine  
SAD: Streptavidin donor beads  
SDS: Sodium dodecyl sulfate

SDS-PAGE: SDS-polyacrylamide gel

T: Threonine

TACE: tumor necrosis factor- $\alpha$ -converting enzyme

TM: Transmembrane



## Chapter 1:

### *Introduction*

#### **1. The Gamma-Secretase Complex and its Regulated Proteolysis**

Gamma-secretase (GS) is a multi-component enzyme found on the membrane of the cell [1, 2]. It was first found to cleave Amyloid Precursor Protein (APP) in the transmembrane region [2-5]. APP is a single-pass integral membrane protein, whose primary function is unknown, but it may be related to trafficking and neurite pruning. Also, the cleavage products of APP have been implicated in Alzheimer's Disease [2, 3, 5, 6]. Later, additional cleavage targets, including the Notch family of proteins, were subsequently identified [5, 7]. There are over ninety different substrates for gamma-secretase, giving GS the name "proteasome of the membrane" [8, 9]. Due to its library of substrates, side effects are very common when pharmacologically or chemically altering GS cleavage ability [10-12].

The GS complex is made of 4 main subunits, Nicastrin, Presenilin, Anterior pharynx-defective-1 (APH-1), and Presenilin enhancer-2 (PEN-2) [1, 13, 14]. These four subunits are necessary and sufficient for the complex to form and to become catalytically active (figure 1). Stoichiometrically, a subunit ratio of 1:1:1:1 is needed, but it is also possible that larger complexes form with altered or multiplied stoichiometry. In addition, due to the large library of substrates that gamma-secretase has, additional proteins or modulators must interact with gamma-secretase to help specify which proteins it should be targeting within specific cellular microenvironments. For example, Hif1 $\alpha$  has been shown to directly activate GS in breast cancer [15].

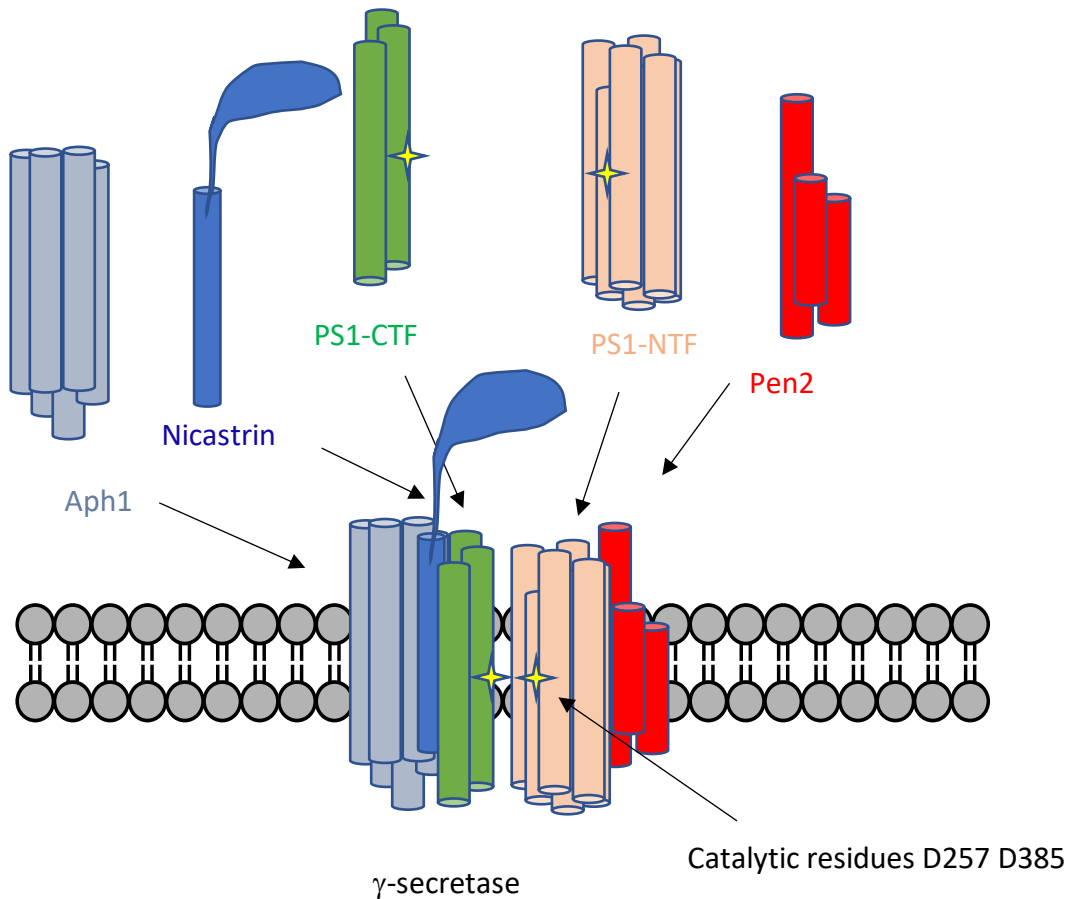


*Figure 1: The four proteins that make up the Gamma-secretase complex: Presenilin (PS1), which needs to be proteolyzed into PS1 c-terminal and n-terminal fragments. Presenilin enhancer 2 (Pen2), which helps with the endoproteolysis of PS1. Nicastrin, which is used for substrate recognition. Lastly, Anterior pharynx-defective1 (Aph1), which is used for structural stability. The substrate docks within the complex allowing residues D257 and D385 to cleave the protein.*

Not all GS that resides in the cell is activated. First Presenilin must be endoproteolyzed into c-terminal and n-terminal fragments for GS to be activated [3, 16]. Gamma-secretase's active site resides on Presenilin, residues D257 and D385 [3, 16]. Nicastrin, which extends above the GS complex is used for substrate recognition and docking [17, 18]. APH-1 and PEN-2 give structural stability to the overall complex. Cleavage occurs when

the substrate docks within Gamma-secretase, and then the aspartyl proteases use water to cleave the protein the mechanism is shown in figure 2 [2].

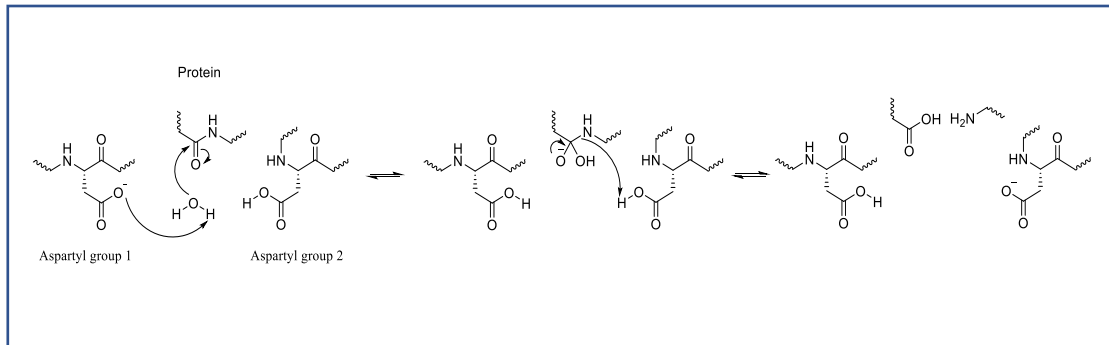


*Figure 2: General cleavage mechanism of aspartyl proteases. One aspartyl protease attacks a water molecule which then attacks the carbonyl which is stabilized by the other aspartyl residue. The carbonyl reforms and the hydroxyl group takes a hydrogen from the second aspartyl residue. This reforms the carbonyl bond, cleaves the amide-bond, and releases a molecule of water from the protein.*

Due to cleavage products of APP being associated with Alzheimer's Disease, initial treatments towards treating Alzheimer's Disease consisted of complete inhibition of GS which will prevent the creation of APP cleavage products. All these pan-GS inhibitors failed in various stages of clinical trials due to toxicities related to GS's function not associated with APP. This shows the importance of GS's function, and that GS cannot be completely inhibited. Rather to properly modulate the substrates of GS to prevent the diseases associated with them, the regulation must happen with the substrate and not with GS to limit the associated toxicities.

## 2. Notch Protein Cleavage and Function

The Notch protein was first discovered in 1917 by Thomas Morgan who, while studying drosophila genetics, found that this protein when absent or mutated caused a characteristic notch in the fly wing [19]. The Notch

protein, which is a transmembrane receptor, and its signaling pathway are so complex that even decades later the structure of Notch, and mechanism of activation, are still being elucidated [20]. This complexity is needed due to the numerous roles Notch plays in various stages of development, differentiation, proliferation and apoptosis [21-26].

There are four Notch proteins (Notch1-4), which share similar structural organization, with Notch1 and Notch2 having the highest sequence homology [27]. The four receptors have varying amounts of epidermal growth factor (EGF)-like repeats external to the membrane, with humans having between 29 and 36. Each EGF-like repeat consisting of about 40 residues and they contain six cysteines that form a characteristic disulfide bond formation [28]. Binding occurs on this domain, with EGF repeats 11-13 being the binding domain for Notch1. The EGF-like repeats are followed by the notch regulatory region (NRR) that protects the ADAM10/17 cleavage site [29, 30]. Next is the transmembrane region where the gamma-secretase cleavage site resides. The intercellular region has seven ankyrin repeats, which are integral for Notch function and are conserved throughout the isotypes. Each ankyrin domain is about 33 residues long [31]. Lastly, the c-terminal portion of the protein is a PEST domain to allow for speedy degradation of the protein (figure 3) [20].

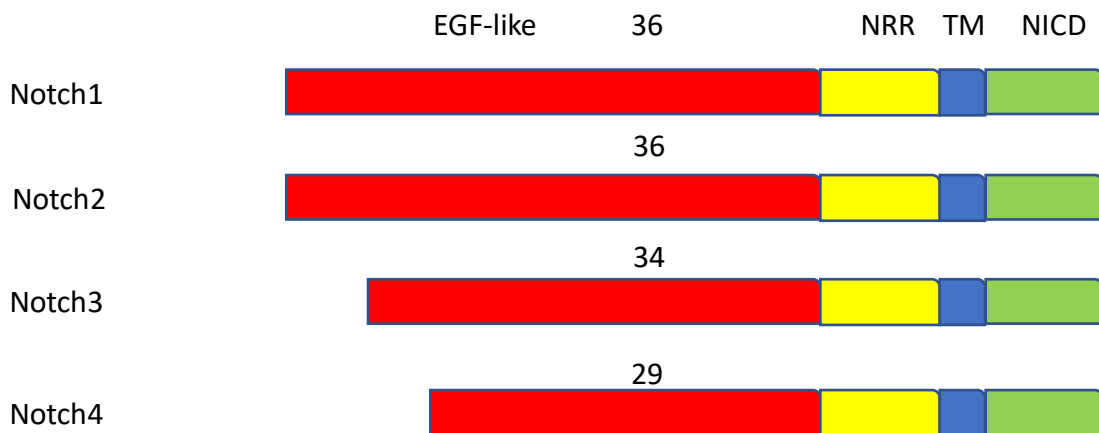


*Figure 3: The four mammalian Notch receptors. Binding occurs in the EGF-like repeat domain. The four Notch receptors mainly differ in how many EGF repeats are in the EGF-like repeat domain. Notch1 and Notch2 have 36, Notch3 has 34, and Notch4 has 29 EGF-like repeats. The Notch regulatory region (NRR) region is where ADAM10/17 cleaves the Notch receptors, and then within the transmembrane region (TM) Gamma-secretase cleaves the Notch receptors. The Notch intracellular domain (NICD) then translocates to the nucleus.*

The family of Notch proteins are first synthesized as ~300kDa proteins, and then in the Golgi apparatus, a furin-like convertase (S1 cleavage) cleaves the protein to generate a mature, non-covalent heterodimers [32]. It is generally understood that the mature Notch protein is trafficked to the surface of the cell, and, once exposed on the cell surface, a neighboring cell's Notch ligand (Delta1, 3,4 or Jagged1,2 in mammals) binds to the EGF-like regions [20, 33]. As mentioned previously, in Notch1 in mammals the ligand binds in between EGF-like regions 11-13 [34, 35]. Once binding occurs, the NRR moves and uncovers the ADAM10/17 cleavage site (S2), which is the rate-limiting step in Notch signaling [29, 30]. Then Gamma-secretase cleaves within the membrane [5, 36]. Once Notch is cleaved by Gamma-secretase the intracellular domain (NICD) translocates into the nucleus, where it associates with the CBF1-Se(H)-lag1 complex and converts the complex from being a

repressor complex to being an activating complex [37]. The downstream genes upregulated by Notch signaling include HES (hairy enhancer of split) and HEY (hairy-related transcription factor) which are the Notch effector genes (figure 4) [38-40].

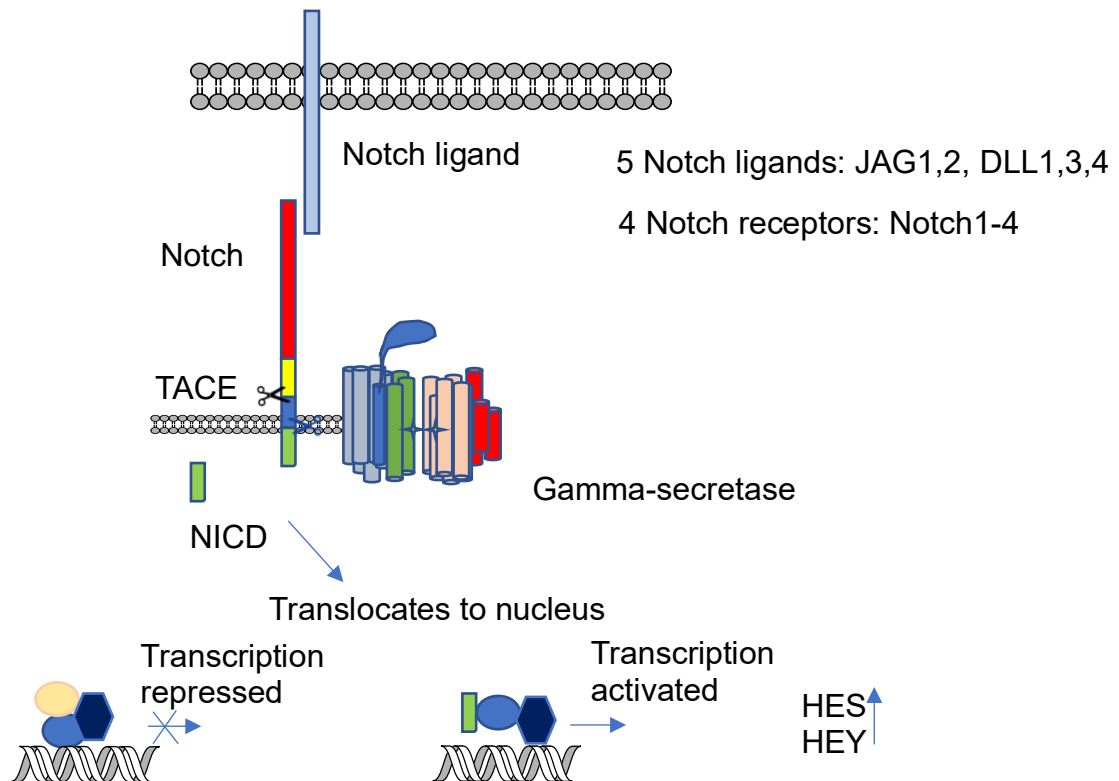


*Figure 4: The Notch signaling system: The Notch ligand, of which there are 5 (JAG1,2, DLL1,3, and 4), binds to the Notch receptor, of which there are 4 (Notch1-4). ADAM10/17 then cleaves the Notch receptor. Once ADAM10/17 cleaves the Notch receptor, Gamma-secretase cleaves the Notch receptor within the membrane. Then the NICD translocates into the nucleus and transcription of the Notch-downstream genes (HES and HEY) occur.*

Due to the ubiquity of the components of Notch signaling, additional and specified regulation is required to achieve the desired signaling endpoint [41]. Some of these additional layers of regulation include spatial and temporal regulation of the expression of the components of Notch signaling [42]. In

addition, differential post-translational modifications (i.e. O-fucosylation), trafficking and degradation of the components are also used by the cell to regulate Notch signaling [43-46].

Notch is needed in regular development and differentiation, as mentioned previously. For example, in hematopoiesis, the regulated balance of self-renewal and differentiation of hematopoietic stem cells is based on whether Notch1 or Notch2 are signaling [47]. In the myeloid lineage Notch1 and Notch2 are increased in granulocytes, whereas in erythroid progenitor cells Notch1 has decreased expression [48]. Also, Notch1 expression in early lymph cell development influences B-cell versus T-cell lineage determination [49, 50]. In the intestines Notch is crucial for differentiation into the stem, progenitor and crypt cells. Notch inhibition causes reduced proliferation, differentiation into only a subset of the intestinal cells, and apoptotic cell death [12, 51, 52].

Functionally, Notch can have various signaling determinations, and mutations in Notch can cause various maladies, including cancers and genetic disorders [53, 54]. For example, in the early 90's a chromosomal translocation (t(7;9)(q34;q34.3) in T-cell acute lymphoblastic leukemia (T-ALL) involved a translocation of the Notch gene [55]. Other translocations also lead to increase, and unregulated, transcription of the downstream proteins [56]. In other T-ALL cases there are activating mutations in Notch1 itself, causing Notch1 to be oncogenic [57, 58]. Not only is Notch1 implicated in cancer, but other parts of the Notch signaling pathway are also associated with cancer like Jagged2 overexpression in breast cancer, or Notch2 activation in bladder cancer, for example [59, 60]. On the other hand, Notch can also act as a tumor suppressor. Decreased Notch activity has been shown to correlate with poor

prognosis for patients with certain gliomas [61]. Certain Notch ligands may also work antagonistically, with some binding regions or ligands being more oncogenic and some portions act more like a tumor suppressor within the same cancer. [62].

#### **a. Notch Therapeutic potential**

Due to the breadth of Notch's signaling, its roles as both oncogene and tumor suppressor, and its essentiality for cell differentiation and development, as shown previously, interfering with Notch signaling can cause more issues than it solves. Practically, this is the reason why many therapeutic avenues are closed off, as both full inhibition of Notch signaling and further activation of Notch signaling can result in disease. [63]. For example, inhibitors of gamma secretase were used to prevent APP aggregation in patient's brains [64]. Gamma secretase inhibitors were able to properly block gamma secretase activity and prevent buildup of APP cleavage products, but inhibition of other GS substrates, including Notch, resulted in negative outcomes [65]. Specifically, as mentioned before, there were reports of toxicities within the intestines, where there was no Notch signaling. Enterocytes whose main function is to absorb nutrients in the intestine were not being differentiated due to the lack of signaling [66].

An alternative approach would be to reduce pathological signaling, while simultaneously maintaining healthy levels of Notch signaling thereby preventing off-target toxicities [67, 68]. Optimally, a modulation of signaling should be spatially defined and target specific. This is especially important, since the cell that is being targeted does not, necessarily, have the Notch receptors perform the same, or even similar, functions.



We want to approach this issue by using peptides to interfere with Notch signaling. One advantage that a peptide has to target a specific protein, as opposed to a small molecule, is that there are multiple points of contact that the peptide has with the protein, whereas the small molecule only interacts with a small part of the protein. Also, it is easy to modify, cheap to make and much smaller than an antibody, while only having perhaps a slightly lower specificity.

### **3. Phage Display**

Bacteriophages (phage) are viruses for bacteria [69]. They contain circular DNA encased in a long protein capsid cylinder [70]. The phages infect the host bacterial cell and use a combination of host and self-machinery to replicate their DNA [70]. There has been shown to be a symbiotic relationship between the bacteria and the phage, since the bacteria have an increased lifespan relative to uninfected bacteria, with subsequent generations of bacteria continuing to grow phage particles [71].

The phage structure consists of pVIII, which is the major coat protein, pVII and pIX at one end, pIII and pVI at the other. The DNA within the structure is oriented with the packaging signal positioned towards the pVII and pIX end. The genome encodes 11 genes. Genes 3,6,7, 8, and 9 are for the capsid structure, genes 1,4, and 11 are for capsid assembly, genes 2 and 10 are for DNA replication, and gene 5 is for binding single stranded DNA [72] (figure 5).

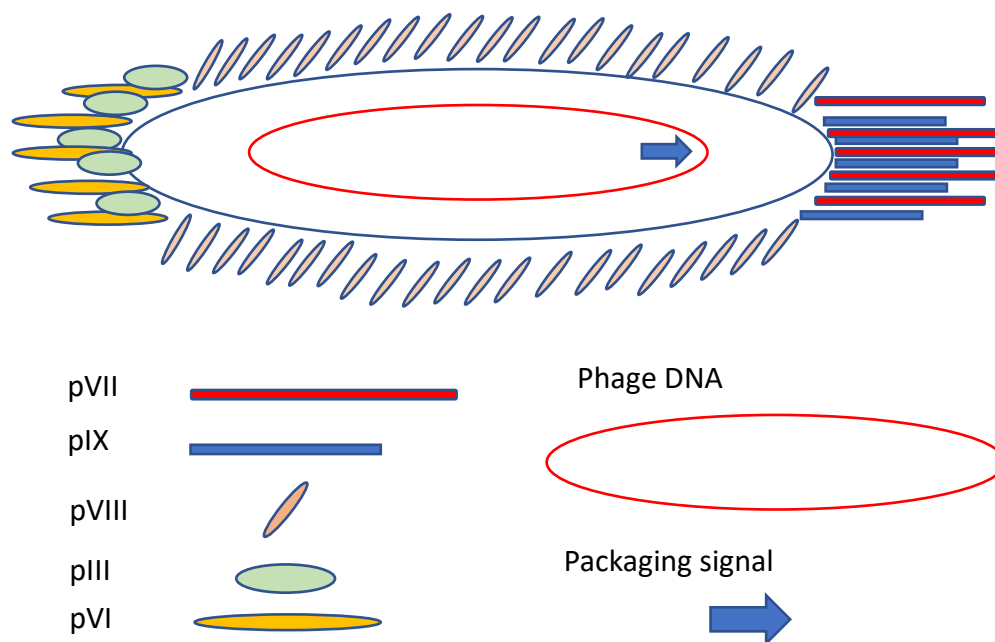


*Figure 5: Bacteriophage structure: pVII and pIX are localized to one end of the bacteriophage, and pIII and pVI localize to the other end. The DNA is oriented with the packaging signal towards the pVII and pIX end. The bulk of the structure of the bacteriophage is pVIII which covers the surface of the bacteriophage besides the two ends of the bacteriophage.*

Due to the flexibility of phage DNA and the amount that is incorporated into the phage capsid, large amounts of foreign DNA can be added to non-essential parts of the phage DNA [73]. This process makes it possible to display foreign peptides or proteins on the surface of the phage particle [74]. Since the amino-termini are external to the phage most of the foreign peptides and proteins that phages have expressed have been chimeric proteins connected to the amino-terminus of capsid structure proteins [75]. Historically, pIII and pVII have been used to display proteins and peptides, and large libraries have been expressed fused to these proteins. Other proteins have been used, but with much lower efficiency [73]. Since these proteins are small it is possible that this lower efficiency is due to the inability of these proteins,

with the added length of the library, to be trafficked to appropriate locations in the phage.

Usually, proteins expressed via pVIII are inserted between the sequence for the pVIII signal peptide and the amino-terminal coding region for the mature capsid protein [76]. This type of display, which is displayed on every pVIII on the surface is limited to 8 or fewer amino acids, due to structural considerations [77]. To express longer peptides, hybrid systems are used. Either through encoding on the phage gene (an 88 system), or a phagemid (a plasmid for phages an 8+8 system) [78]. In these systems an extra pVIII gene, which encodes for the individual peptides in the library, usually under an inducible promotor, is inserted along with the original pVIII [79]. In these situations, most of the surface pVIII is wild type and a portion are the new pVIII, but enough of the library peptide is exposed on the surface to be immunogenic and interact with specific ligands (figure 6) [78]. At least 80% of pVIII expressed by the hybrid phages are wild type. Interestingly, many proteins that bind to phages of the 8+8 system have lower affinity but bind due to higher valency [80].

pIII can also be used to express these libraries, but it can tolerate much longer peptides directly inserted in the original pIII [78]. The main drawback is, that the infection efficiency is down. Once again, a hybrid approach, with similar systems, solves this issue and wild type pIII can be expressed along with modified pIII [81].

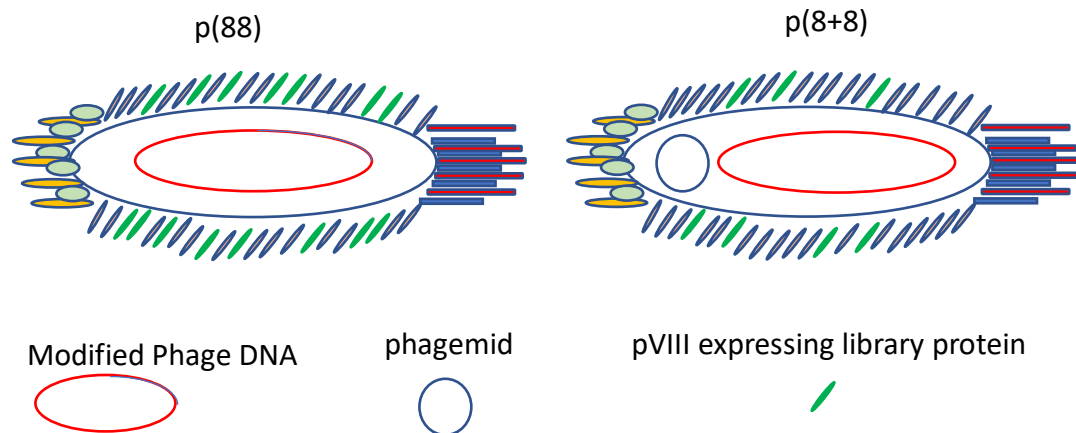


*Figure 6: Phages displaying the two libraries. In the p(88) library the library DNA is on the same DNA strand as the rest of the phage DNA. More copies of the peptide from the library are displayed, but there is more structural instability conveyed to the phage. In the p(8+8) library the library DNA is on its own phagemid (plasmid for phage). Therefore, fewer modified pVIII proteins are expressed on the surface, and the peptides resulting from a p(8+8) screen have higher avidity than from the p(88) screen.*

#### **a. Phage Screening**

The purpose of the screening of a phage library is always the same -to find something that, to some extent, binds to another specific molecular structure. In this thesis, for the sake of uniformity, I will be speaking about a peptide library screen, but this can be generalized to other types of phage screens. The modality of the screening can change depending on the type of data one seeks. For example, if the researcher desires very high affinity (tight binding) phages to the structure, increasingly stringent washing steps are used to remove the background and lower affinity phages.

In solid-phase panning either the phage, or the protein of interest is immobilized on a plate surface [79]. In our case, cells, which displayed the protein of interest, were immobilized on the plate surface. The phage is then incubated with the immobilized cells. The unbound, and weakly bound, phages are then washed off, leaving the bound phages of interest. Also, the protein

can be biotinylated and immobilized via streptavidin on plates and then the phage can be incubated with the immobilized protein [79]. Subsequent rounds of screening can introduce increasingly stringent washing conditions to remove lower affinity phages (figure 7).

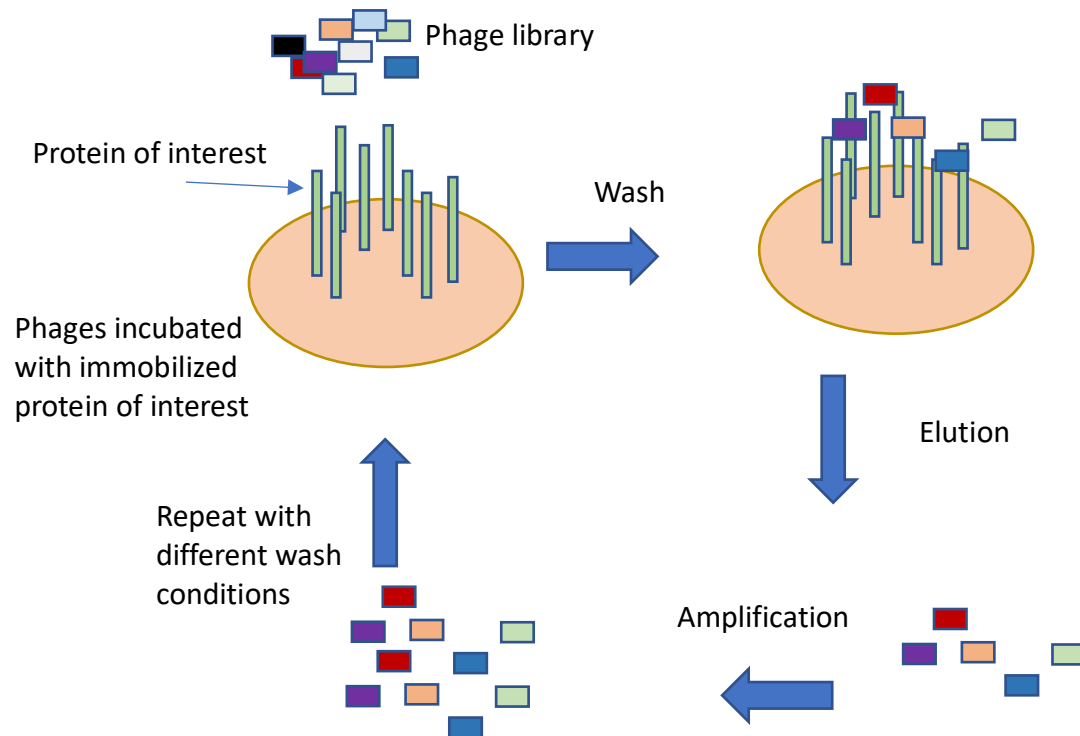


*Figure 7: Solid-phase phage display screening: In solid-phase phage display the protein of interest is immobilized on the surface and the phage is flowed across the immobilized protein. The non-binding phage are washed off. The bound phage is eluted off the protein and amplified. The process is repeated through multiple rounds of screening, with the phage being washed-off with increasingly stringent washes (ex. decreasing pH) leaving just strongly bound phage at the end of the process.*

An alternative to the above methods is liquid-phase panning. In liquid-phase panning an extra step of immobilization is used [79]. For example, biotinylated proteins are incubated in solution with a phage library. Next, the proteins are captured by immobilized Streptavidin. Then the unbound phage is washed off, the bound phage is amplified, and the process repeated. Other

tags are also used to immobilize the protein and bound phage and wash off the unbound phage. It is also possible to use biotinylated phage particles and let the proteins and phage equilibrate in solution [79]. At equilibrium, higher affinity phages will bind more molecules than lower affinity phages, if the lower affinity phages bind any screening molecules at all [71]. Next, the proteins are captured by immobilized Streptavidin. This step is inefficient, which reduces yields relative to the solid-phase method. The phages that are isolated are relatively higher affinity. For example, with pVIII-peptide displaying libraries there is a linear correlation between peptide affinity to the amount of screening molecules bound per phage (figure 8).

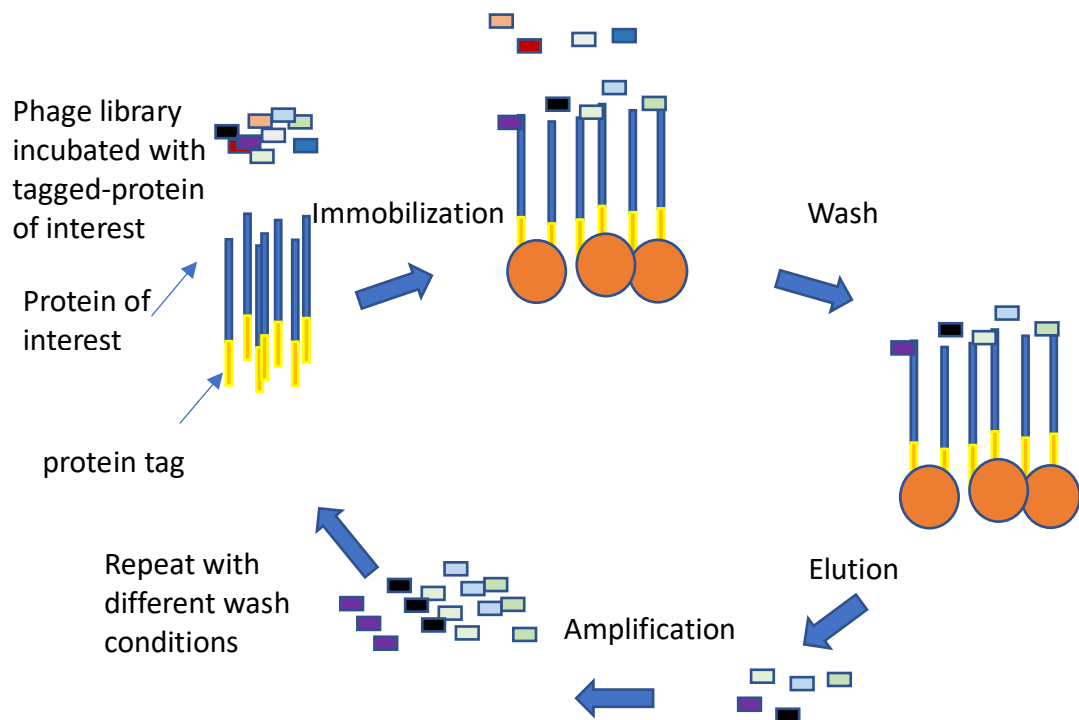


*Figure 8: Liquid-phase phage screening: The tagged-protein is incubated with the phage until binding equilibrium happens. Then the phage is immobilized and the unbound phage is washed off. The bound phage is eluted and then amplified in *E. coli*. The process is repeated with increasingly stringent washes.*

#### 4. Amyloid precursor protein structure and cleavage

Amyloid precursor protein is a single-pass transmembrane protein whose function is not known, is heavily associated with Alzheimer's disease [82, 83]. Previous studies looking at postmortem brains of Alzheimer's Disease patients shows characteristic amyloid plaques made from APP-derived peptides [84]. The human APP protein has several isoforms ranging in length from 365 to 770 amino acid residues, with the APP695 isoform predominantly associated with neurons [85].

Full length APP is processed by either  $\alpha$ - or  $\beta$ -secretase and then  $\gamma$ -secretase [86, 87]. Cleavage by  $\alpha$ -secretase generates an 83-residue fragment that is further cleaved by GS that is not pathogenic [88-91]. Whereas, a  $\beta$ -secretase, usually BACE1, cleaves APP leaving behind a 99-residue peptide that is further cleaved by GS that is pathogenic and does generate the amyloid plaques that are associated with Alzheimer's Disease (figure 9) [92, 93].

GS cleaves the 99-residue fragment either at residue 49 ( $A\beta$ -49) or 48 ( $A\beta$ -48) and then proceeds to cleave in multiple other points along the peptide fragment, usually in 3 amino acids steps. If GS first cleaves at  $A\beta$ -49 then it cleaves at  $A\beta$ -46 then  $A\beta$ -43 then  $A\beta$ -40 and possibly  $A\beta$ -37. On the other hand, if GS first cleaves at  $A\beta$ -48 it then cleaves at  $A\beta$ -45 then  $A\beta$ -42 and then  $A\beta$ -38 [94-96]. The biggest fragment that makes up the plaques is  $A\beta$ -40 followed by  $A\beta$ -42 (figure 10) [97, 98]. It is assumed that  $A\beta$ -42 is the crucial peptide for forming plaques due to its increased hydrophobicity, with the additional amino acids isoleucine and alanine, even though it accounts for less than 10% of the mass of the plaques [99-102]. The other fragments have only

been seen *in vitro* through mass spectrometry however the tools have not been developed yet to see these fragments *in vivo* [103-105].

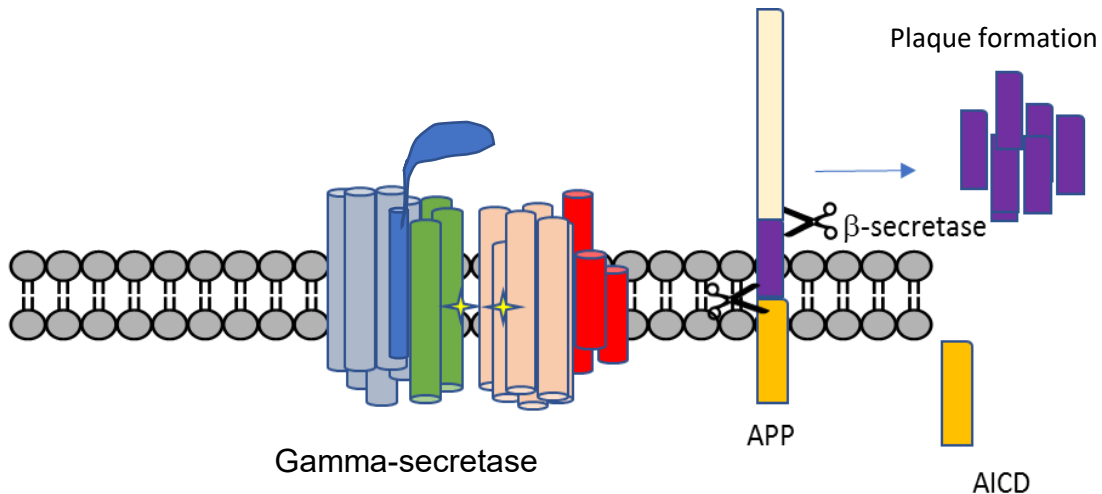


Figure 9: Plaque formation caused by APP cleavage by Gamma-secretase. APP is first cleaved by  $\beta$ -secretase and then cleaved subsequently by GS. Depending on how GS cleaves APP plaques can be formed with the cleavage products. Some researches have shown an affect with AICD, which translocates into the nucleus and may have implications in Alzheimer's Disease.

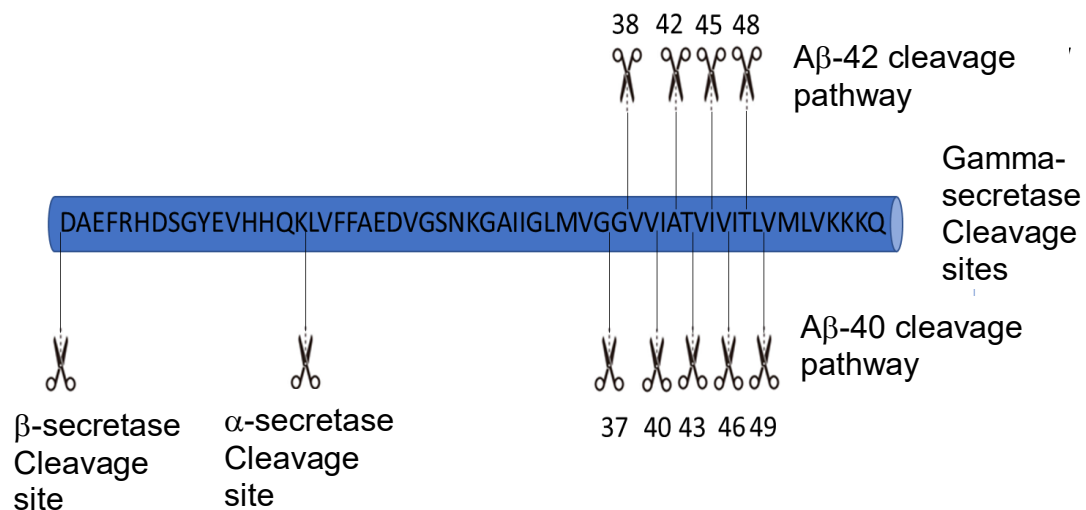


Figure 10: The two possible pathways that GS can take to cleave APP. In the A $\beta$ -42 cleavage pathway GS first cleaves at A $\beta$ -48 and then continues down to A $\beta$ -42. Whereas in the A $\beta$ -40 pathway, cleavage starts at A $\beta$ -49 and then continues down to A $\beta$ -40. With both pathways perhaps continuing one step further to A $\beta$ -38 and A $\beta$ -37, respectively.



### **a. APP cleavage inhibition and mutations**

Due to APP's plaque deposition being correlated with Alzheimer's Disease, initially the therapeutic avenue was to inhibit all forms of processed APP [106]. This led to pan-GS inhibitors, and then, as mentioned above, to resulting toxicities [10, 107]. One of the next possibilities was to focus on altering GS and making it follow the A $\beta$ -49 pathway as opposed to the A $\beta$ -48 pathway, thereby creating more A $\beta$ -40 in place of A $\beta$ -42 [108]. One of the reasons for this was based on the mutations found in hereditary Alzheimer's Disease patients (Table 1). Multiple mutations within APP itself and within Presenilin led to increased amounts of A $\beta$ -42 as opposed to A $\beta$ -40 and a correlated increase in morbidity [109, 110]. The next idea was to inhibit A $\beta$ -42 generation while limiting interference with A $\beta$ -40 generation [111]. At this point, two ways were thought of how to do this. Either to increase A $\beta$ -38, which would mean that the A $\beta$ -42 that was being generated is being cleaved by GS into a smaller fragment which is less hydrophobic. The amino acids that are cleaved are 2 glycines, isoleucine, and alanine. Or, it was to increase A $\beta$ -40, which would mean that GS would be starting its cleavage path down A $\beta$ -49 as opposed to A $\beta$ -48. There is a third possibility which is to limit the amount of A $\beta$ -42 that is being generated without increasing A $\beta$ -38 or A $\beta$ -40, rather by increasing A $\beta$ -45 or even A $\beta$ -48. This would mean that GS is inhibited higher up in its cleavage pathway. The current drawback is that there are no tools sensitive enough to see this *in vivo*. One of the most sensitive tools that would work in this situation would be antibodies, which are sensitive enough to differentiate between the A $\beta$  fragments, except antibodies have never been generated towards these epitopes. If antibodies were generated to these

epitopes then even *in vivo*, we would be able to test for the generation of these substrates.

*Table 1: Mutations in APP and PSEN1. Red residue mutations are known mutations that are pathogenic. Green residue mutations are protective mutations.*

Residue number	Amino acid	Possible mutation	Biological affect
709 (38) APP	G	<b>S</b>	
713 (42) APP	A	<b>T, V</b>	
714 (43) APP	T	<b>A, I</b>	Increased A $\beta$ 42/A $\beta$ 40 ratio
715 (44) APP	V	<b>A, M</b>	Increased A $\beta$ 42/A $\beta$ 40 ratio.
716 (45) APP	I	<b>F, M, T, V</b>	Increased A $\beta$ 42/A $\beta$ 40 ratio
717 (46) APP	V	<b>F, G, I, L</b>	Increased A $\beta$ 42/A $\beta$ 40 ratio
719 (48) APP	T	<b>P</b>	
246 PSEN1	A	<b>E, P</b>	Increased A $\beta$ 42/A $\beta$ total ratio.
248 PSEN1	L	<b>P, R</b>	
250 PSEN1	L	<b>S, V</b>	
384 PSEN1	G	<b>A</b>	Increased A $\beta$ 42/A $\beta$ 40 ratio; Increased A $\beta$ 42; decreased A $\beta$ 40.
386 PSEN1	F	<b>I, S</b>	
388 PSEN1	F	<b>L</b>	Increased A $\beta$ 42 and A $\beta$ 42/A $\beta$ 40 ratio.

## 5. Antibodies and their structure

Antibodies are proteins secreted by B-cell lymphocytes. The general structure of the monomeric antibody is four peptide chains, that are coordinated to make the larger protein structure -two similar heavy chains and two similar light chains (figure 11). Each heavy and light chain is connected via several disulfide bonds, and this region is known as the hinge region of the antibody. The end of the light chain is the hypervariable region, which, based on genetic recombination, has unique amino acid sequences, and gives the antibody binding selectivity and perhaps specificity.

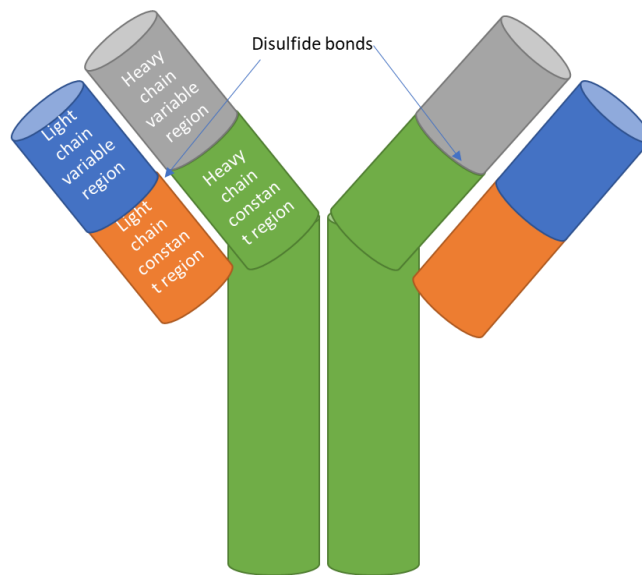


*Figure 11: Structure of an IgG antibody. The antibody is made up from a set of heavy chains and a set of light chains that are held together by disulfide bonds. The variable region is where the antibody displays its specificity and the constant region is what defines the antibody type.*

There are five isotypes of antibodies and several subtypes of the isotypes, with each serving specific functions [112, 113]. The five isotypes of antibodies are Immunoglobulin(Ig) A (IgA), IgD, IgE, IgG, IgM. IgA is secreted in the mucus and has 2 subtypes and is either in a monomer or dimer form. IgD is a monomer and its exact function still is not clear. IgE are the source of allergies, it is also a monomer that the body makes in response to being introduced to an allergen. IgM is the early response of the B-cell when presented with an antigen, and it exists usually as a pentamer. IgG is the most abundant of all antibodies. It exists as a monomer, but it has 4 isotypes IgG1, IgG2, IgG3, IgG4. They bind to receptors in the descending strength.  $IgG3 > IgG1 > IgG4 > IgG2$ . Also, IgGs usually have the longest half-life of over 20 days, besides for IgG3, which has a half-life of a week similar to the half-life of IgM and IgA. IgD and IgE have half-lives of 3 and 2 days, respectively [114, 115].

### **a. Antibody uses**

The most significant attribute that antibodies have is their ability to recognize specific epitopes and ignore others. This can include minor modifications. If the epitope is methylated the antibody will have decreased recognition of the epitope. This specificity is used in the lab to create affect as a tool, but antibodies can also be used in therapies [116]. Some modalities for therapy include targeting specific epitopes for degradation by macrophages, or the antibody can be used as a drug-conjugate to increase the specificity of the drug [117, 118].

## Chapter 2:

### *Discovery of Notch1 modulating peptides*

#### **1. Introduction:**

Notch signaling is present during all stages of development [119]. It is a highly conserved signaling system that enables short-range communication between cells. Contact between cells is required for signaling to occur, and the resulting signaling is dependent on cellular microenvironment [120]. For example, Notch can trigger cell proliferation, cell differentiation, and cell death throughout an organism's lifespan [20, 119-124]. This Notch signaling is triggered in the same fashion, but the resulting effect can be different depending the cellular microenvironment [62, 125, 126]. Because of Notch's omnipresence in organismal development, understanding aberrant Notch signaling is critical to our examination of many disorders including Alagille syndrome, CADASIL (cerebral autosomal dominant arteriopathy with subcortical infarcts and leukoencephalopathy) and multiple types of cancer and for the future pharmacological manipulations of the Notch signaling system [121, 127-132].

Notch is a single-pass transmembrane protein, found on the surface of the cell [120, 125]. There are four members of the Notch receptor protein family (Notch 1-4), with Notch 1 and 2 having the largest sequence overlap [125]. For signaling to occur, Notch requires a neighboring cell to express one of five, Delta1, 3, or 4, or Jagged1 or 2, ligands. Binding occurs along the "epidermal growth factor (EGF) like-region," which is where the Notch proteins have multiple copies of EGF domains, with Notch1 binding to its ligands at EGF domain 11-13 [133-136]. Once the ligand binds to the Notch receptor, there is a conformational change in the Notch regulatory region and the

metalloprotease ADAM 10 and ADAM 17 cleavage site is revealed [125]. The metalloprotease cleaves Notch external to the cell membrane. Gamma-secretase then cleaves within the cell membrane and the Notch intercellular domain (NICD) is released and translocates to the nucleus. In the nucleus, NICD complexes with DNA-bound CSL repressor complex and recruits Mastermind and binds with RBPJ to make a transcriptionally active complex. Notch activation then transcribes the Notch downstream effector genes, most significantly HES and HEY [20, 125]

Notch may act as both an oncogenic or a tumor suppressing ligand, depending on the cellular microenvironment of the specific tissue [132, 137]. Sixty percent of all T cell lymphoblastic leukemias have activating (oncogenic) mutations in Notch1, including a fusion of the 3' end of Notch1 to the T cell receptor  $\beta$  generating a truncated dominant active Notch1 protein [126, 137]. However, many squamous cell carcinomas have inactivating mutations, stopping the tumor suppressor function of Notch, including head and neck, cutaneous and esophageal squamous cell carcinomas [138-140]. In addition, alterations of Notch signaling too drastically can cause other toxic side-effects. For example, Clevers et al. showed that Notch inhibition turns proliferative cells in intestinal crypts and adenomas into goblet cells [141].

Pharmacological manipulations of the Notch signaling system can become very complicated, as outlined above. While the principle drug target may be to inhibit gamma-secretase cleavage of notch1, it has become well known that inhibitors of notch cleavage have many off-target side effects [5]. This is due to the fact that gamma secretase, the main protease involved in Notch cleavage, has over 90 substrates [9]. Because Notch plays a role in various signaling pathways, it is critical to acknowledge this during drug

development. Ultimately, complete inhibition of notch signaling is toxic. Therefore, drug development is critical to specifically target pathologic Notch signaling [131].

In order to specifically target Notch signaling, we have designed a pooled peptide screen to identify ones that bind to Notch1. Peptides represent a reemerging class of drugs because of their modular design, cost and overall ease to work with [142]. Due to their modular design, they represent an ideal pooled screen with the ability to screen different sequences, epitopes and conformations in a high throughput manner. To find a good peptide candidate, we used a bacteriophage that displayed a peptide library. A bacteriophage is a virus that infects bacteria, that can express a library of peptides on the surface of the phage allowing us to screen large possibilities of peptides easily. This screening will help us discovery new peptide-protein interactions. In our case, we will use high-throughput to screen the large library of peptide expressing M13 bacteriophages to find peptide sequences that can recognize Notch1 and then rescreen them to see if, and how much, they inhibit, or modulate, Notch signaling [78, 79]. Here, to perform the pooled screen, we screened a phage library ( $>10^9$  diversity) to find a sequence that can recognize Notch1 and modulate Notch signaling. We not only found a sequence that recognizes Notch1, but is also specific for Notch1, and does not recognize other homologs of Notch including Notch2, which is highly homologous ( $>60\%$ ) [123, 143]. In addition, we were able to make a dimer of the peptide sequence and it partially inhibited Notch1 signaling.

## 2. Results:

Phage display is a versatile way to test numerous, diverse peptide sequences. Here we used a library with a linear 20 amino acid variable region with a library size  $>10^9$ . In order to be able to display such a long peptide, without compromising the structural stability of the phage, the phage library uses a p(8+8) system. In this system a library of peptides is added via an additional library displaying pVIII protein that is located on a phagemid and not on the phage's native DNA [144]. The structural integrity is provided by the native pVIII, which expresses about 2500 proteins on the surface. While the library is expressed on a separate pVIII that only has about 200 copies displayed on the phage surface (figure 12). Due to the need for structural stability, the library can only be expressed on a minority of the surface pVIII proteins [78, 144, 145].

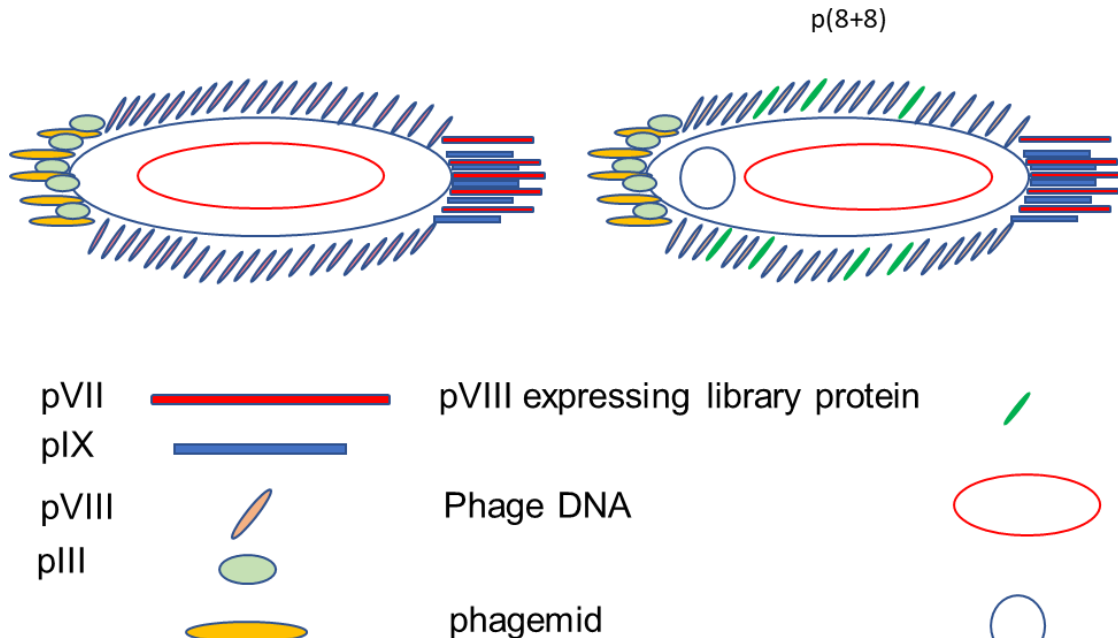


*Figure 12: M13 bacteriophage structure. Most of the surface is pVIII with pVI and PIII at one end and pVII and pIX at the other end. In the modified M13 bacteriophage, about 10% of the surface express a modified pVIII protein that is located on the phagemid. This is where the library is expressed and exposed on the surface of the bacteriophage.*



We screened the peptide library against stable Flp-in U2OS cells that upregulate human Notch1-Gal4 chimeric receptors in a doxycycline dependent manner (U2OS-N1) [146, 147]. First, cells that were expressing Notch1 were immobilized via paraformaldehyde (PFA) and incubated with the phage library. The unbound phage was washed off and the bound phage was dissociated and amplified in *E. coli*. Then, for a negative selection, the recovered phage was rescreened against U2OS cells that did not upregulated Notch. This negative selection removed phages that only recognized the surface of the cell and not Notch1. The phages that did not bind the U2OS surface were then amplified in *E. coli* and rescreened against U2OS cells that upregulated Notch1 for three more rounds, with each round using increasingly stringent dissociation steps (each dissociation was with a lower pH). The remaining phages after the multiple steps of biopanning would leave behind only peptides that strongly bound to Notch1 [148]. After all the five rounds of biopanning the resulting phages were sequenced and there was enrichment for just one peptide sequence VGGLAQLVRAYSGLNGSTTA (P1 phage) (Table 2). An ELISA was performed to show that the phage does recognize Notch1 when Notch1 is upregulated via doxycycline (figure 13).

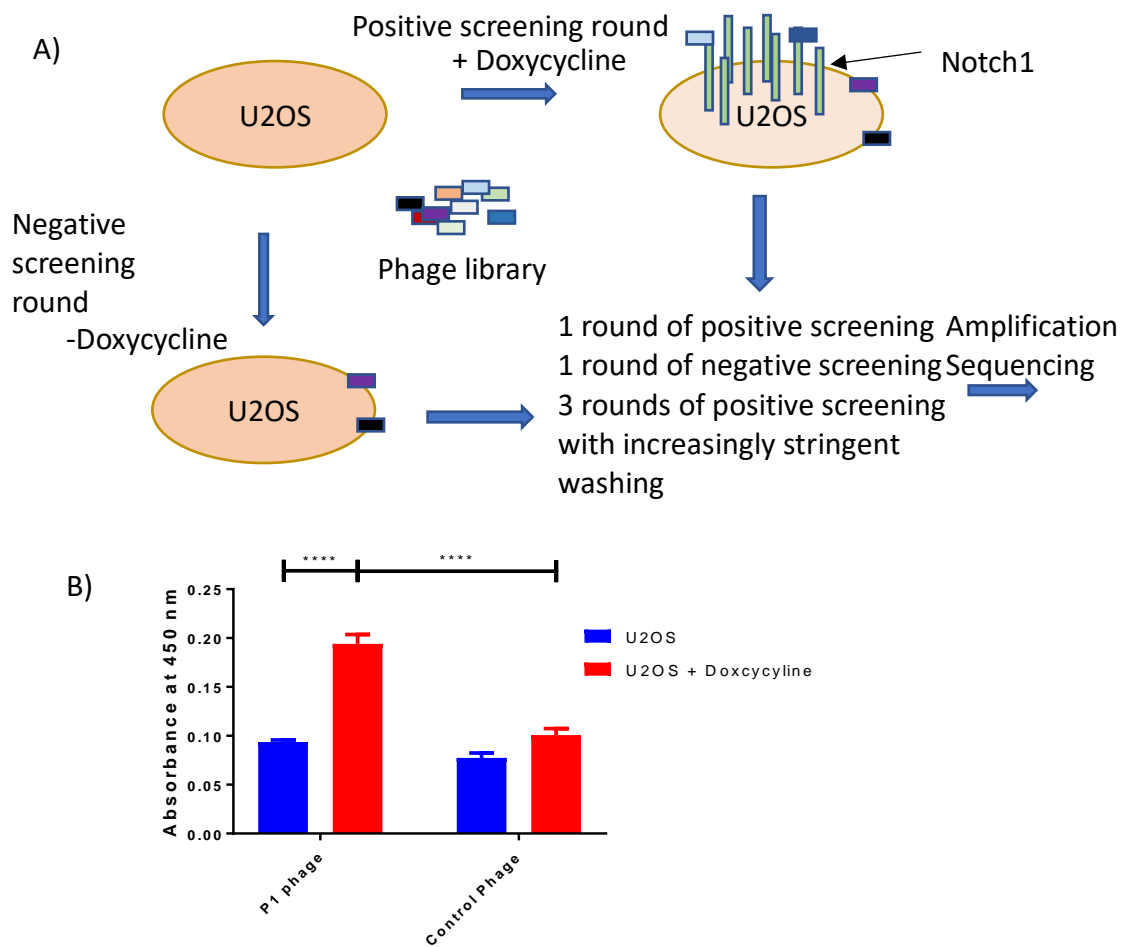


**Figure 13: Method used to screen the phage library to discover peptides that recognize Notch1.** A) The phages were first screened against U2OS cells that upregulated Notch1 in the presence of doxycycline. The phages that bound were then screened against U2OS cells that did not upregulated Notch1. The phages that did not bind when Notch1 was not present were then reincubated with U2OS cells that upregulated Notch1. The phages were washed off with subsequent stringent washes. The result of the screen was the phage P1 phage B) P1 phage recognizes Notch1 in a doxycycline dependent manner. After five rounds of screening of the phage library against immobilized cells, an ELISA showed that P1 Phage recognizes Notch1 preferentially when it is upregulated and compared to a control phage. ANOVA test \*\*\*\*<0.0001 P-value ns = not significant P-value. Data from Dr. Villa.

Table 2: Sequences recovered over multiple rounds of biopanning

Enrichment of Sequences after Biopanning		
	P1 Phage	P2 Phage
Round 2	0%	0%
Round 3	3.03%	3.03%
Round 4	87.23%	2.13%
Round 5	97.78%	0%

After the identification of the P1 phage from the phage screen, and its sequencing, the binding abilities of P1 phage were assessed. P1 phage itself was fluorescently labeled with an Alexa Fluor 568 dye [149]. First Flp-in U2OS cells were plated that were, incubated with 1 ug/ml doxycycline to induce Notch1 expression. After 24 hours the cells were fixed with 4% formaldehyde. Once the cells were fixed, we incubated 10 nM of fluorescently-labeled P1 phage with the U2OS cells. As controls we also incubated these modified P1 phages with U2OS cells that did not upregulate Notch1. Also, we conjugated a control phage at the same concentration with U2OS cells that upregulated, and did not upregulate, Notch1 (Figure 14). Then we incubated the fixed cells with a human antibody that was developed to bind to the Notch regulatory region (anti-NRR) [150]. Lastly, a mouse anti-human Alexa Fluor 488 was incubated with the cells to bind to the anti-NRR antibody, which showed that both the fluorescently-labeled P1 phage overlapped in binding with the anti-NRR antibody (Figure 14).

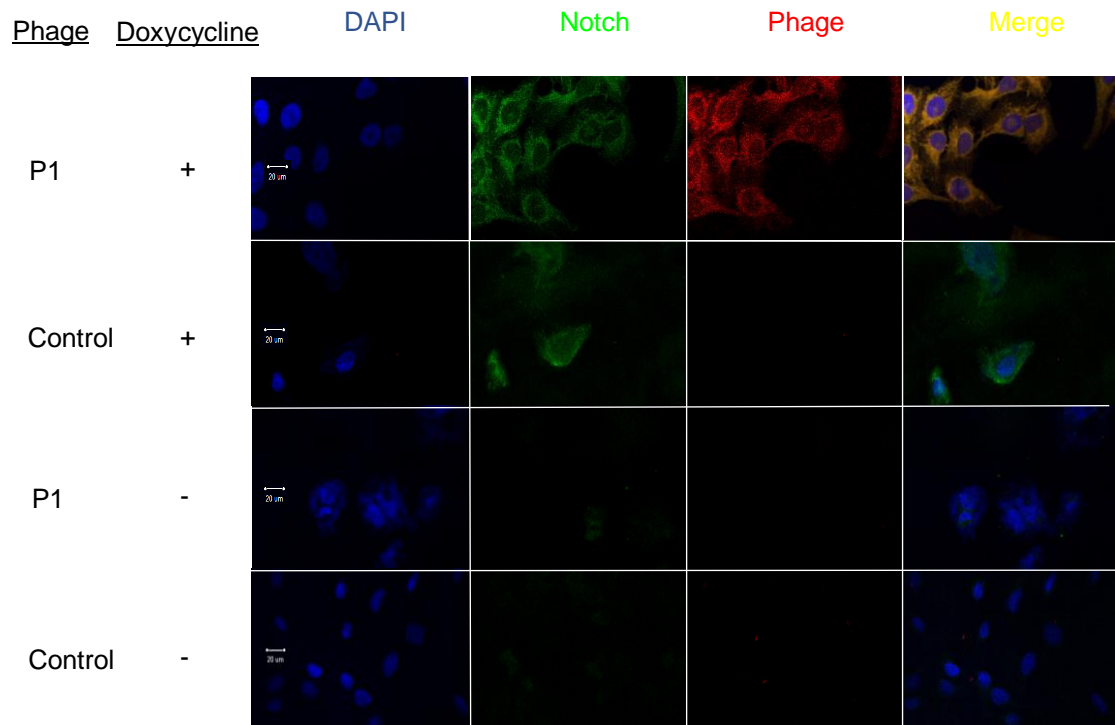


*Figure 9: P1 phage binds to cells that upregulate Notch1. Top two rows, cells were first incubated with doxycycline (1 $\mu$ g/ml), to upregulate Notch1. After 24 hours the cells were fixed and P1 phage and control phage at 10 nM, that were previously conjugated to Alexa Fluor 568 was added. Bottom two rows. Labeled-P1 phage does not bind to cells that do not upregulate Notch1. No doxycycline was added and Notch1 was not upregulated. Therefore, neither the conjugated P1 phage nor anti-notch1 antibody bound. 10 $\mu$ g of human anti notch1 antibody was added to bind to Notch1. Alexa-488 anti-human was used as a secondary (1:2000).*

The four Notch receptors have some sequence homology, especially between Notch1 and Notch2, with Notch4 showing the least homology [123, 143]. The signaling of the different receptors is context dependent. For example, Notch1 signaling causes T-cell differentiation in lymphocyte development, without it Notch2 cause cell differentiations into the B-cell lineage [151]. This shows that different Notch receptors' signaling responses can actively oppose one other's signaling [62, 132]. To see if P1 phage can differentiate between the different Notch receptors we incubated fluorescently

labeled P1 phage with cells that inducibly, via doxycycline, express Notch1, Notch2, and Notch3 (Figure 15). Notch4 was not used since its homology is <40%. The strong red signal by the labeled-P1 phage as opposed to the other Notch receptors shows that P1 phage only recognizes, and therefore only binds to, Notch1.

Previously, we showed that P1 phage and the Notch1 antibody colocalize together. However, this does not demonstrate that P1 phage directly binds to Notch1. In order to show direct labeling of Notch1 by P1 phage we performed a co-immunoprecipitation pull down of Notch1 and P1 phage (Figure 16). First, Notch1 was upregulated in U2OS cell. Next, the cells were lysed and harvested and then incubated with P1 phage and control phage separately. Then we incubated the lysate with P1 phage and control phage. Using anti-M13-antibodies, which recognize the M13 bacteriophage, we performed a pulldown, ran the components on in an SDS-PAGE gel and blotted with the anti-NRR antibody to show direct binding to Notch1. Then we probed the blot with the anti-NRR antibody showing that the P1 phage directly bound to Notch1.

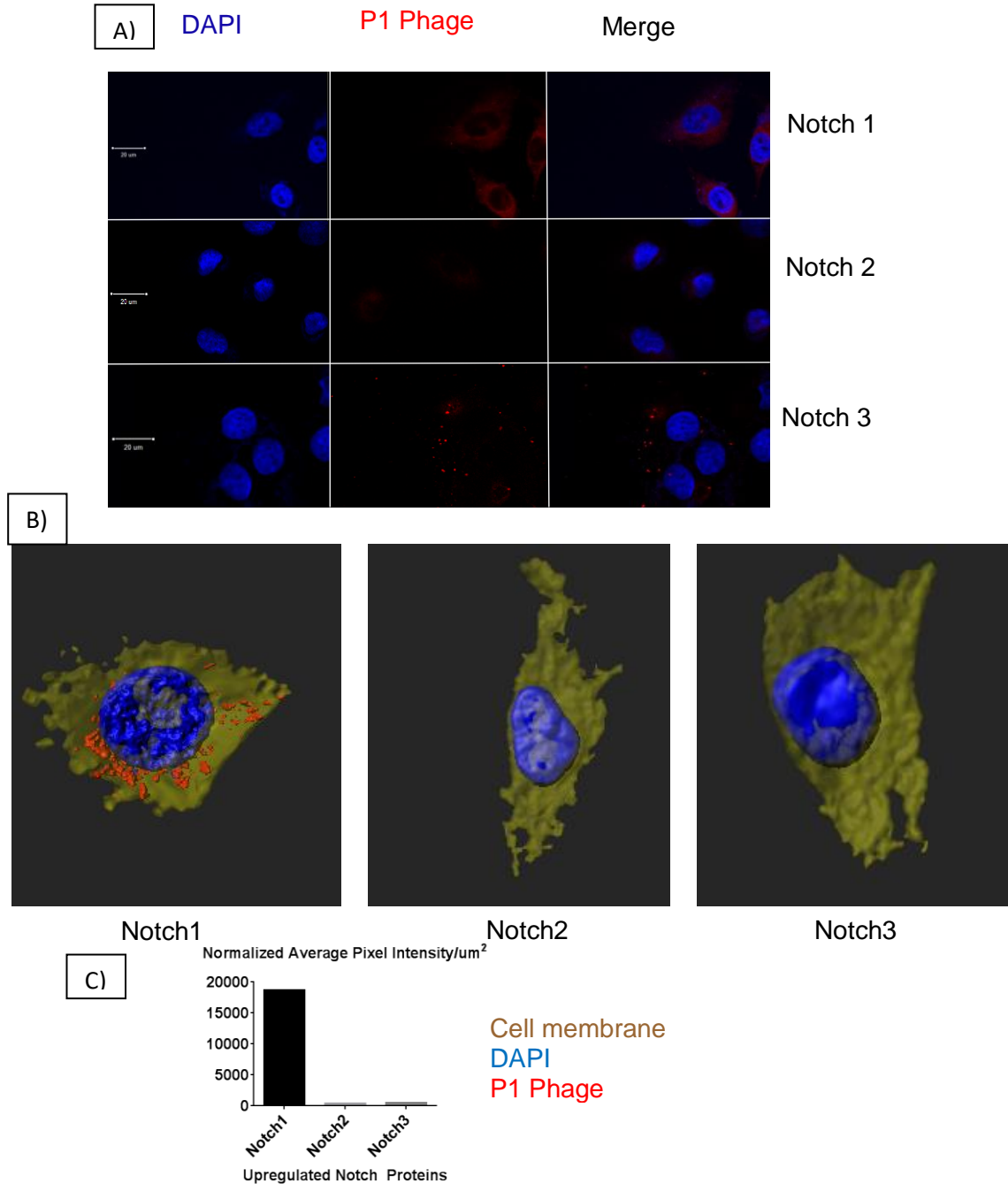


**Figure 15: P1 phage only recognizes Notch1 and no other isoforms of the Notch receptor.** A) U2OS cells that are Flp-in for Notch1, Notch2, and Notch3 were incubated with 1 $\mu\text{g}/\text{ml}$  of doxycycline, and then fixed with formaldehyde 24 hours later. Then 10 nM of labeled-P1 phage was incubated with each of the cells expressing a different Notch receptor isoform, and the cells were imaged. P1 showed binding to Notch1. B) A 3d-rendering was done by reconstruction of the z-stacks of images of U2OS-Notch1, Notch2, and Notch3, with P1. C) Pixel intensity for B of as a correlation of P1 recognizing of the three Notch isoforms.

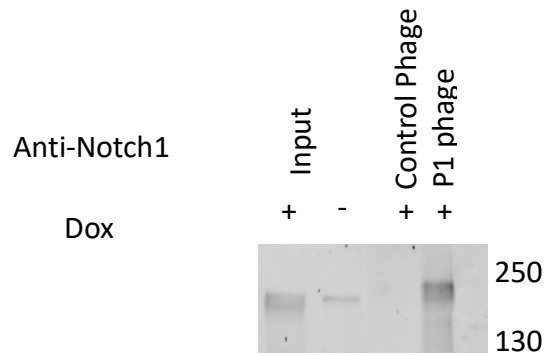


*Figure 16: Co-immunoprecipitation of Notch1 and P1 phage. Flp-in-U2OS Notch1 cells were incubated for 24 hours with doxycycline. The cells were lysed and P1 phage was mixed with the lysate. The phage-lysate was then incubated with biotinylated anti-m13 to bind the phage. The bound phage/Notch1 complex was subsequently concentrated via magnetic streptavidin beads. The beads were boiled, and the eluent was run on a western blot and probed with the anti-NRR Notch1 antibody.*

Since the Notch1 construct is an inducible chimeric construct with Gal4 at the c-terminus, it signals in a manner mimicking Notch1 but upregulates a protein downstream of the GAL4 DNA binding sequence instead of the Notch downstream genes. To measure Notch1 signaling we co-cultured NIH-3T3 cells that constitutively upregulate the Jagged2 (J2) ligand. We also transiently transfected firefly luciferase that has an upstream signaling sequence that will be upregulated in the presence of Notch1-Gal4's cleavage and translocation to the nucleus. As a control, renilla luciferase, which does not require any extraneous signaling to fluoresce, was also added. Incubating P1 phage itself within this culture system showed an interference with Notch1 signaling signal relative to the positive control. Incubating with P1 phage with U2OS Flp-in cells that inducible express Notch2 and Notch3 did not show a significant change in signaling. This experiment demonstrated that P1 phage only recognizes Notch1, and it also interferes with Notch1 signaling (Figure 17).

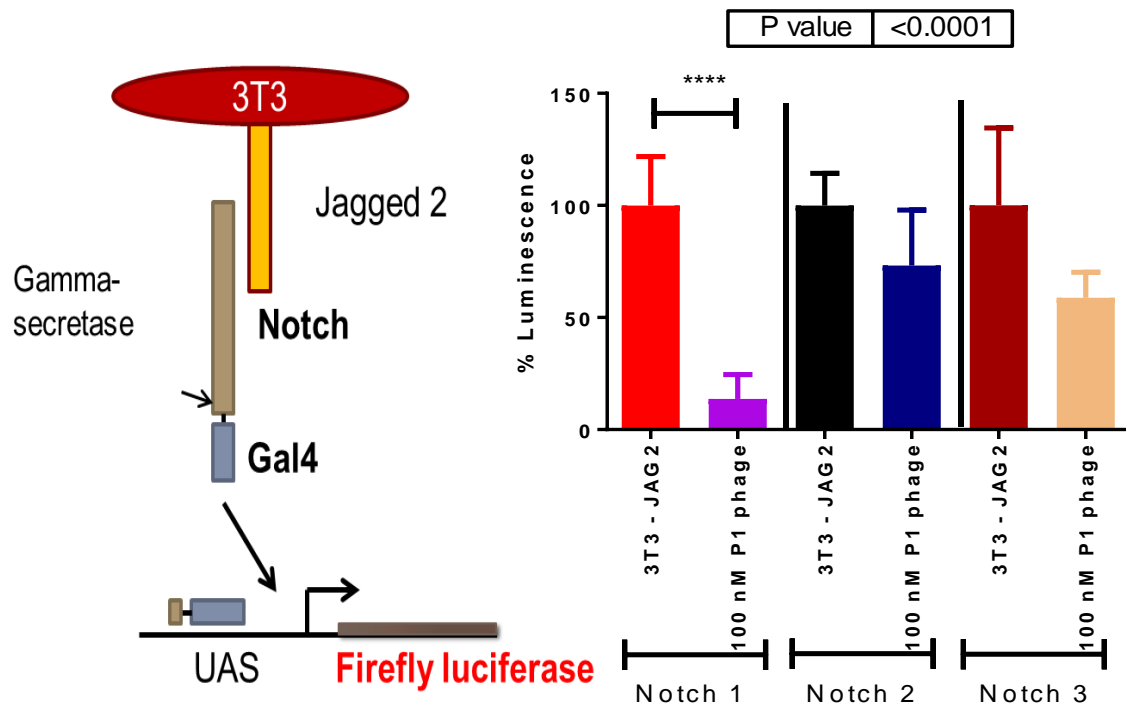


Figure 17: Notch signaling is partially inhibited by P1 phage: The Notch reporter signaling system is depicted with 3T3 cells expressing Jagged2, which is a Notch ligand, co-cultured with Notch expressing cells. The Jagged ligand binds to the Notch receptor and the Notch receptor is cleaved. The internal part of the protein, which is Gal4, translocates to the nucleus and binds to the UAS domain and increases transcription of firefly luciferase. Here, U2OS cells expressing Notch1, Notch2, and Notch3 were separately co-cultured with 3T3-Jagged2 expressing cells. Only Notch1 signaling is interfered with by adding P1 phage at 100 nM. ANOVA testing for significance. \*\*\*\*<0.001 p-value. Background was calculated by incubating with jc2 ( $\gamma$ -secretase inhibitor).

Recently, there has been some data that showed that Notch1 does not always require a ligand on a neighboring cell to signal, also known as *trans*-signaling [152]. It is possible for Notch to signal with ligands presented on the same cell, in what is known as *cis*-signaling. One possible explanation for our inability to completely inhibit Notch signaling is that P1 phage is binding along the EGF region where it may interfere with Jagged2 presented by the 3T3



cells, which is *trans*-signaling, perhaps, binding along this region would not interfere with *cis*-signaling.

The next question we asked, was whether the bacteriophage itself contributing to the affect that we saw. In order to show that just the peptide sequence is needed we synthesized the monomeric peptide through solid-phase peptide synthesis. When it was incubated with the U2OS-flp in cells that were upregulating Notch1, we did not see any interference with Notch1 signaling. Also, when we directly labeled the peptide with fluorescent dyes, we did not see any binding of the peptide to Notch1. This can mean that the peptide has a high off-rate, or it a monomer of VGGLAQLVRAYSGLNGSTTA is not able to adopt a conformation that will be able to bind to the Notch1. It is also possible that the dye interfered with peptide binding, but that would not explain the lack of modulation of Notch1 signaling. Since we used a p(8+8) library, which expresses around 200 copies of the VGGLAQLVRAYSGLNGSTTA peptide on the surface of the phage, we focused next on an avidity approach. To do this we synthesized a VGGLAQLVRAYSGLNGSTTA dimer(dVGG) with a PEG spacer using the Universal PEG NovaTag resin [153]. The synthesized VGGLAQLVRAYSGLNGSTTA dimer was purified through C-18 reversed-phase HPLC and its identity was confirmed by mass spectrometry. The synthetic steps are shown in figure 18.

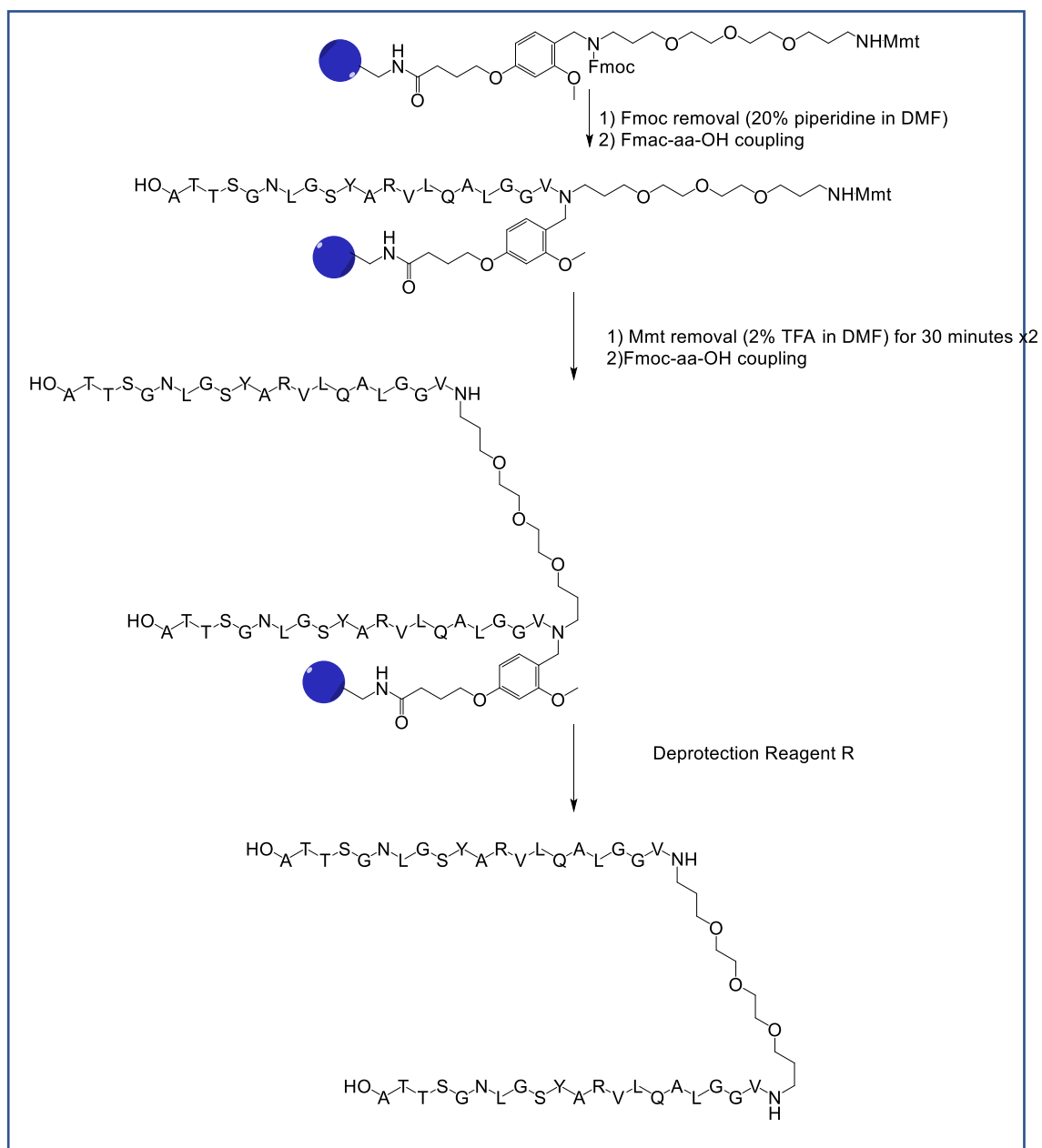


*Figure 18: Synthetic scheme to synthesize dVGG. Step one, was deprotecting the Fmoc from the resin and then SPPS to build the first monomer with a Boc protecting group after the final valine. Next, 2% TFA in DMF was used to deprotect the Mmt protecting group and then SPPS was performed to synthesize the second monomer. Lastly, reagent R was used to deprotect the peptide from the protecting groups and cleave it off the resin.*

Once we synthesized dVGG, we incubated the dimer and monomer with the luciferase system that we used before. The peptide did not significantly interfere with signaling, whereas the dimer did inhibit the signal on a similar level to what the phage was able to do on its own (figure 19).

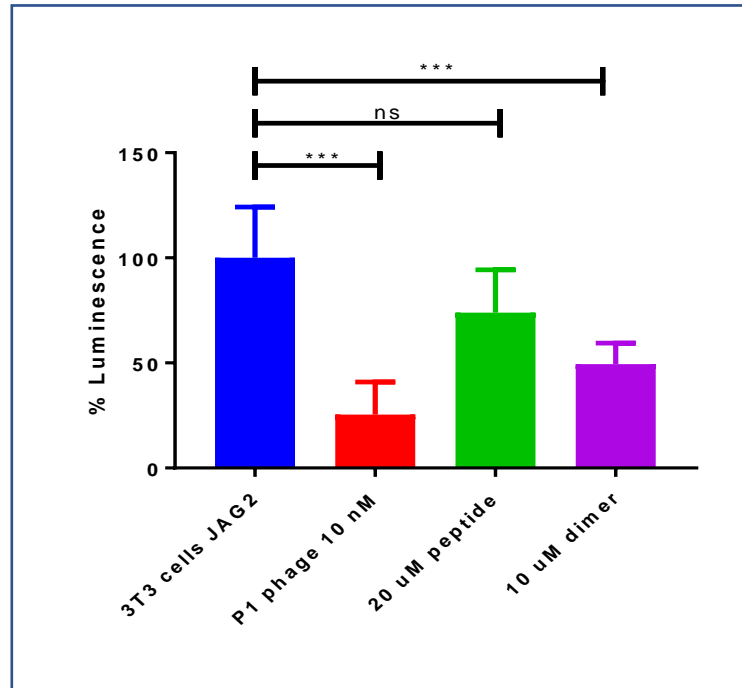


*Figure 19: dVGG inhibits cells signaling. Incubating our co-culture luminescence system individually, with monomeric peptide and dVGG, showed that dVGG does interfere with signaling while the monomer does not. (\*\*\*\*<0.0001 P-value, \*\*\*<0.001, ns = not significant P-value*

### 3. Conclusion:

As illustrated here, the bacteriophage can modulate Notch1 signaling. This modulation can be useful in that, as seen with gamma-secretase inhibitor clinical trials, inhibiting all Notch signaling will lead to toxic side-effects, whereas modulating the signal would be more useful and helpful. The seeming inability for the phage to completely inhibit signaling would be a step in this direction. As a therapy, this are multiple different diseases based on Notch signaling where this peptide will not be useful, due to those diseases being able to signal in a non-normal ligand receptor binding way. For example, certain T-ALLs have mutations in the NRR of Notch1. These cancers can grow and signal without normal ligand binding since they do not require the Notch regulatory region to adopt a conformational change that would allow signaling to occur. In these models, the peptide seemingly would not abrogate signaling. Whereas in other diseases in which the ligands are being over expressed, the dimeric peptide would be more useful.

In addition, the dimeric peptide that was made from the phage surface does not necessarily mimic the surface of the phage, in that the peptide is locked in place on each end on the phage, and there are more copies of the sequence. Nevertheless, the peptide is able to interfere with signaling. This does broaden the tools to both study Notch signaling and at the same time shows a focus one a possible avenue to further look at modulating Notch signaling.

### 4. Materials and Methods:

**Cells Lines, Transfections:** The U20S-flp-in Notch1, U20S-flp-in Notch2, and U20S-flp-in Notch3 cells were a gift from the Blacklow lab in Harvard University. NIH 3T3-J2 were purchased from ATCC. All cells were cultured in

DMEM media with 10% heat inactivated FBS with penicillin and streptomycin. The pRL renilla luciferase under the CMV promotor was purchased from Promega. The pFR firefly luciferase under the GAL4 promoter was purchased from Agilent.

**Discovery of Notch1-binding phage:** A  $10^9$  library of bacteriophages that encoded a 20-mer randomized peptide was screened against U2OS-Flp-in tet-on Notch1-Gal4 cells. The cell (U2OS control, U2OS-N1) were plated at 10,000 cells/well. After 24 hours the cells were induced for 24 hours with doxycycline (Sigma-Aldrich) at  $1\mu\text{g/ml}$ . Then the cells were fixed with 10% formalin buffer pH 7 (Electron Microscopy sciences) and incubated for 20 minutes at room temperature, washed with tris buffered saline and 0.1% tween20 (wash buffer) (Sigma-Aldrich) two times, and quenched with 1%  $\text{H}_2\text{O}_2$ , 0.1%  $\text{NaN}_3$  (Sigma-Aldrich) in wash buffer. The cells were blocked for one hour with PBS and 3% milk (Bio-rad) at room temperature. In the meantime, the phage was blocked in a 96-well plate with 2xPBS and 6% milk for 1 hour at room temperature. The cells were washed, and the blocked phage was added to the cells for 2 hours at room temperature. Afterwards the plate was washed and anti-M13 (Abcam ab24229) detection at 1:2000 dilution was incubated with the cells at room temperature for an hour. The plates were washed and incubated with 50  $\mu\text{l}$  of TMB (Surmodics) for 10 minutes and then 50  $\mu\text{l}$  of 1M  $\text{H}_2\text{SO}_4$  (Sigma-Aldrich) and read on an Envision (Perkin Elmer) at 450 nm.

**Labeling of P1 phage:** Following the protocol found in Jaye et al, Alexa Fluoro 568 carboxylic acid, succinimidyl ester was conjugated to the phage [149]. An Alexa Fluoro 568 solution prepared at  $10\mu\text{g}/\mu\text{l}$  in DMSO. Also, P1 at  $1 \times 10^{13}$  colony forming units (cfu) was resuspended in 100  $\mu\text{l}$  1 M  $\text{Na}_2\text{CO}_3$ /1 M

NaHCO<sub>3</sub> pH 9.0 (bicarbonate conjugation buffer). 5 µl of the Alexa Fluoro 568 solution was incubated with P1 phage. The conjugation was performed in the dark at room temperature rotating for 1 hour. Following incubation P1 phage was resuspended twice with 200 µl of 20% PEG/NaCl.

**Co-immunoprecipitation:** U2OS-Flp-in Notch1 cells were seeded at 100,000 cells per well in a six well plate. The cells were incubated with doxycycline for 24 hours. The media was aspirated, and the cells were washed with PBS two times. The PBS was then aspirated and lysis buffer (1x RIPA buffer, 100µM phenylmethylsulfonyl fluoride (Sigma 10837091001), protease inhibitor cocktail (1 mM Benzamidine (Fluka 12072), 2.9µM Leupeptin (Sigma L9783), 5µM Antipain (Fluka 10791), 100µM EDTA (ethylenediaminetetraacetic acid)(Sigma 798681))) was added to lyse the cells and the plate was gently mixed at 4°C for 1 hour. The cells were transferred to an Eppendorf tube and the debris was pelleted by spinning at 13000 rpm for 10 minutes. The lysate was incubated with 10 nM of P1 phage or control phage for 2 hours at 4°C while rotating. Then 1µg/ml of biotinylated anti-M13 (Abcam ab17269 E1 clone) phage coat protein was added and rotation continued overnight at 4°C. Streptavidin magnetic beads (Pierce 88816) were then added to the tube and the rotation was then done at room temperature for 2 hours. The beads were washed with 0.05 % PBST three times. The samples were boiled at 90°C for 5 minutes and then loaded on an SDS-PAGE gel. The gel was transferred to nitrocellulose paper and the human anti-NRR Notch1 antibody was used to blot for Notch1.

**Peptides:** The peptides were synthesized via solid phase peptide synthesis on a tribute peptide synthesizer (Protein Technologies, Inc.). Amino acids and (2-(1H-benzotriazol-1-yl)-1,1,3,3-tetramethyluronium hexafluorophosphate

(HBTU) were purchased from Advanced Chemtech, Dimethylformamide (DMF) and methylene chloride from Fisher Scientific, and methylmorpholine and piperidine were purchased from Sigma-Aldrich. Double coupling was done on 17<sup>th</sup> amino acid leucine, based on Protein Technology's analysis. The dimer was synthesized using the Universal PEG NovaTag resin from Millipore Sigma (catalog number 855058). The Fmoc was first removed with 20% piperidine in DMF. Then the individual Fmoc-AA-OH were coupled to the resin. The n-terminus of the final valine was protected by the *t*-butyloxycarbonyl group, in place of Fmoc. Once the first monomer was synthesized on the resin, the (4-methoxyphenyl)diphenylmethyl (Mmt) protecting group was removed with 1.0 M *N*-hydroxybenzotriazole in trifluoroethanol/dichloromethane, and then the second monomer of the dimer was synthesized. The final deprotection was done with reagent R (0.2:0.3:0.5:9 anisole:1,2-ethanedithiol:thioanisole:trifluoroacetic acid). The cleaved peptide was vacuum filtered and extracted several times with ethyl ether (Fisher Scientific), and purified on a reversed-phase HPLC with a C-18 column (ZORBAX 300 eclipse xdb-c18 Agilent Technologies), using a 15-60% water/acetonitrile gradient in the presence of 0.1% trifluoroacetic acid. The resulting solution was lyophilized, and the peptide identity was confirmed using liquid chromatography/tandem mass spectrometry (Agilent Technologies).

## Chapter 3:

### *Development of antibodies to bind to multiple Amyloid Beta cleavage sites*

#### **1. Amyloid beta cascade hypothesis and cleavage targets**

Post mortem Alzheimer's Disease (AD) patients' brains are mainly characterized by two proteins -Tau and Amyloid beta ( $A\beta$ ) [154]. When Tau is hyperphosphorylated it forms tangles, while the  $A\beta$  protein aggregates into plaques [155, 156]. That  $A\beta$  plaques deposits are associated with the onset of AD has been the mainstream consensus for over a quarter of a century [157]. In both healthy and unhealthy subjects APP is cleaved either by  $\alpha$ -secretase or  $\beta$ -secretase and then is processed by  $\gamma$ - secretase [158-161]. The n-terminal fragment of the protein is released extracellularly and, in healthy patients, degraded [162]. However, in a pathological state, there is accumulation of  $A\beta$  peptides, most of them being peptides cleaved at the 40 ( $A\beta$ -40) or 42 ( $A\beta$ -42) [4, 163]. This increase in  $A\beta$  results in the accumulation of  $A\beta$  peptides into plaques, which are presumed to be the cause of neurotoxicity ( $A\beta$  cascade hypothesis) [4].

Tau tangles are formed from hyperphosphorylated tau proteins, which form unique structural twists called neurofibrillary tangles (NFTs). In human pathology NFTs are found first in the entorhinal cortex region and then is found to spread to the limbic and neocortical areas [164]. The spreading of the pathology is highly correlated with a decline in cognitive ability and other clinical symptoms of AD [165].

Historically, the AD field has focused on the  $A\beta$  cascade hypothesis as the reason to pharmacologically target plaques and protease activity, with the hope of decreasing peptide processing and the subsequent plaque



accumulation that causes neurodegeneration [4, 166]. Numerous clinical trials and studies have focused on ameliorating AD by interfering with the A $\beta$  cascade. Several avenues have been investigated, including trials with small molecules that work to inhibit different steps in the cleavage pathway of A $\beta$ , or testing with antibodies against various forms of A $\beta$  to decrease deposition [167, 168]. However, these clinical trials all ended in failure. Possible reasons for these failures include researchers' narrow interpretations of the amyloid hypothesis leading to ineffective scientific approaches (i.e. inhibiting gamma secretase alone will halt A $\beta$  production), or drug targeting focused on singular pathogenic species of A $\beta$  versus a more multiplexed approach looking at all peptides generated in this pathway [169].

A $\beta$ -40 and A $\beta$ -42 are important because initially when the plaques that were found in post mortem brains were analyzed A $\beta$ -40 and A $\beta$ -42 were found to be the predominant form of A $\beta$  [170]. It is possible that there were other forms of A $\beta$  in these samples, however researchers were unable to identify them with the current tools and technologies. The questions that we still do not have a clear answer for are, while A $\beta$ -40 and A $\beta$ -42 are the most reported peptide species, the cleavage of A $\beta$  at additional sites indicates that there may be alternative pathological cleavages of GS. Why are these other cleavage products produced at such low levels, and why are they not found in Alzheimer's patients' A $\beta$  plaques?

Recently, mass spectrometry has been used to find other forms of A $\beta$ . Studies have shown through MS analysis, multiple forms of amyloid beta peptides that exist. Takami et al. found a stepwise processing of A $\beta$  with the release of three amino acid (tripeptide) residues [105]. These tripeptide

residues are grouped into two sets of peptides that each can be from a different cleavage pathway. In one set of peptide cleavage, cleavage was found to start at the 49<sup>th</sup> position and the rest of the set of tripeptides showed cleavages at A $\beta$ -46, A $\beta$ -43, and A $\beta$ -40. The other set of tripeptides showed cleavage starting at the 48<sup>th</sup> position and then proceeding to A $\beta$ -45 and A $\beta$ -42. The mechanism of this tripeptide cleavage indicates that there may be pocket within gamma-secretase that the substrate can fit within while it gets cleaved, that is the size of a tripeptide [103]. These cleavage sites are shown in figure 20. Interestingly, many Familial Alzheimer's Disease mutations are found within this (A $\beta$ -40- A $\beta$ -49) region of APP and perhaps can contribute to the increase prevalence of Alzheimer's Disease in those patients as seen in Table 1 [171]. These A $\beta$  fragments were only seen *in vitro* via mass spectrometry, since the tools have not been developed yet that will see these fragments *in vivo* [105].

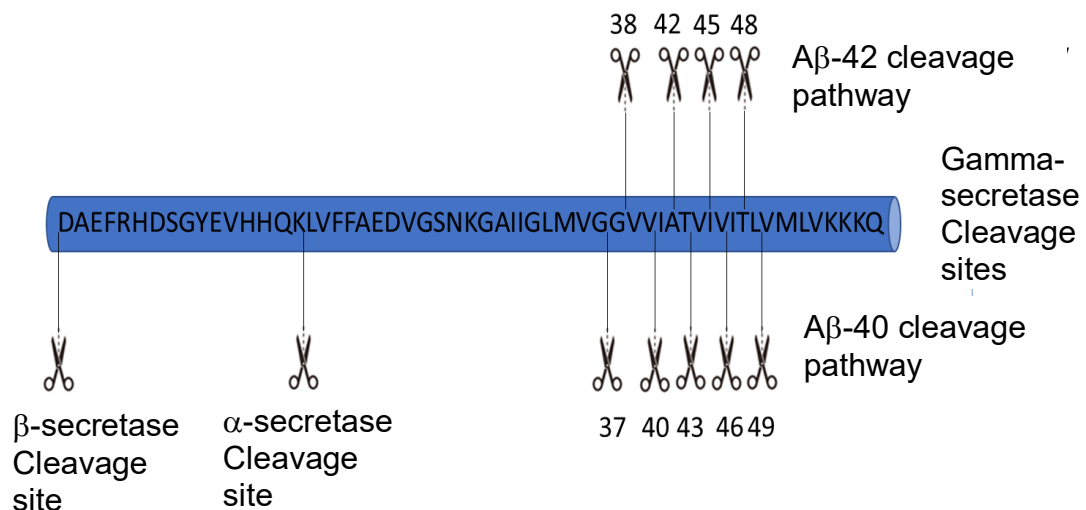


**Figure 20:** Amyloid Beta sequence that includes the  $\beta$ -secretase,  $\alpha$ -secretase, and the purported Gamma-secretase cleavage sites. The two possible cleavage pathways “A $\beta$ -40” and “A $\beta$ -42” for Gamma-secretase are illustrated, with the possible cleavage sites for each pathway noted.

Table 3: Pathologic Mutations in APP

713 (42) APP	A	T	
714 (43) APP	T	A, I	Increased A $\beta$ 42/A $\beta$ 40 ratio
715 (44) APP	V	A, M	Increased A $\beta$ 42/A $\beta$ 40 ratio.
716 (45) APP	I	F, M, T, V	Increased A $\beta$ 42/A $\beta$ 40 ratio
717 (46) APP	V	F, G, I, L	Increased A $\beta$ 42/A $\beta$ 40 ratio
719 (48) APP	T	P	

In order to further investigate and identify these differentially cleaved A $\beta$  peptides *in vivo*, we developed monoclonal antibodies for the detection of specific A $\beta$  peptides. Monoclonal antibodies, through their antigen binding site can recognize specific protein epitopes. These epitopes can be designed as an overall structure or shape that a protein folds into or it can be designed to bind a specific sequence of amino acids. Antibodies can be produced that are specific enough that the change of an amino acid at any location on the sequence can prevent the antibody from recognizing the epitope, and properly binding [172]. Ultimately, the specificity of these monoclonal antibodies should prove effective when detecting peptides *in vivo*.

## 2. Target development

First, using solid-phase peptide synthesis (SPPS) we have synthesized nine amino acid sequences for A $\beta$ -37, A $\beta$ -38, A $\beta$ -40, A $\beta$ -42, A $\beta$ -43, A $\beta$ -45, A $\beta$ -46, A $\beta$ -48, and A $\beta$ -49, which were confirmed through mass spectrometry. We chose nine amino acid fragments so that the c-terminus can be exposed, in order for antibodies to be made against the c-terminus of the peptide as opposed to other less-specific regions. The additional sequences were for fragments that were purported to be cleavage products of gamma secretase.

Antibody production requires that the introduction of a foreign species elicits an immune response in the organism. Since peptides themselves are rarely immunogenic, we synthesized the sequences with an additional cysteine at the N-terminus. Keyhole limpet Hemocyanin (KLH) is used extensively as a carrier protein due to its plentiful sites for antigen conjugation, its large size, and its ability to stimulate the immune system.

With the help of the people in the MSKCC Antibody and Bioresource core 3-month old BALB/c mice were inoculated with the proper peptide-adjuvant, and the response in the mice blood was tested via ELISA after 2 months. For each peptide we inoculated 5 mice and boosted them twice. If the signal did not titer out to less than 50% loss in signal at 1:10000 as compared to 1:100 then the mice were boosted with repeated injections of the proper peptide-adjuvant. After the mice were boosted, they were retested 2 weeks later to see if the ELISA signal strengthened. The animals were split into two cohorts with A $\beta$ -37, A $\beta$ -38, A $\beta$ -40, A $\beta$ -42, A $\beta$ -43 tested first, and the others followed in the second cohort. Several of these peptides do have antibodies available, either commercially, or otherwise, to their epitopes, and we will use those antibodies to compare to our antibodies as controls and as the current gold standard.

**a. First cohort A $\beta$ -37, A $\beta$ -38, A $\beta$ -40, A $\beta$ -42, A $\beta$ -43**

Since the epitopes for the antibodies were very similar, with some antigens differing by only one amino acid, we ran cross-reactivity ELISA assays between similar antigens (figures 21). Cross-reactivity shows non-specificity, whether the antibody being tested only recognizes its intended

target, or whether it can recognize other epitopes. In the first cohort, after injecting with peptide A $\beta$ -37 conjugated to KLH the mice produced a very low immunogenic response to A $\beta$ -37. Mice inoculated with KLH-A $\beta$ -38 also produced antibodies that were cross-reactive, but the highest signal was against the A $\beta$ -38 peptide. The blood from A $\beta$ -40 mice had a very strong signal to the A $\beta$ -40 peptide with very low cross-reactivity. This is not unexpected in that A $\beta$ -40's epitope is at least two amino acids different from the other peptides that we screened it against. Some success was found with A $\beta$ -42 injected mice, as one antibody (mouse 5) generated an antibody against A $\beta$ -42 with little cross-reactivity. Mouse 2 did recognize A $\beta$ -42 but had some cross-reactivity to A $\beta$ -43. Lastly, A $\beta$ -43 had two mice that produced antibodies to the peptide (mouse 3 and mouse 5), but both had cross-reactivity to other peptides. Mouse 3 recognized both A $\beta$ -42 and A $\beta$ -43, while mouse 5 recognized A $\beta$ -38 and A $\beta$ -43, even though the sequence overlap (position 34 to position 38 MVGG) between the peptides is low. At this point in antibody development the entire mouse sera which includes all antibodies that the mouse is making are being tested. Therefore, it is expected that some antibodies were made to other epitopes along the peptide or are not necessarily specific for one c-terminus.

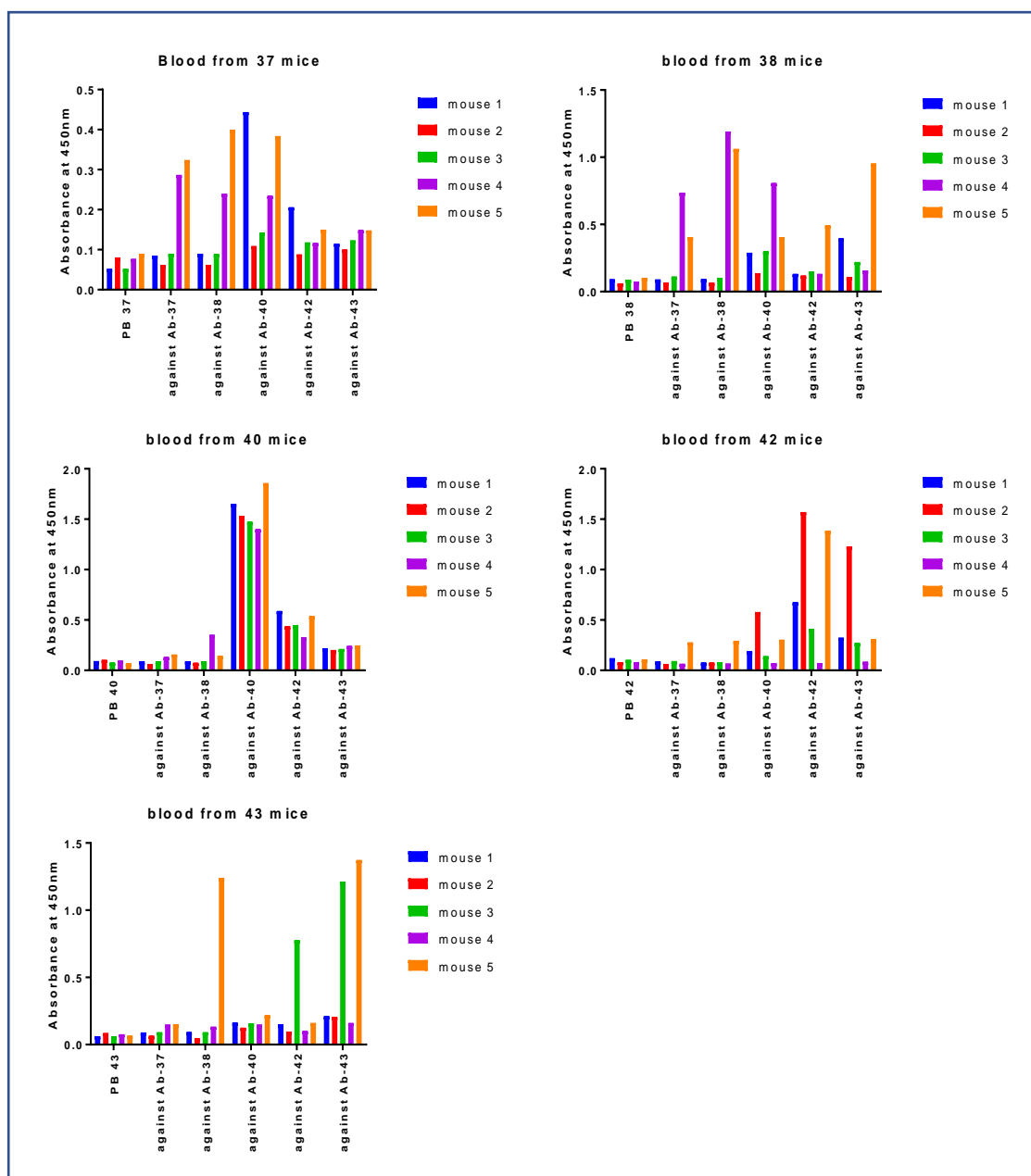


Figure 21: Signal and cross-reactivity between the inoculated mice from the peptides in the first cohort. The blood sera from all the mice in the cohort were screened against all the possible peptides in the screening library. A $\beta$ -37 mice had very low signal and lots of cross-reactivity. A $\beta$ -38 mice had signal in mice 4 and 5 but had cross-reactivity to peptides from A $\beta$ -37, A $\beta$ -40, and A $\beta$ -43. A $\beta$ -40 mice had very strong signal to the A $\beta$ -40, which they were inoculated with and low cross-reactivity. Mouse 2 and mouse 4 that were inoculated with A $\beta$ -42 had strong signal but mouse 2 cross-reacted with A $\beta$ -43. The A $\beta$ -43 mice had signal in mice 3 and 5, but mouse 5 also recognized A $\beta$ -38 and mouse A $\beta$ -43 recognized A $\beta$ -42.

After we saw a large immunogenic response, the mice were sacrificed. The persons within the MSKCC Antibody and Bioresource Core harvested their B cells, which produced the antibodies, and immortalized the B cells by fusing them with a myeloma cell line, which created a hybridoma. Once the hybridoma was generated, we prepared dilutions of the supernatant taken from the hybridoma and were screened in a similar fashion to the mice sera against the peptide of interest, as well as against the other peptides for cross-reactivity. After the initial screen was completed and the hits selected, the hybridomas from the wells were regrown and subcloned to see if the well was heterogenous or homogenous for the antibodies. Since each well that we screened can have up to six different immortalized hybridomas generating antibodies, the wells that should bind to a specific peptide were grown up diluted until one cell is plated per well. Therefore, if a heterogenous populations was in the original well when we screen at the one-cell-per-well level we will find the specific hybridoma expressing the clone of interest.

Due to the size of the cohort and the need to check for cross-reactivity, we split the cohort into two sets, A $\beta$ -38, A $\beta$ -40, and A $\beta$ -42, and A $\beta$ -37, A $\beta$ -40, A $\beta$ -43. The A $\beta$ -40 mice were part of both since the screening in the first set did not result in any specific antibodies, and in the second set we only found two specific antibodies.

We screened serial dilutions of the supernatant fluid from the hybridomas. In the first set the cross-reactivity was differentiated through serial dilutions showing signal only remained for the specific peptide. In the second set we had signal only for the specific peptide and it was repeated from supernatant over multiple days and maintained strength over several days.

This showed that the B-cell that was producing this antibody was immortalized and only recognizing the peptide of interest.

#### **i. A $\beta$ -37**

We sacrificed mouse four and mouse five for A $\beta$ -37 (peptide CGAIIGLMVG), however we were unsuccessful in recovering any specific hits from the screen. The mice's low immunogenic response to the conjugated peptide may indicate the possible causes for the low hit rate. It is possible that one or both conjugations of the peptide to the larger proteins did not occur. Either the peptide did not conjugate well to the KLH when the mice were inoculated, or to the BSA when the sera was screened, or both. Optimization is required for the generation of a sufficient immune response against these peptides, and furthermore for the development of an Ab-37 specific antibody.

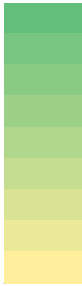
#### **ii. A $\beta$ -38 – 18A05**

From the Ab-38 (peptide CAIIGLMVGG) group of mice mouse four and mouse five were sacrificed and their B cells were immortalized. The resultant screen generated one specific clone -18a5. Table two shows the results of the ELISA screen of the B-cell supernatant for clone 18a5 against each of the peptides in the screening set. Specificity was found towards A $\beta$ -38 at dilutions ranging from 1:100 to 1:1000 when tested against the other peptides in the set (A $\beta$ -40 and A $\beta$ -42).



Table 4: ELISA results of 18A05

	18A05
A $\beta$ -38	High
A $\beta$ -40	Medium
A $\beta$ -42	Low




### iii. A $\beta$ -40 – 12F04, 11G10

Mice injected with A $\beta$ -40 (peptide CIGLMVGGVV) conjugated peptides showed high immune response and low cross-reactivity, as measured by ELISA. This response allowed for the increased probability of recovering a specific hit. When testing the generated antibodies in the first set, there was no specific hit. In the second set of screening mouse 3 and mouse 4 were sacrificed and we were able to generate to specific clones, 12F04 and 11G10. Both clones showed high specificity to A $\beta$ -40, even when prepared at a 1:10 dilution as seen in table 5.

Table 5: ELISA results of 11G10 and 12F04

	11G10		12F04
A $\beta$ -37	Low	A $\beta$ -37	Low
A $\beta$ -40	High	A $\beta$ -40	High
A $\beta$ -43	Low	A $\beta$ -43	Low




#### iv. A $\beta$ -42 – 13B8, 15G11, 27G11, 29A11, 30A2, 32A6

Mouse two and mouse five for A $\beta$ -42 (peptide CLMVGGVIA) were sacrificed. We found six highly specific clones in this screen as seen in table 6.

Table 6: ELISA results of 13B08, 27G11, 29A11, 30A02, 32A06, and 15G11

	13B08		15G11		27G11	
A $\beta$ -38		A $\beta$ -38		A $\beta$ -38		High
A $\beta$ -40		A $\beta$ -40		A $\beta$ -40		
A $\beta$ -42		A $\beta$ -42		A $\beta$ -42		
	29A11		30A02		32A06	
A $\beta$ -38		A $\beta$ -38		A $\beta$ -38		Low
A $\beta$ -40		A $\beta$ -40		A $\beta$ -40		
A $\beta$ -42		A $\beta$ -42		A $\beta$ -42		



Because A $\beta$ -42 is the most studied and considered to be the most pathogenic in AD, we decided to focus on these antibodies for further optimization. In order to show further specificity of these antibodies for the A $\beta$ -42 epitope we synthesized an amidated A $\beta$ -42 using a Rink resin. This adds an amide group to the terminal carboxylate and mimics a peptide bound. Binding to the amidated peptide would show that the c-terminus is not important for binding. We then performed an ELISA comparing the amidated and non-amidated versions of A $\beta$ -42. The majority of recovered hits, (not including 13B08) showed specificity towards site 42 indicating that a free carboxylic acid terminus is necessary in order to recognize the peptide (figure 22).

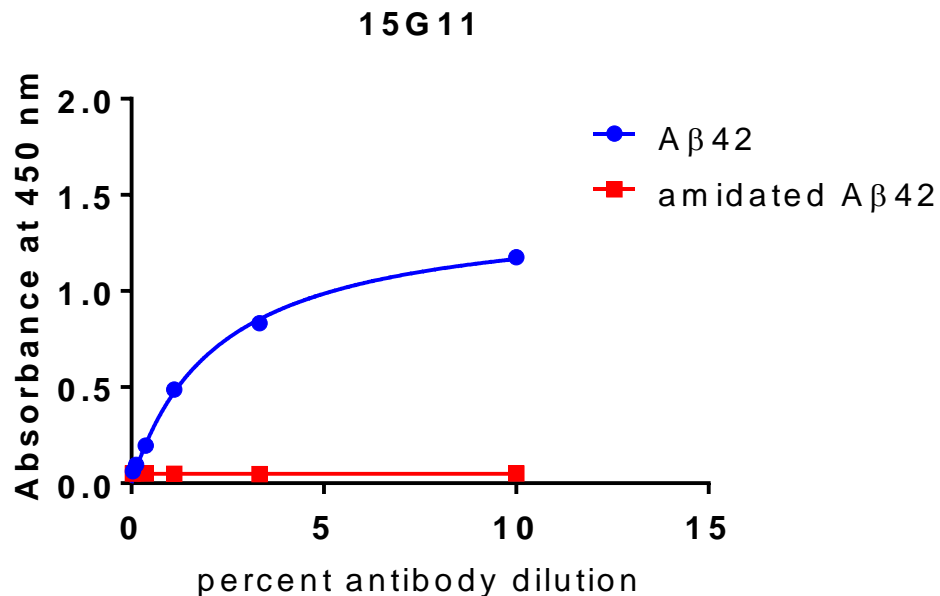


Figure 22: ELISA results comparing the A $\beta$ -42 peptide and amidated A $\beta$ -42 peptide. The red is the ELISA signal of the amidated peptide, and the blue is the signal with the regular carboxylate peptide. There is only signal with the carboxylate peptide showing that a free c-terminus is needed for recognition. 15G11 is representative of the rest of the anti-A $\beta$ -42 antibodies.

#### v. A $\beta$ -43 – 20B11

Mouse three and mouse five were sacrificed for harvesting of potential A $\beta$ -43 (peptide CMVGGVVIAT) antibodies. One successful clone, 20B1, was recovered and was able to show high specificity. The results are in table 5.

Table 7: ELISA results of 20B11

	20B11
A $\beta$ -37	Low
A $\beta$ -40	Low
A $\beta$ -43	High

High

Low

**b. Second cohort A $\beta$ -45, A $\beta$ -46, A $\beta$ -48, A $\beta$ -49**

The second cohort of mice were injected with conjugated peptides of A $\beta$ -45, A $\beta$ -46, A $\beta$ -48, and A $\beta$ -49. The bleeds from these mice were first tested for cross-reactivity against A $\beta$ -42, A $\beta$ -43, A $\beta$ -45, A $\beta$ -46, A $\beta$ -48 and A $\beta$ -49.

Unfortunately, high cross-reactivity was found for all the mice. We screened these mice in two sets A $\beta$ -45/A $\beta$ -46 and A $\beta$ -48/A $\beta$ -49. For A $\beta$ -45 we chose mouse three and mouse four, which both showed some specificity and strong signal (figure 23). For mouse A $\beta$ -46 we chose mouse two and mouse three, these showed strong signal, but not necessarily strong specificity.

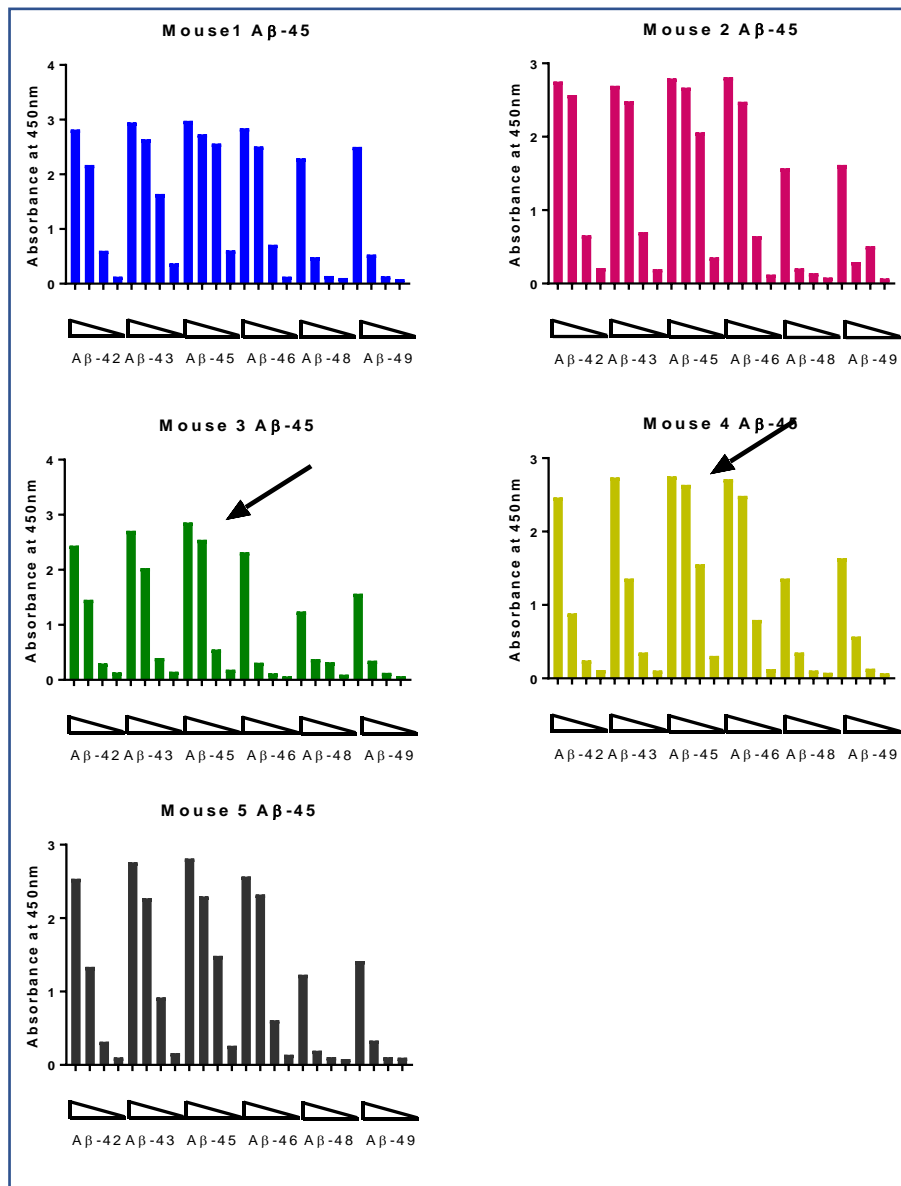


*Figure 23 Signal and cross-reactivity results of the mice that were injected with KLH-maleimide-CGGVVIATVI (Aβ-45). The mice did recognize all the rest of the peptides in the screen. We chose mice three and four which showed some specificity and strong signal.*

The mice that were initially injected with the peptides CVIATVIVIT and CIATVIVITL, A $\beta$ -48 and A $\beta$ -49, respectively, did not show any response. We reconstituted the peptide to KLH and injected a new set of mice. Again, we were unable to detect a strong immune response in the mice. The A $\beta$ -48 mice had a response after the third injection, but the A $\beta$ -49 mice did not have a very strong response even after a fourth injection. Because the signal was so low, we did not check for cross-reactivity. We immortalized the cells from mouse one and two for A $\beta$ -48 and mouse 3 and 4 for A $\beta$ -49 (figure 24).

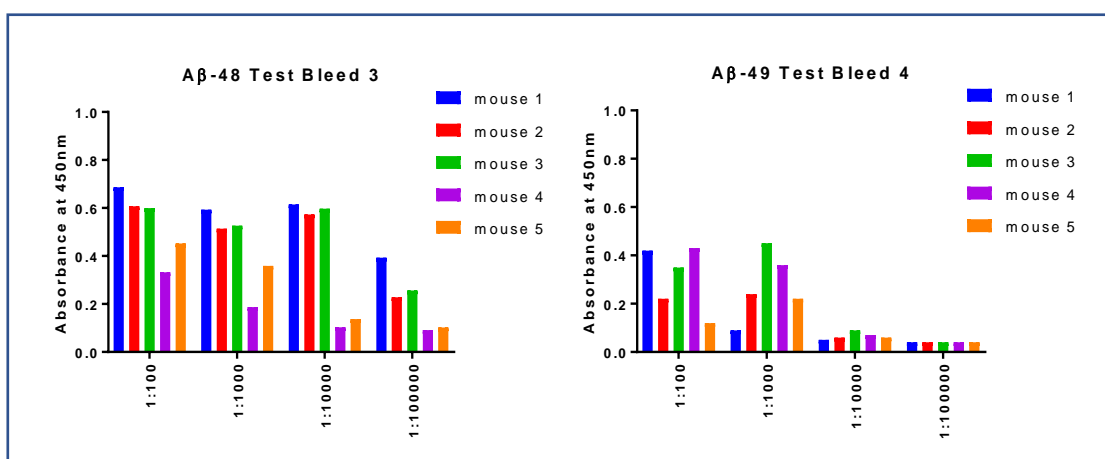


Figure 24: The signal from the mice injected with the peptides for A $\beta$ -48 and A $\beta$ -49, respectively. The signal was very low especially for A $\beta$ -49, and we did not check for cross-reactivity.

#### vi. A $\beta$ -45 – 05B01, A $\beta$ -46 – 32F09

The screening for A $\beta$ -45 and A $\beta$ -46 (peptides CGGVVIATVI and CGVVIATVIV) was done in tandem. After initially screening against A $\beta$ -45 and A $\beta$ -46 the hits were rescreened against A $\beta$ -42 and A $\beta$ -43 to show specificity. There was one hit that was specific for A $\beta$ -45 05B01 (Table 8). 32F09 was

also chosen since it showed some selectivity, even if it did not show specificity (Table 9).

*Table 8: ELISA results of 05B01*

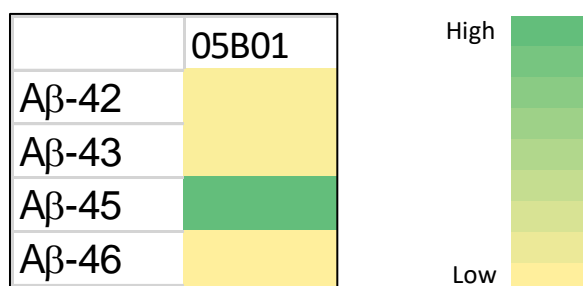
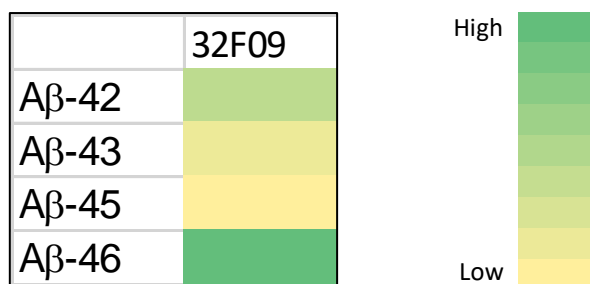


*Table 9: ELISA results of 32F09*



### **vii. A $\beta$ -48 and A $\beta$ -49**

There were no specific hits for A $\beta$ -48 (CVIATVIVIT) and A $\beta$ -49 (CIATVIVITL). Any hit that recognized A $\beta$ -48 had about the same or more recognition for A $\beta$ -49. A $\beta$ -49 hits were selective to A $\beta$ -48, but when screened against A $\beta$ -46 they lost all selectivity.

## **3. Antibody characterization**

The next step in developing the antibodies is characterizing them, including their K<sub>d</sub>, specificity, isotype, and its ability to bind in different assays. Since the maleimide-BSA has at least 20 moles of maleimide per mole of BSA it is very difficult to properly assess the K<sub>d</sub> values of the antibodies. To make proteins with exactly one binding site per protein for K<sub>d</sub> evaluations, we

inserted stop codons into the pIAD16 plasmid for CT1, which is an MBP-avitag-Amyloid Beta protein under a T7 promoter. We inserted the stop codons by using restriction-free cloning, which uses hybrid primers containing complementary sequences to both the desired insert and the target plasmid, to insert the stop codons. The stop codons were inserted for A $\beta$ -37, A $\beta$ -38, A $\beta$ -40, A $\beta$ -42, A $\beta$ -43, A $\beta$ -45, A $\beta$ -46, A $\beta$ -48, and A $\beta$ -49, as seen in figure 25.

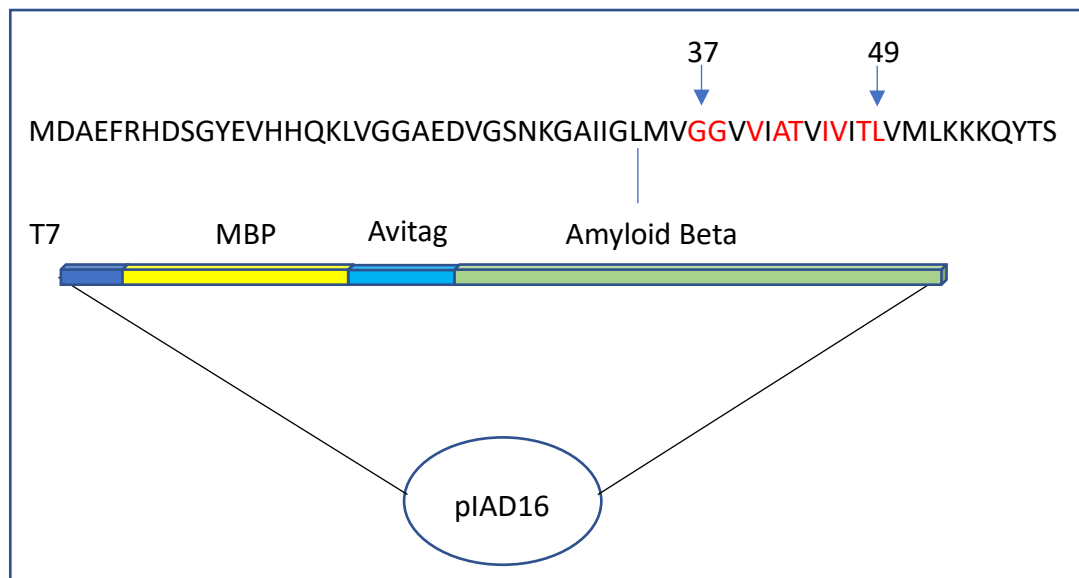


*Figure 25: MBP-protein construct with an Avitag region and amyloid beta sequence. The red amino acids are the amino acids where we put stop codons in different constructs, starting with the 37<sup>th</sup> amino acid until the 49<sup>th</sup> amino acid.*

To ascertain the Kds of the antibodies, we ran the purified proteins in an amplified luminescent proximity homogenous assay- linked immosorbent assay (AlphaLISA) [173]. AlphaLISA, is an immunological assay that is able to detect a signal with picomolar sensitivity. In the assay the analyte, is used to bring together a donor bead and an acceptor bead. A laser irradiates the donor beads at 680 nM which generates a singlet oxygen that can diffuse up to 200 nm in solution. If the acceptor bead is within this proximity, then the singlet oxygen converts a thioxene of the acceptor bead to a bridged



intermediate, which relaxes into a di-ketone derivative and emits light at 340 nm. The 340 nm light excites an electron of a chelated Europium. When that electron returns to its ground state it emits light at 680 nm [174]. The reaction is shown in figure 27 and the mechanism is in figure 26. In this case the analyte is the MBP-biotin-amyloid beta protein, which is captured by the streptavidin-coated donor beads and by either Protein-A or anti-mouse acceptor beads.

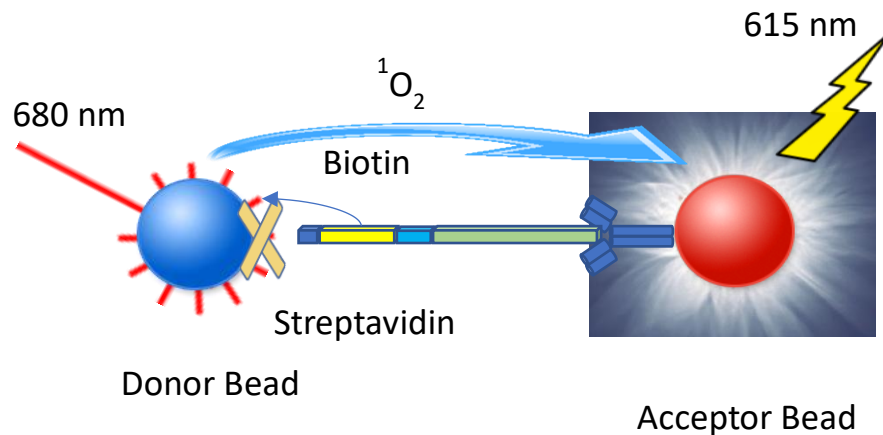


*Figure 26: AlphaLISA reaction: The donor bead is excited at 680 nm. A singlet oxygen is transferred to the acceptor bead, which emits light at 615 nm. This signal is then read by the plate reader.*

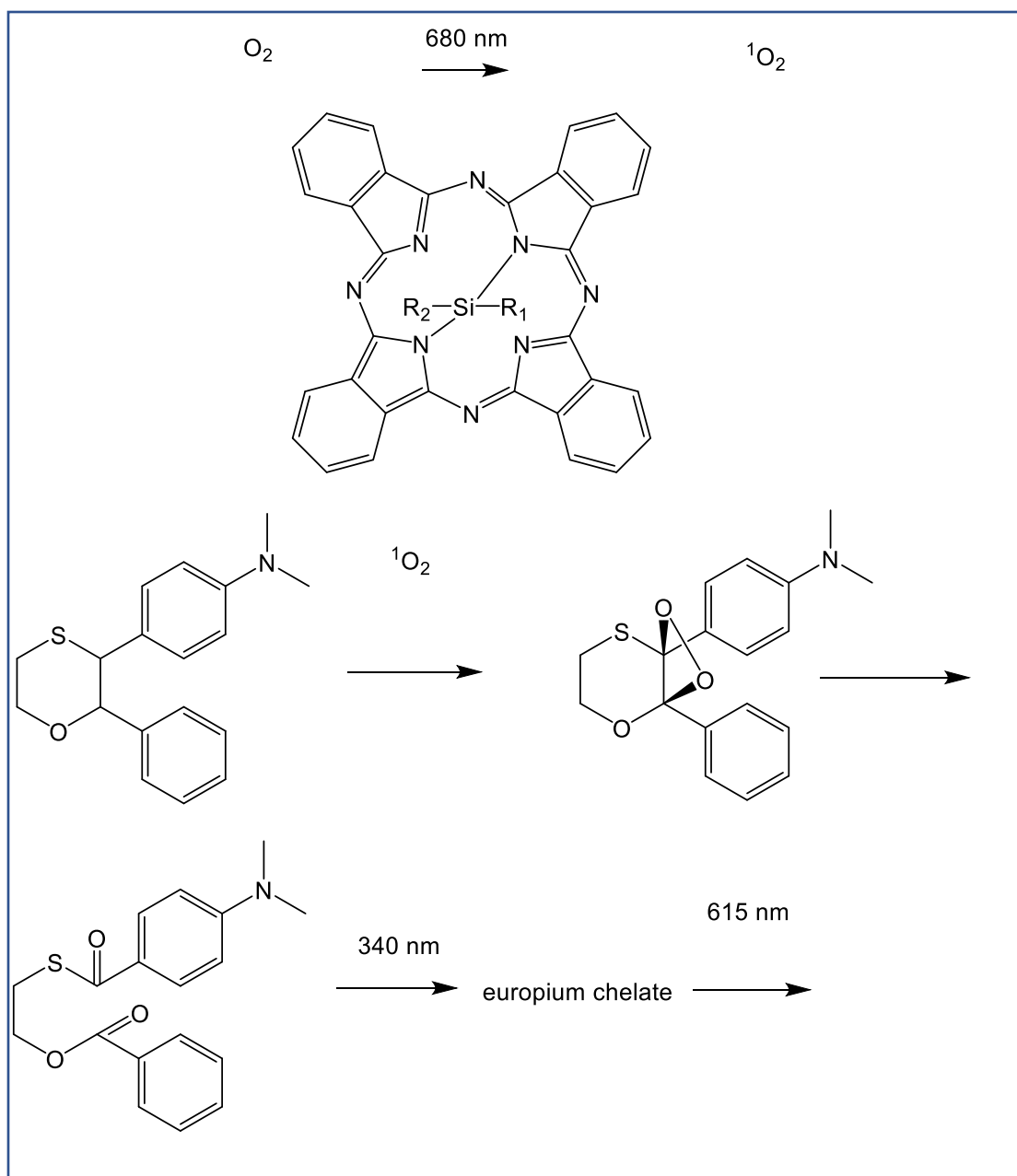


**Figure 27: Mechanism of AlphaLISA reaction.** Upon illumination at 680 nm phthalocyanine converts ambient oxygen to an excited singlet  $O_2$ . The singlet oxygen diffuses to the acceptor bead where a thioxene molecule is converted into a bridged intermediate, which then relaxes into a di-ketone. This emits light at 340 nm which excites the nearby chelated europium, which emits light at 615 nm when it relaxes, which is then read by the plate reader.

### a. Kd determination

Once we had the purified proteins, the next step was purifying the antibodies. The antibodies were grown for 1-2 weeks, and the supernatant fluid containing the generated antibodies was collected. We then purified the antibodies from this supernatant fluid and screened them against our purified MBP-avitag-peptides to confirm the antibody's specificity to the correct A $\beta$  epitope. For the screen, controls were used to confirm accurate signals, specifically G210, a commercially available A $\beta$ -40 antibody and 10G3, an A $\beta$ -42 antibody generously gifted from Pfizer. From the assay it was determined that 13B08 and 11G10 did not have a high signal, and therefore did not bind strongly. Alpha-LISA detection requires the use of acceptor beads that are able to recognize the antibody. 15G11 is not recognized well by the anti-mouse beads that we usually used. We isotypized the antibody and it is actually IgG2a [175]. The anti-mouse beads were not binding to it. Also, the 10G3 that we received from Pfizer is not an IgG1. For those proteins we used Protein A beads which recognizes all the other IgGs besides IgG1 (figure 28).

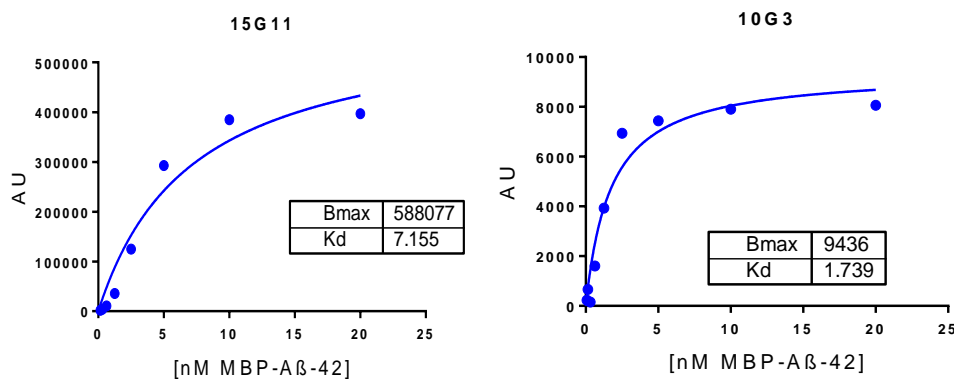


*Figure 28: Kd for 15G11 and 10G3 against A $\beta$ -42. 15G11 was our strongest antibody and 10G3 is the positive control*

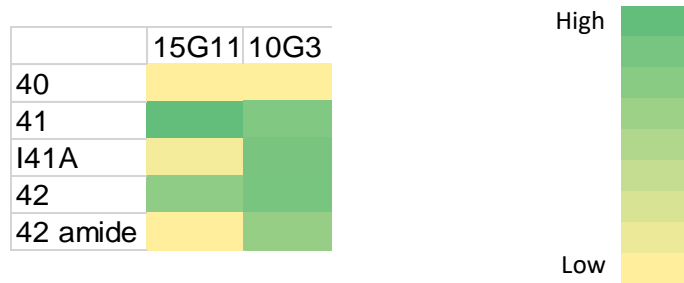
*Table 10: Table of Kd values for the antibodies. G210 is a commercial available antibody against A $\beta$ -40 and 10G3 was a gift from Pfizer. The rest of the antibodies are ones we developed.*

Target	Antibody	Kd in nM
A $\beta$ -38	18A05	2.437
A $\beta$ -40	12F04	6.888
A $\beta$ -40	G210	18.62
A $\beta$ -42	10G3	1.739
A $\beta$ -42	15G11	7.155
A $\beta$ -42	27G11	9.275
A $\beta$ -42	29A11	16.41
A $\beta$ -42	30A02	10.98
A $\beta$ -42	32A06	12.95
A $\beta$ -43	20B11	5.159

#### **b. Epitope specificity**

We continued to characterize the binding epitope of 15G11 vs. 10G3. We chose 15G11 since it had the strongest Kd. First, we synthesized peptides corresponding to A $\beta$ -41 and A $\beta$ -42 but with an alanine in the 41<sup>st</sup> position instead of an isoleucine, which we called I41A, and conjugated them to maleimide-PEG and ran an ELISA. The results in table 11 show that 10G3 is more promiscuous than thought previously. Not only does it recognize an amidated A $\beta$ -42 but it also recognizes the peptide where isoleucine is replaced by an alanine.

*Table 11: Table of  $K_d$  values for the antibodies against modified peptides (next page). 15G11 is more selective than 10G3, with regards to modified A $\beta$ -42 peptides, but both antibodies recognize A $\beta$ -41, which has not been seen to exist in vivo.*



### c. Aggregated A $\beta$ -42 recognition

Once we saw that 10G3 and 15G11 recognized different epitopes, we aggregated biotinylated-A $\beta$ <sub>1-42</sub> to see how the antibodies recognized a more physiologically relevant species [176]. First, that the biotinylated-A $\beta$ <sub>1-42</sub> aggregated was affirmed by atomic force microscopy (AFM). Then 15G11 and 10G3 were incubated with the aggregated and none aggregated biotinylated-A $\beta$ <sub>1-42</sub> to visualize binding, and hence recognition, by Alpha-LISA. 10G3 binding of the aggregated biotinylated-A $\beta$ <sub>1-42</sub> was about 5% of the binding to the non-aggregated biotinylated-A $\beta$ <sub>1-42</sub>. Whereas, binding of 15G11 was about 1% showing that 15G11 barely recognized the aggregated biotinylated-A $\beta$ <sub>1-42</sub> at all. Presumably the aggregated fibrils occluded the binding epitope of 15G11, but for 10G3, as we saw before, the antibody is not as specific and was still able to bind to the aggregate (figure 29).

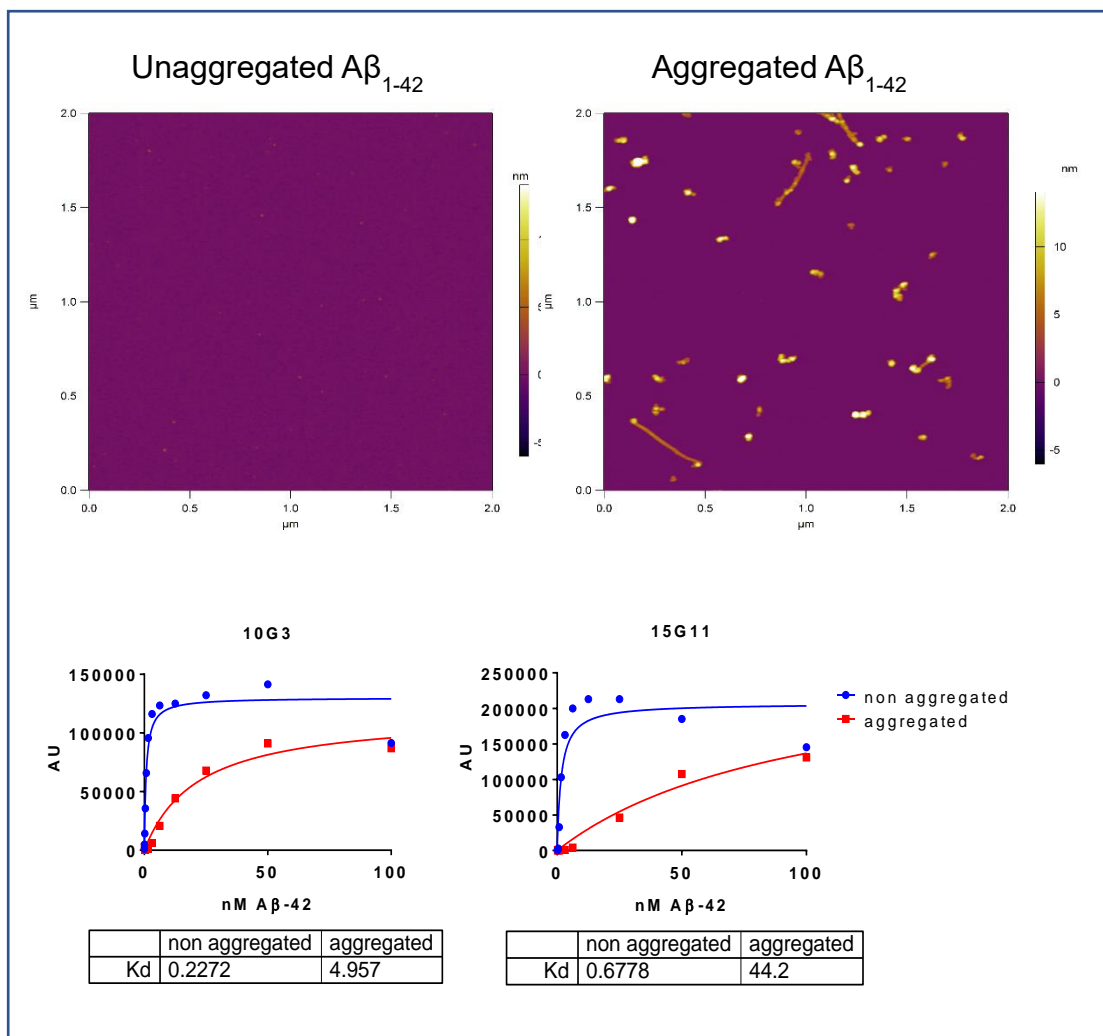


*Figure 29: Aggregated biotinylated- $A\beta_{1-42}$ . The AFM images show that biotinylated- $A\beta_{1-42}$  alone does not aggregate, but when we add HCl, aggregation is induced onto the peptides. 10G3 binding of the aggregate is about 1/20<sup>th</sup> of its binding to the non-aggregated form, but 15G11's Kd is only about 1% of the aggregates to the non-aggregated forms of biotinylated- $A\beta_{1-42}$*

#### **d. In vivo-immunohistochemical characterization**

To further characterize the binding of 15G11 versus 10G3, we employed immunohistochemistry (IHC) to see if antibody binding was successful on fixed mouse tissue. Using our 5xFAD mice, we sacrificed the mice in order to isolate their brains. 5xFAD, have five Familial Alzheimer's Disease

mutations that cause early formation of plaques (3 months) in the mice brains. Three of the mutations are in APP, KM670/671NL by the  $\beta$ -secretase site, and the I716V and V717I mutations, which are positions 45 and 46 on A $\beta$ , respectively. They also have two additional mutations M146L and L286V in presenilin [100]. In order to carry out IHC, mice were sacrificed at 12 months of age transcardially perfused with 4% PFA, before being cryo-preserved by the Histology Core. 10  $\mu$ m brains slices were then mounted on slides. Once the slides were mounted, tissue was incubated with both 15G11 and 10G3. Consistent with what we saw with our binding assay 10G3 was able to recognize the plaques in the 5xFAD brains, and 15G11 was not able to recognize the plaques as well as seen in figure 30.

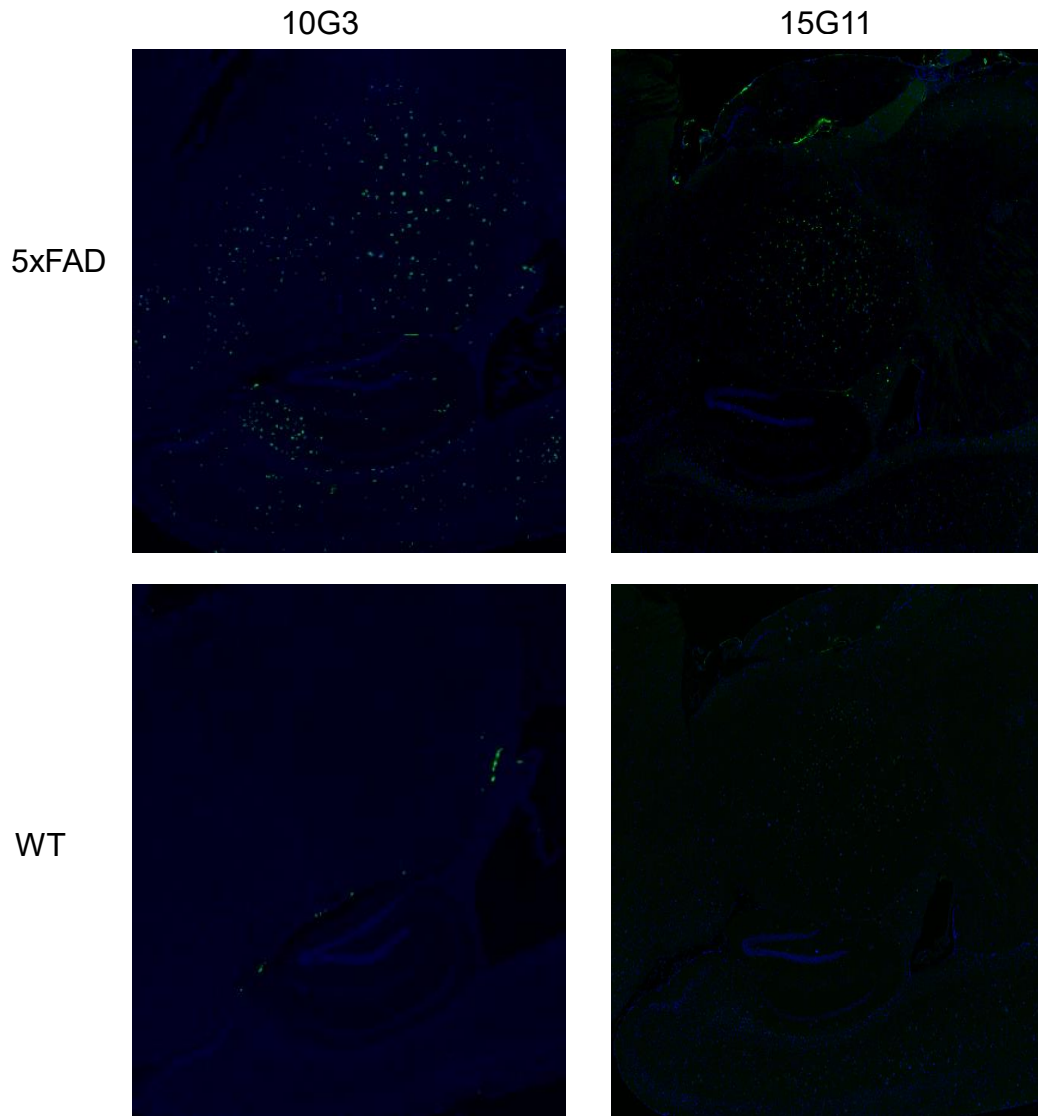


*Figure 30: 5xFAD brains and wild type brains incubated with 10G3 and 15G11 antibodies. The antibodies both were able to recognize plaques in the 5xFAD brains as opposed to the wild type brains, but 15G11's binding is much lower. Also ,15G11 saw plaques in the thalamus and not in the cortex as expected.*

#### **e. In vitro gamma secretase activity assay**

In order to quantify the ability of gamma secretase to cleave amyloid beta, our lab uses an *in vitro* assay. In this assay Hela membrane is used as a



source of gamma secretase and CT6, which is an MBP-biotin-Amyloid beta protein, as an A $\beta$  source [159]. The two are incubated together and the resulting cleavage is quantified using the Alpha-LISA assay. As seen in figure 31, 15G11 was unable to recognize cleavage occurring over the control which used JC2 as a gamma secretase inhibitor.

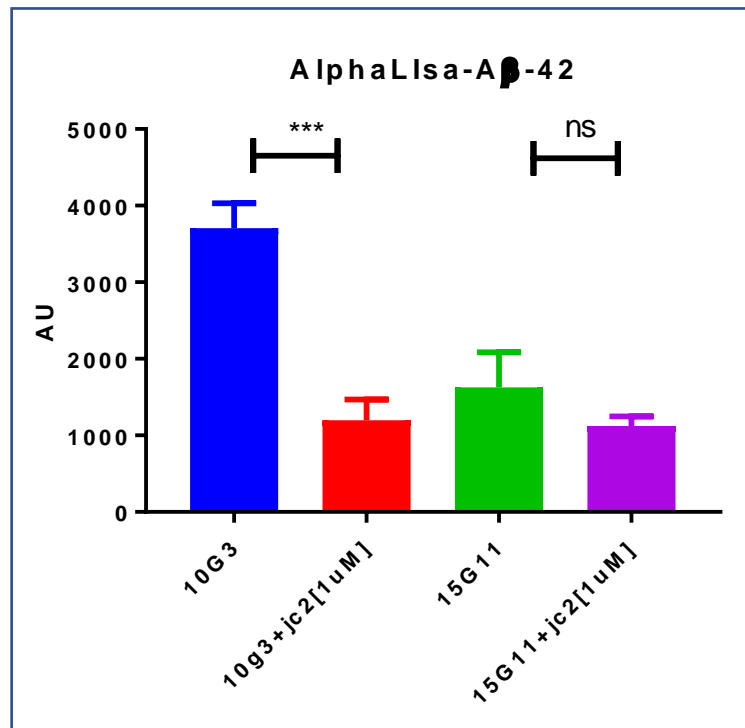


*Figure 31: Alpha-LISA assay of Hela membrane cleaving CT6. 10G3 has a signal to noise ratio of about 3, showing that we can recognize CT6 being cleaved by GS. 15G11 does not have a recognizable signal over noise. \*\*\*<p-value 0.001. ns not significant P-value.*

There are several possibilities for this occurrence. One possibility for this lack of signal is that, what is being detected by 10G3 is not a form of A $\beta$ -42 that 15G11 is able to recognize. A more likely explanation is that there is too much CT6 in the system and it is occluding the ability of 15G11 to enough

substrate to bring the donor and acceptor beads together in the Alpha-LISA assay. As seen in figure 32, spiking in (adding in CT6 to an assay right before reading the signal) one-tenth the amount of CT6 that we use in the *in vitro* assay to an Alpha-LISA assay of MBP-biotin-A $\beta$ -42 that 15G11 can recognize very strongly and give off a very high signal, blocks all signal. When other biotinylated proteins were also used, the signal was also blocked. Since other biotinylated proteins occlude the signal from the 15G11 recognizing MBP-42, it can be that the lack of signal is due to that fact that over 99% of the substrate is not cleaved and that can occlude the signal.

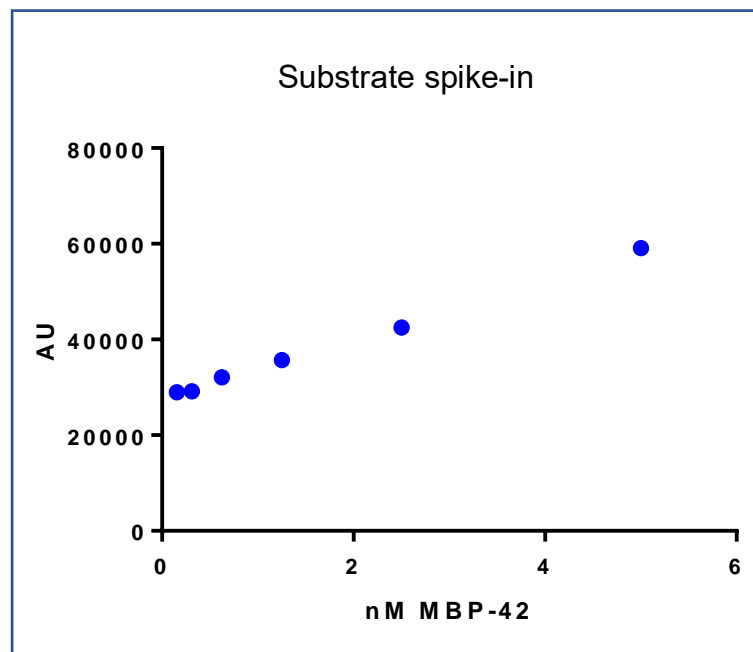


*Figure 32: CT6 spike-in blocks 15G11 signal. Spiking-in CT6 into the Alpha-LISA with MBP-biotin-A $\beta$ -42 blocks all 15G11's signal except for the highest amount of MBP-biotin-A $\beta$ -42 showing that any biotinylated protein is enough to block signal in the *in vitro* assay.*

Interestingly, we were not able to get any signal from any of our antibodies made against A $\beta$ -42, but when we compare 12F04 to G210, which are both antibodies to A $\beta$ -40, we are able to see signal, albeit 12F04 does not a signal as strong as G210 (figure 33).

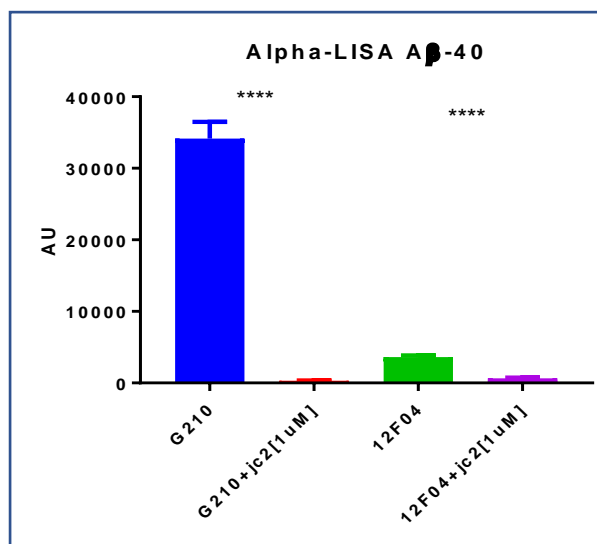
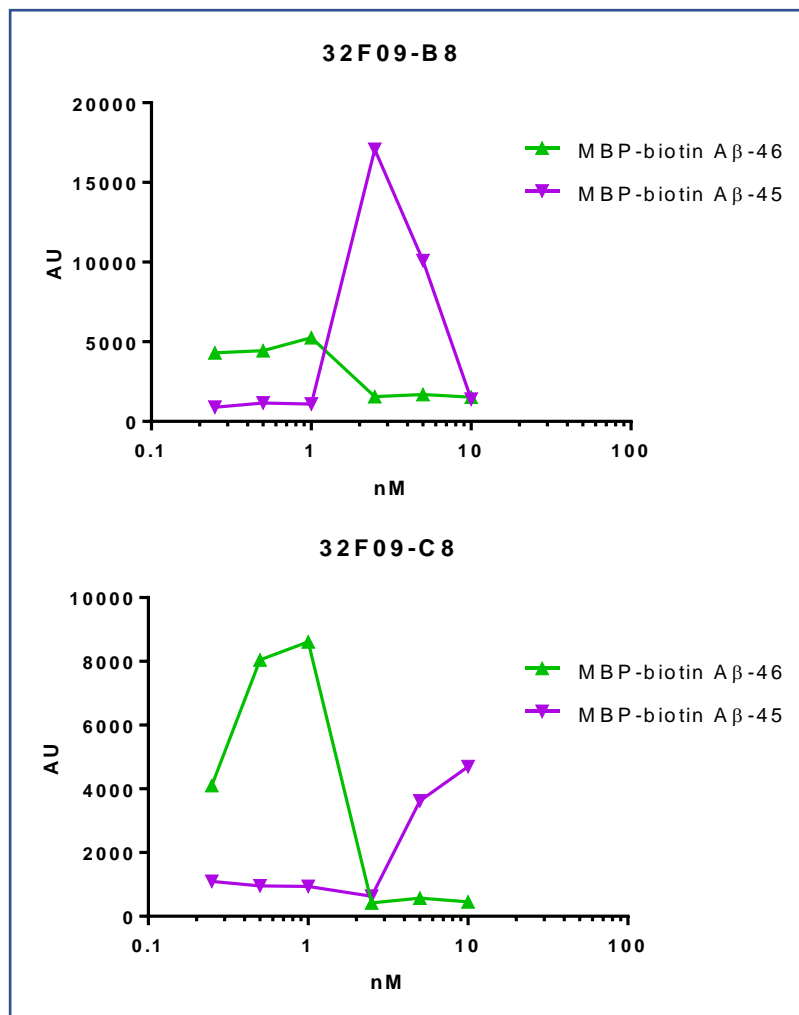


Figure 10: In vitro Alpha-LISA measuring the amount of A $\beta$ -40 generated by Gamma-secretase cleavage of CT6. G210 and 12F04 both can recognize cleaved A $\beta$ -40. \*\*\*\*<math>p</math>-value 0.0001

#### f. Kd determination and characterization of second cohort of antibodies

Once we saw the relative success of our ability to create, and characterize, antibodies for known cleavage sites of amyloid beta by gamma-secretase we pivoted to the assumed cleavage sites higher up amyloid beta. Once we found clones (05B01 and 32F09) against A $\beta$ -45 and A $\beta$ -46, respectively, we subcloned them to make sure that they were monoclonal. We then screened the supernatant of the subclones in an Alpha-LISA to determine specificity. The results were very heterogenous. We did not get any specific clones, and even clones that we did get a signal from they recognized both MBP-biotin-A $\beta$ -45 and MBP-biotin-A $\beta$ -46, albeit at different concentrations. Ostensibly at this point, we should only have one clone per well, and therefore one epitope recognized per well. Although, the subclones seem to have selectivity based on concentration, as seen in figure 34, nevertheless we

chose subclones that had trends over several concentrations showing a preference for one A $\beta$  species or another for further purification.



*Figure 11: Alpha-LISA of two subclones from 32F09 screen. The clone 32F09, at lower concentrations, shows selectivity for A $\beta$ -46, but at higher concentrations it shows selectivity for A $\beta$ -45.*

32F09, as demonstrated earlier should be selective for A $\beta$ -46, which we do see at lower concentrations for both clones depicted in figure 34. We grew them up and purified them and ran Alpha-LISAs on the purified antibody. Both clones gave us a similar signal (a representative is in figure 35), showing that they are really the same subclone from the original screen. Interestingly, the screen shows that there is a lower K<sub>d</sub> for the clone to bind to MBP-A $\beta$ -46, as

opposed to MBP-A $\beta$ -45, nevertheless the Ab-46 signal seems to max-out and we get a higher signal from MBP-A $\beta$ -45. This recapitulates a shift in the specificity at different concentrations.

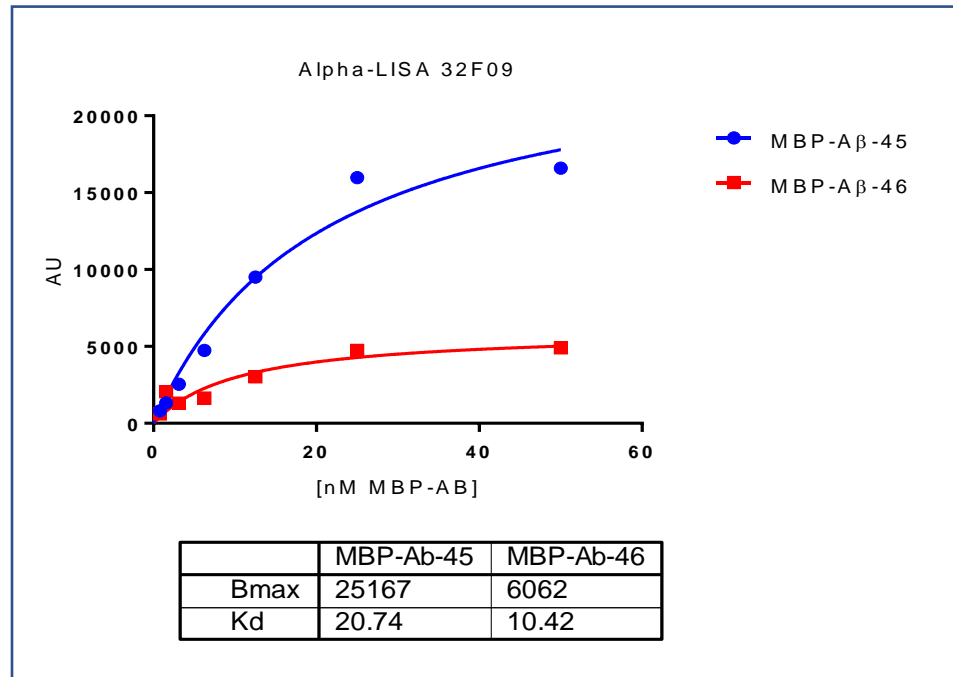


*Figure 12: The Alpha-LISA of 32F09 against MBP-A $\beta$ -45 and MBP-A $\beta$ -46. The antibody does recognize both epitopes of A $\beta$ -45 and A $\beta$ -46, even though based on the initial ELISA screen it should only recognize A $\beta$ -46. It does have a slightly lower Kd for A $\beta$ -46.*

The other clone that we found 05B01, which from the sera screen should shows some selectivity towards A $\beta$ -45, the purified antibody only shows a slight selectivity towards it (figure 36).

Now that we had these antibodies and we showed that they both had selectivity towards Ab-45 over Ab-46 we performed a HELA Alpha-LISA to see how much of Ab-45/Ab-46 can be detected by the antibodies. The results are in figure 37 for 32F09, but 05B01 had a similar result, which show that we had no signal above background.

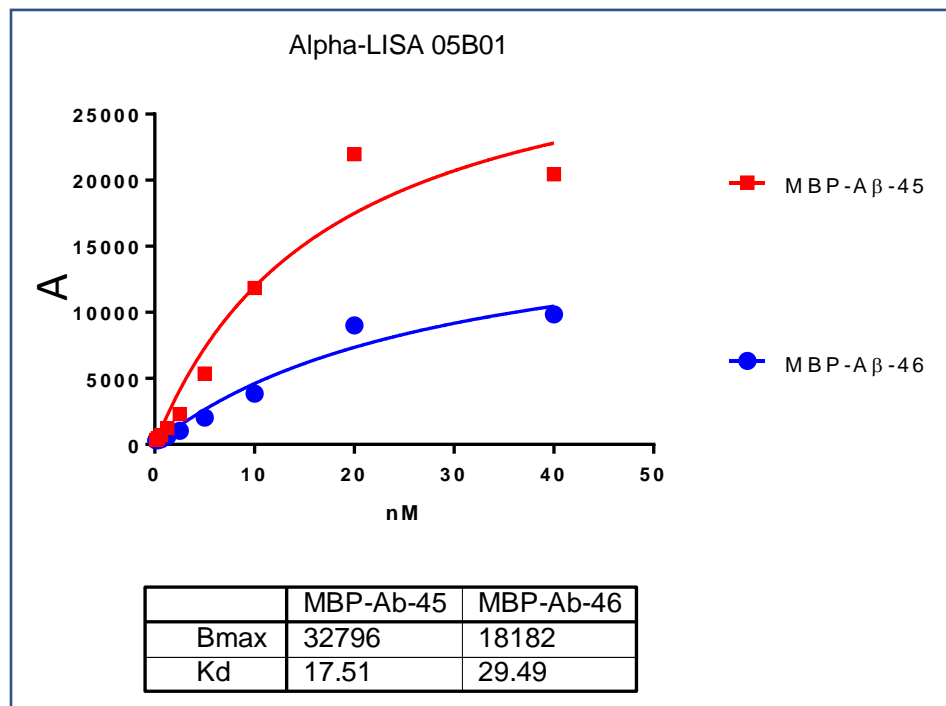


Figure 36: Second selective clone found in the A $\beta$ -45 and A $\beta$ -46 screen. As was seen in the ELISA, there is a slight selection towards A $\beta$ -45

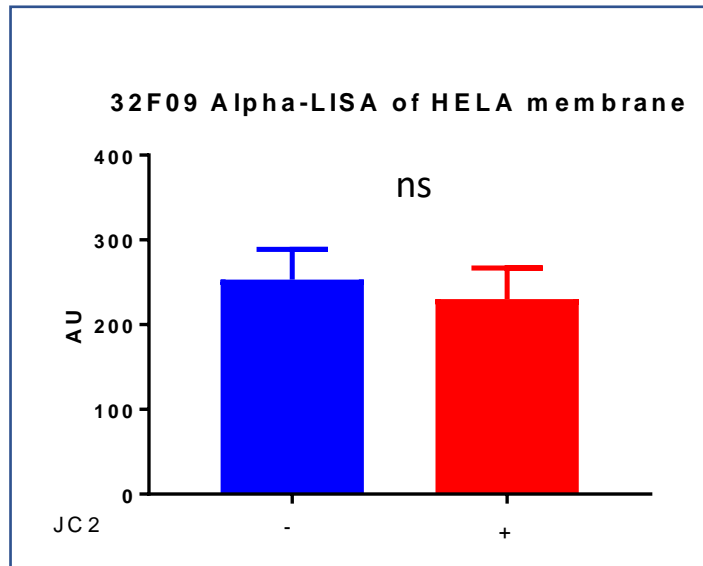


Figure 37: Alpha-LISA of HELA cleavage of CT6 detected by 32F09. There was no cleavage of CT6 that was detected by the 32F09.

In addition, when we screened the two antibodies against the group of MBP-A $\beta$  proteins a different picture emerges, and it does not seem that these

antibodies are as selective as we would have hoped (figure 38). Even with the increased in range of epitopes that the antibodies are able to recognize, we still did not see any signal.

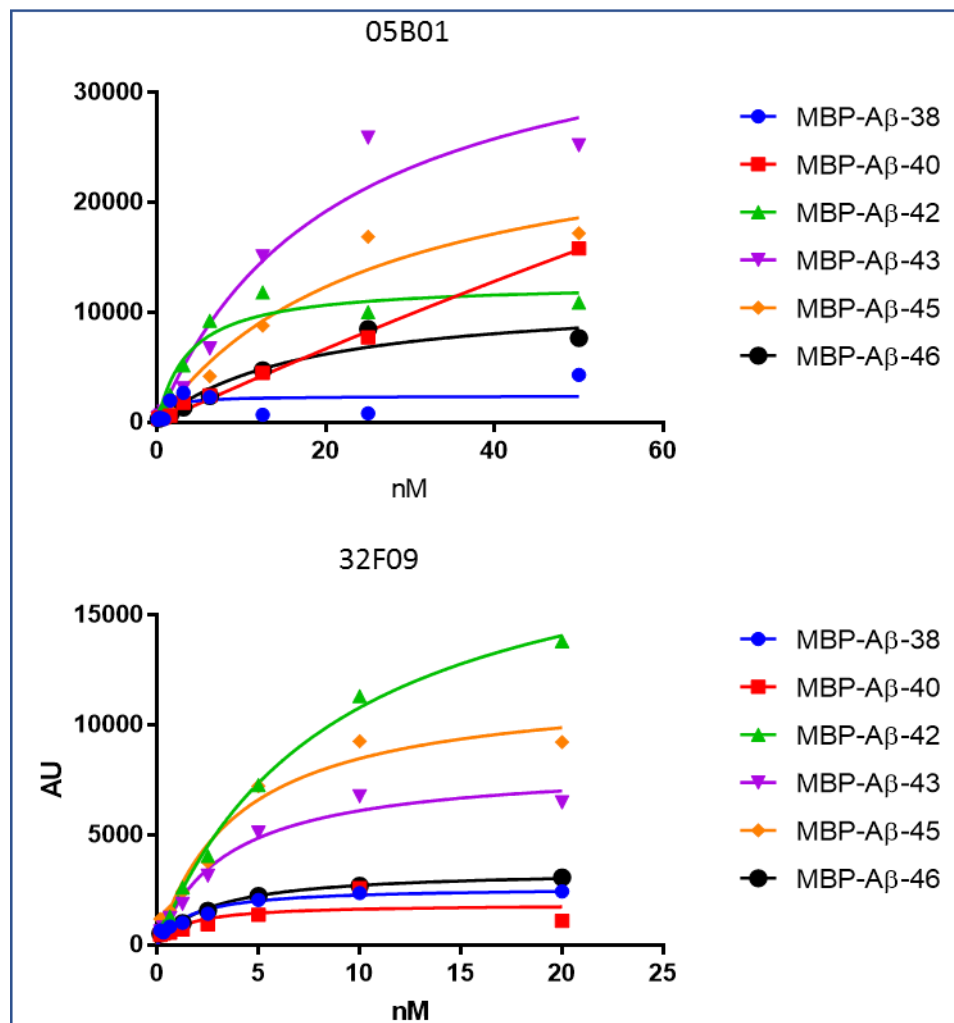


Figure 38: Screening 05B01 and 32F09 against the group of MBP-Aβ proteins. When the two hits that were selective for Aβ-45 were rescreened against an enlarged group of MBP-Aβ proteins, we do see the recapitulation of the selectivity of Aβ-45 vs. Aβ-46, but those are not the only epitopes that the antibodies recognize.

#### 4. Conclusion

We were successful in generating the antibodies towards several epitopes of interest. Nevertheless, after antibody characterization, only 12F04 was able to work in the Alpha-LISA screen. It is assumed that at most 1% of all CT6 is cleaved by gamma secretase in the Hela Alpha-LISA. If so, as demonstrated with spiking-in CT6, our antibodies would not be able to detect any signal. As a modality to detect the cleavages of A $\beta$  that are currently undetectable, antibodies will be very successful, and the antibodies discovered here, should be able to help.

The next step is to figure out how to modify the Hela Alpha-LISA to detect the higher order species (A $\beta$ -43 – A $\beta$ - 49). It is possible that longer incubation times are needed to be able to detect higher-order species because they are quickly cleaved down to lower-order species (A $\beta$ -40 and A $\beta$ -42) and only in time, perhaps with a feedback inhibition loop, is there a buildup of higher order species that will be detectable. It could also, be that there is never a feedback inhibition of GS cleaving from the higher-order species to lower-order species and only short incubation times can be used to find these Ab species.

These antibodies can be useful both as a tool and hopefully further down the line as a therapeutic agent. They are used to detect the cleavages sites of these specific A $\beta$  species *in vitro*. Once specificity is optimized, they will be used to detect A $\beta$  species *in vivo*. Later, their use will be helpful in imaging to perhaps show an increase or a decrease in Alzheimer's Disease models and eventually patients. Finally, they can be as a therapeutic agent. Similar to how the A $\beta$  antibodies are being used now, to bind to plaques, either to prevent plaque growth, as carrier proteins to bring a therapy to the plaques,



or for macrophage detection of plaques and subsequent engulfment of plaques. The current antibodies are directed against the wrong epitopes, which leaves a broad field for the antibodies discovered here.

## **5. Materials and Methods**

**Peptide development and injection:** The peptides were synthesized via solid phase peptide synthesis on a tribute peptide synthesizer (Protein Technologies, Inc.). Amino acids and (2-(1H-benzotriazol-1-yl)-1,1,3,3-tetramethyluronium hexafluorophosphate (HBTU) were purchased from Advanced Chemtech, Dimethylformamide (DMF) and methylene chloride from Fisher Scientific, and methylmorpholine and piperidine were purchased from Sigma-Aldrich. Using maleimide activated KLH (Imject™ Maleimide PEGlyated mCKLH item 77663) we conjugated the N-terminus to the protein via the cysteine, in conjugation buffer. The c-terminus, where the major differences between peptide exists, was then available to be recognized by the immune system.

**Rink resin:** Coupling to the resin is the same, but decoupling, since the resin is extremely acid-labile, is done using only 10% TFA in DCM (dichloromethane). The resin shakes in 10% TFA in DCM for 1 hour and then vacuum filtered in to a glass flask. The resin is washed with 5% TFA in DCM 2 more times. The peptide in TFA/DCM is removed under reduced pressure and the side chains are then cleaved in the usual manner.

**ELISA:** To perform the ELISA, first, we conjugated the peptide to maleimide-BSA in a similar fashion to the KLH (Imject™ Maleimide-Activated BSA 77116). Using MaxiSorb plates we coated each well with 50 ng/well and either the plate was left in 4°C overnight or 37° for an hour. The wells were washed 3

times with 0.5% PBST (was buffer). Next, the wells were blocked with 1% BSA in was buffer (blocking buffer) for an hour. Afterwards they were washed again with wash buffer and then the blood of the inoculated mice was diluted in blocking buffer starting at 1:100 down to 1:100000. Then the wells were washed 3 more times with wash buffer and then incubated with Jackson Immuno research (item 115-035-003) peroxidase affinityPure Goat Anti-Mouse IgG (H+L) diluted 1:3000 in blocking buffer for 40 minutes. Then one last set of 4 washes. Lastly, 50ul of TMB substrate (fisher nc038303) was added for 10 minutes to each well, and the reaction was stopped with 50 ul of 1M H<sub>2</sub>SO<sub>4</sub>.

**Antibody purification:** Once the antibodies showed specificity, the antibodies were purified by growing large amounts of cells and pooling the supernatant until we had about 400 mls. We purified the antibodies using Hi Trap Protein G columns (GE item 29-04850-81) at 4°C. The antibody supernatant was also diluted 1:2 in binding buffer (0.02 M sodium phosphate, pH 7.0). Using a peristaltic pump 5 columns of binding buffer flowed through the column as 1 ml/min. Then the diluted antibody supernatant also flowed through the column at 1 ml/min. Once the antibody was loaded onto the column, 10 column volumes of binding buffer were used to wash off anything that did not bind to the protein G. Then, to break the affinity between the protein G column media and the antibody we used a low pH elution buffer (0.1 M glycine-HCl, pH 2.7), but to preserve the activity of the acid-labile antibody the tubes had 100 uls of neutralizing buffer (1 M Tris-HCl, pH 9.0). The purified antibody was then buffer exchanged into 20 mM sodium acetate pH 5.5, with 0.02% sodium azide. The concentration was determined at absorbance at 280 with an extinction coefficient of 210,000M<sup>-1</sup>cm<sup>-1</sup>.

**Restriction-free cloning:** In this method a primer is designed half that is a complementary sequence overlap with the insertion site on the CT1 half with the target plasmid. First the primers are used to amplify the insert using regular PCR. The resulting primer is known as a “mega-primer” and is used in a second PCR reaction with CT1. The mega primer inserts the stop codon by the insertion site. Then we use Dpn1 to break up the parental DNA.

*Table 12: Primers for MBP-A $\beta$  species*

Primer name	Primer sequence
A $\beta$ -49_F	GTGATCGTCATCACCTTG TAGTAGAAGCTTGCGGCC
A $\beta$ -49_R	GGCCGCAAGCTTCTACTA CAAGGTGATGACGATCAC
A $\beta$ -48_F	ACAGTGATCGTCATCAC TAGTAGAAGCTTGCGGCC
A $\beta$ -48_R	GGCCGCAAGCTTCTACTA GGTGATGACGATCACTGT
A $\beta$ -46	ATAGCGACAGTGATCGTC TAGTAGAAGCTTGCGGCC
A $\beta$ -46_R	GGCCGCAAGCTTCTACTA GACGATCACTGTGCTAT
A $\beta$ -45	GTCATAGCGACAGTGATCTAGTAGAAGCTTGCGGCC
A $\beta$ -45_R	GGCCGCAAGCTTCTACTA GATCACTGTGCTATGAC
A $\beta$ -43	GGTGTTGTCATAGCGACATAGTAGAAGCTTGCGGCC
A $\beta$ -43_R	GGCCGCAAGCTTCTACTA TGTCGCTATGACAACACC
A $\beta$ -42	GGCGGTGTTGTCATAGCGTAGTAGAAGCTTGCGGCC
A $\beta$ -42_R	GGCCGCAAGCTTCTACTA CGCTATGACAACACCGCC
A $\beta$ -40	ATGGTGGGCGGTGTTGTC TAGTAGAAGCTTGCGGCC
A $\beta$ -40_R	GGCCGCAAGCTTCTACTA GACAACACCGCCACCAT
A $\beta$ -38	GGACTCATGGTGGGCGGT TAGTAGAAGCTTGCGGCC
A $\beta$ -38_R	GGCCGCAAGCTTCTACTA ACCGCCCACCATGAGTCC
A $\beta$ -37	ATTGGACTCATGGTGGGC TAGTAGAAGCTTGCGGCC
A $\beta$ -37_R	GGCCGCAAGCTTCTACTA GCCCACCATGAGTCCAAT

**MBP-peptide:** The proteins were made in BL21 competent cells. 25 ng of the plasmid was added with 25 ng of the BirA (biotin ligase) were added to the BL21 competent cells. The mixture was placed on ice for 30 minutes. Then for the DNA to be able to enter the cells, the BL21s were heat shocked at 42°C for 15 seconds and placed on ice for 30 minutes. 450 ul of SOC was added and then the cells shook at 37°C for 60 minutes. 50 uls of the cells were plated

on Kanamycin (for MBP plasmid) and Chloramphenicol (BirA) selection. The colony was picked and grown in 25 mls of LB overnight. The overnight culture is then poured into 2 liters of LB with the appropriate antibiotics and shaken until OD 600 is 0.6. Then 0.1 mM IPTG (**Isopropyl  $\beta$ -D-thiogalactoside**) (**Sigma I6758**) and 50  $\mu$ M of biotin (**Sigma B4501**). LB was grown for 5 hours and then centrifuged at 5000g for 40 minutes at 4°C. The supernatant was poured off and the cells were frozen overnight at -80°C. The cells were resuspended in buffer A (20 mM Tris base, 200 mM NaCl, pH 7.4) and 100 $\mu$ M phenylmethylsulfonyl fluoride (Sigma 10837091001), and protease inhibitor cocktail (1 mM Benzamidine (Fluka 12072), 2.9 $\mu$ M Leupeptin (Sigma L9783), 5 $\mu$ M Antipain (Fluka 10791), 100 $\mu$ M EDTA (ethylenediaminetetraacetic acid) (Sigma 798681))). The cell solution was then lysed by French Press (Spectronic Instruments). The lysed cells were then centrifuged at 15000 rpm for 40 minutes at 4°C to pellet the debris. The supernatant was transferred to a superloop and purified on an Acta prime with a maltose column. The fractions were run on a gel and then the protein concentration was visualized using InstaBlue (Fisher ISB1L). The fractions with the pure protein were concentrated (usually fractions 18-26) and protein concentration was determined at absorbance at 280.

**Isotyping Antibodies:** Antibodies were diluted at 0.5  $\mu$ g in PBS. 150  $\mu$ l of the diluted antibodies was put into the development tube and one Isostrip (Sigma 11493027001) black end at the bottom into each of the development tubes. The positive bands appear after 5-10 minutes.

**Hela Alpha-LISA:** Hela (S3) cell pellet (mid-log) for membrane preparation was purchased from Biovest. The frozen pellet was resuspended in 1X MES

buffer (50 mM MES, pH 6.0, 5 mM MgCl<sub>2</sub>, 5mM CaCl<sub>2</sub>, and 150 mM KCl) containing 100μM phenylmethylsulfonyl fluoride (Sigma 10837091001), and protease inhibitor cocktail (1 mM Benzamidine (Fluka 12072), 2.9μM Leupeptin (Sigma L9783), 5μM Antipain (Fluka 10791), 100μM EDTA (ethylenediaminetetracaacetic acid) (Sigma 798681))) and lysed by French Press (Spectronic Instruments). Cell debris and nuclei were removed by centrifugation at 800g for 10 min. Supernatants were collected and centrifuged at 100,000g for 60 minutes. The resulting pellet was resuspended in MES buffer and stored at -80°C.

The gamma secretase in Hela membrane was incubated with biotinylated substrate (CT6) at 1 μM in the presence of 0.25% CHAPSO (**3-([3-Cholamidopropyl]dimethylammonio)-2-hydroxy-1-propanesulfonate) (Sigma C3659)** and **PIPES buffer** (50 mM PIPES, pH 7.0, 5 mM MgCl<sub>2</sub>, 5mM CaCl<sub>2</sub>, and 150 mM KCl) for 3 hours at 37°C. Afterwards the antibodies are incubated with the Hela membrane incubated solution with streptavidin-conjugated donor beads (40 μg/ml Perkin Elmer 6760002) and with Protein-A or anti-mouse acceptor beads (10 μg/ml Perkin Elmer AL101M and AL105M) overnight. The Alpha signal is read on an envision plate reader (Perkin Elmer)

**Aggregating Aβ<sub>1-42</sub>:** Biotinylated-Aβ<sub>1-42</sub> (Anaspec as23523-05) was dissolved in DMSO to a 5 mM concentration. 10mM of HCl was added to an end concentration of 100 uM Aβ<sub>1-42</sub>. The sample was vortexed for 15s and then incubated at 37°C for 24 hours. After 24 hours 2 uls of aggregated and non-aggregated Aβ<sub>1-42</sub>

**AFM:** Fluid Imaging was acquired using a MFP-3D-BIO AFM (Asylum Research), with an Olympus BL-AC40TS AFM probe (Asylum Research) in

tapping mode. Probes were tuned using an Auto Thermal method. The scanning was done in air.

**FIXING OF BRAINS:** Mice at 12 months of age underwent intracardiac perfusion with 4% paraformaldehyde while under ketamine/xylazine anesthesia. The head was dislocated, and the brain was removed and cryopreserved by the Histology core. The brain was sliced at 10  $\mu\text{m}$  sections.

## Chapter 4:

### *Conclusions and Implications of this Thesis*

GS is a very complex protein, and presumably a heavily regulated enzyme [1, 177]. This regulation is needed due to its large library of substrates which often overlap in their expression, and particularly since many of the substrates are integral for proper cell function [9]. Unregulated cleavage by GS can lead to various disease states [178].

In general, GS cannot be inhibited without causing off-target toxicities [107, 179, 180]. Research has shown that, to successfully inhibit GS, would be to interfere with the mechanism for GS recognition and cleavage of individual substrates. For example, one method that gamma-secretase modulators use to interfere with the cleavage of substrates by GS is by acting as allosteric inhibitors [181, 182]. Assuming, that one mechanism that GS demonstrates specificity is by adopting a specific conformation for a specific substrate, then interfering with the ability of GS to adopt that conformation would effectively inhibit GS safely. Another method of inhibition would be to interfere with the proteins that bind to GS like Hif1 $\alpha$ , which activates Notch signaling in breast cancer models [15, 183].

But a more successful modulation of GS cleavage can be achieved by altering substrate specific cleavage rather than interfering with overall enzymatic ability. In this thesis, we focus on two modalities to study and modulate GS cleavage. These modalities rely on specificity and focuses on the substrate and not on the enzyme. In one system, a peptide is used, and it interferes with Notch1 signaling, but not the other Notch proteins that are closely related. In the other system, antibodies were developed to multiple

cleavage sites of Amyloid beta with a possible use to monitor how small molecules can affect GS's cleavage of Amyloid beta.

The demonstration that dVGG interferes with Notch1 cleavage still leaves many questions unanswered. What amino acids are required for the specific binding to occur along the twenty-amino acid peptide, and can the sequence be optimized for an even better result? The interference was shown in a Notch reporter system since the Notch Intracellular Domain was replaced with Gal4. What happens in a regular Notch system, where feedback mechanisms are in place? When cleavage of Notch1 is inhibited, does that mean that there is increased cleavage of other Notch proteins to compensate?

Also, a more direct question is how P1 phage and dVGG modulate Notch1 signaling? It is possible that a conformational change is occurring on Notch1 that makes S2 cleavage less likely to occur and therefore resulting in less signaling [184]. It could also be binding along Notch1, perhaps around EGF11-EGF13 region, and interfering with how the ligand is binding to Notch1, and therefore less signaling is being transduced [28]. Using photoreactive crosslinkers in the peptide, we can use LC-MS to show binding of the peptide to Notch1. Where dVGG binds along Notch1 would help determine its mechanism of modulating Notch signaling [185].

In the second part of this thesis, antibodies were developed to specific cleavage sites of Amyloid Beta. We were not yet successful in developing antibodies that were specific for A $\beta$ -45, A $\beta$ -46, A $\beta$ -48 and A $\beta$ -49, but these cleavage sites should be monitored for the multiple avenues of therapeutic potential that they can open up. They can be used to screen for other molecules that modulate how GS cleaves different parts of Amyloid Beta.



Second, the antibodies can possibly be used themselves as diagnostics to identify biomarkers in body fluids for the diagnosis of patients [104]. Third, depending on what epitopes are exposed on the surface of the plaque, they can be used to target plaques either for degradation by macrophage or to be used as a carrier protein to transport therapeutics, like  $\alpha$ -particles, to degrade the plaques [186].

Our failure to find antibodies specific for A $\beta$ -45, A $\beta$ -46, A $\beta$ -48 and A $\beta$ -49 is that we did not screen enough clones. For each of these peptides we only screened 30 plates of roughly 400 clones per plate (there are multiple clones per well), and we are looking for the one specific clone. Amino acid 44 is valine, 45 is isoleucine, and 46 is valine again showing that the antibody that we would want needs to be extremely specific. Also, this explains the hit rate that we had with Ab-49, which is leucine, that also recognized Ab-46 (valine).

The development of therapeutics for Alzheimer's Disease is an extremely difficult task as evident by the amount of ideas that have failed at various stages of clinical trials [187, 188]. Initially, many of these ideas focused on a small selection of targets (A $\beta$ -40 and A $\beta$ -42) or a ratio of these targets (the ratio of A $\beta$ -42/A $\beta$ -40) and focuses on GS cleavage products, but since then the Alzheimer's Disease field have moved to focus on other portions of the APP cleavage pathway [189, 190]. Some of these ideas require new tools to be created, but that should not prevent those ideas from being developed. This is a fertile ground for both tool development and therapeutic potential in a specific manner to perhaps finally develop an Alzheimer's Disease cure.

## REFERENCES

1. Kimberly, W.T., et al., *Gamma-secretase is a membrane protein complex comprised of presenilin, nicastrin, Aph-1, and Pen-2*. Proc Natl Acad Sci U S A, 2003. **100**(11): p. 6382-7.
2. Lichtenthaler, S.F., et al., *Mechanism of the cleavage specificity of Alzheimer's disease gamma-secretase identified by phenylalanine-scanning mutagenesis of the transmembrane domain of the amyloid precursor protein*. Proc Natl Acad Sci U S A, 1999. **96**(6): p. 3053-8.
3. Annaert, W.G., et al., *Presenilin 1 controls gamma-secretase processing of amyloid precursor protein in pre-golgi compartments of hippocampal neurons*. J Cell Biol, 1999. **147**(2): p. 277-94.
4. Hardy, J.A. and G.A. Higgins, *Alzheimer's disease: the amyloid cascade hypothesis*. Science, 1992. **256**(5054): p. 184-5.
5. Kimberly, W.T., et al., *Notch and the amyloid precursor protein are cleaved by similar gamma-secretase(s)*. Biochemistry, 2003. **42**(1): p. 137-44.
6. Herreman, A., et al., *Presenilin 2 deficiency causes a mild pulmonary phenotype and no changes in amyloid precursor protein processing but enhances the embryonic lethal phenotype of presenilin 1 deficiency*. Proc Natl Acad Sci U S A, 1999. **96**(21): p. 11872-7.
7. Tarassishin, L., et al., *Processing of Notch and amyloid precursor protein by gamma-secretase is spatially distinct*. Proc Natl Acad Sci U S A, 2004. **101**(49): p. 17050-5.
8. Kopan, R. and M.X. Ilagan, *Gamma-secretase: proteasome of the membrane?* Nat Rev Mol Cell Biol, 2004. **5**(6): p. 499-504.
9. Haapasalo, A. and D.M. Kovacs, *The many substrates of presenilin/gamma-secretase*. J Alzheimers Dis, 2011. **25**(1): p. 3-28.
10. Wong, G.T., et al., *Chronic treatment with the gamma-secretase inhibitor LY-411,575 inhibits beta-amyloid peptide production and alters lymphopoiesis and intestinal cell differentiation*. J Biol Chem, 2004. **279**(13): p. 12876-82.
11. Geling, A., et al., *A gamma-secretase inhibitor blocks Notch signaling in vivo and causes a severe neurogenic phenotype in zebrafish*. EMBO Rep, 2002. **3**(7): p. 688-94.
12. van Es, J.H., et al., *Notch/gamma-secretase inhibition turns proliferative cells in intestinal crypts and adenomas into goblet cells*. Nature, 2005. **435**(7044): p. 959-63.
13. Baulac, S., et al., *Functional gamma-secretase complex assembly in Golgi/trans-Golgi network: interactions among presenilin, nicastrin, Aph1, Pen-2, and gamma-secretase substrates*. Neurobiol Dis, 2003. **14**(2): p. 194-204.

14. LaVoie, M.J., et al., *Assembly of the gamma-secretase complex involves early formation of an intermediate subcomplex of Aph-1 and nicastrin*. J Biol Chem, 2003. **278**(39): p. 37213-22.
15. Villa, J.C., et al., *Nontranscriptional role of Hif-1alpha in activation of gamma-secretase and notch signaling in breast cancer*. Cell Rep, 2014. **8**(4): p. 1077-92.
16. De Strooper, B., et al., *A presenilin-1-dependent gamma-secretase-like protease mediates release of Notch intracellular domain*. Nature, 1999. **398**(6727): p. 518-22.
17. Shirotani, K., et al., *Gamma-secretase activity is associated with a conformational change of nicastrin*. J Biol Chem, 2003. **278**(19): p. 16474-7.
18. Li, T., et al., *Nicastrin is required for assembly of presenilin/gamma-secretase complexes to mediate Notch signaling and for processing and trafficking of beta-amyloid precursor protein in mammals*. J Neurosci, 2003. **23**(8): p. 3272-7.
19. Morgan, T.H., *The Theory of the Gene*. The American Naturalist, 1917. **51**: p. 513-544.
20. Kopan, R. and M.X. Ilagan, *The canonical Notch signaling pathway: unfolding the activation mechanism*. Cell, 2009. **137**(2): p. 216-33.
21. Ahmad, I., P. Zaqouras, and S. Artavanis-Tsakonas, *Involvement of Notch-1 in mammalian retinal neurogenesis: association of Notch-1 activity with both immature and terminally differentiated cells*. Mech Dev, 1995. **53**(1): p. 73-85.
22. Artavanis-Tsakonas, S., K. Matsuno, and M.E. Fortini, *Notch signaling*. Science, 1995. **268**(5208): p. 225-32.
23. Miele, L. and B. Osborne, *Arbiter of differentiation and death: Notch signaling meets apoptosis*. J Cell Physiol, 1999. **181**(3): p. 393-409.
24. Irvin, D.K., et al., *Expression patterns of Notch1, Notch2, and Notch3 suggest multiple functional roles for the Notch-DSL signaling system during brain development*. J Comp Neurol, 2001. **436**(2): p. 167-81.
25. Louvi, A. and S. Artavanis-Tsakonas, *Notch signalling in vertebrate neural development*. Nat Rev Neurosci, 2006. **7**(2): p. 93-102.
26. Ehebauer, M., P. Hayward, and A.M. Arias, *Notch, a universal arbiter of cell fate decisions*. Science, 2006. **314**(5804): p. 1414-5.
27. Weinmaster, G., V.J. Roberts, and G. Lemke, *Notch2: a second mammalian Notch gene*. Development, 1992. **116**(4): p. 931-41.
28. Rebay, I., et al., *Specific EGF repeats of Notch mediate interactions with Delta and Serrate: implications for Notch as a multifunctional receptor*. Cell, 1991. **67**(4): p. 687-99.
29. Gordon, W.R., et al., *Structure of the Notch1-negative regulatory region: implications for normal activation and pathogenic signaling in T-ALL*. Blood, 2009. **113**(18): p. 4381-90.

30. Gordon, W.R., et al., *Effects of S1 cleavage on the structure, surface export, and signaling activity of human Notch1 and Notch2*. PLoS One, 2009. **4**(8): p. e6613.
31. Ehebauer, M.T., et al., *High-resolution crystal structure of the human Notch 1 ankyrin domain*. Biochem J, 2005. **392**(Pt 1): p. 13-20.
32. Logeat, F., et al., *The Notch1 receptor is cleaved constitutively by a furin-like convertase*. Proc Natl Acad Sci U S A, 1998. **95**(14): p. 8108-12.
33. Ehebauer, M., P. Hayward, and A. Martinez-Arias, *Notch signaling pathway*. Sci STKE, 2006. **2006**(364): p. cm7.
34. Hambleton, S., et al., *Structural and functional properties of the human notch-1 ligand binding region*. Structure, 2004. **12**(12): p. 2173-83.
35. Muranyi, A., et al., *<sup>1</sup>H, <sup>13</sup>C, and <sup>15</sup>N resonance assignments of human Notch-1 calcium binding EGF domains 11-13*. J Biomol NMR, 2004. **29**(3): p. 443-4.
36. Song, W., et al., *Proteolytic release and nuclear translocation of Notch-1 are induced by presenilin-1 and impaired by pathogenic presenilin-1 mutations*. Proc Natl Acad Sci U S A, 1999. **96**(12): p. 6959-63.
37. Ansieau, S., L.J. Strobl, and A. Leutz, *Activation of the Notch-regulated transcription factor CBF1/RBP-Jkappa through the 13SE1A oncoprotein*. Genes Dev, 2001. **15**(4): p. 380-5.
38. Jarriault, S., et al., *Delta-1 activation of notch-1 signaling results in HES-1 transactivation*. Mol Cell Biol, 1998. **18**(12): p. 7423-31.
39. Iso, T., L. Kedes, and Y. Hamamori, *HES and HERP families: multiple effectors of the Notch signaling pathway*. J Cell Physiol, 2003. **194**(3): p. 237-55.
40. Palomero, T., et al., *NOTCH1 directly regulates c-MYC and activates a feed-forward-loop transcriptional network promoting leukemic cell growth*. Proc Natl Acad Sci U S A, 2006. **103**(48): p. 18261-6.
41. Artavanis-Tsakonas, S., M.D. Rand, and R.J. Lake, *Notch signaling: cell fate control and signal integration in development*. Science, 1999. **284**(5415): p. 770-6.
42. Schweisguth, F., *Regulation of notch signaling activity*. Curr Biol, 2004. **14**(3): p. R129-38.
43. Chastagner, P. and C. Brou, *Tracking trafficking of Notch and its ligands in mammalian cells*. Methods Mol Biol, 2014. **1187**: p. 87-100.
44. Okajima, T. and K.D. Irvine, *Regulation of notch signaling by o-linked fucose*. Cell, 2002. **111**(6): p. 893-904.
45. Yamamoto, S., W.L. Charng, and H.J. Bellen, *Endocytosis and intracellular trafficking of Notch and its ligands*. Curr Top Dev Biol, 2010. **92**: p. 165-200.
46. Guruharsha, K.G., M.W. Kankel, and S. Artavanis-Tsakonas, *The Notch signalling system: recent insights into the complexity of a conserved pathway*. Nat Rev Genet, 2012. **13**(9): p. 654-66.

47. Suresh, S. and A.E. Irvine, *The NOTCH signaling pathway in normal and malignant blood cell production*. J Cell Commun Signal, 2015. **9**(1): p. 5-13.
48. Yan, Q., et al., *O-fucose modulates Notch-controlled blood lineage commitment*. Am J Pathol, 2010. **176**(6): p. 2921-34.
49. Bigas, A., T. D'Altri, and L. Espinosa, *The Notch pathway in hematopoietic stem cells*. Curr Top Microbiol Immunol, 2012. **360**: p. 1-18.
50. Bigas, A. and L. Espinosa, *Hematopoietic stem cells: to be or Notch to be*. Blood, 2012. **119**(14): p. 3226-35.
51. VanDussen, K.L., et al., *Notch signaling modulates proliferation and differentiation of intestinal crypt base columnar stem cells*. Development, 2012. **139**(3): p. 488-97.
52. Demitrack, E.S. and L.C. Samuelson, *Notch regulation of gastrointestinal stem cells*. J Physiol, 2016. **594**(17): p. 4791-803.
53. Louvi, A., J.F. Arboleda-Velasquez, and S. Artavanis-Tsakonas, *CADASIL: a critical look at a Notch disease*. Dev Neurosci, 2006. **28**(1-2): p. 5-12.
54. Miyamoto, Y., et al., *Notch mediates TGF alpha-induced changes in epithelial differentiation during pancreatic tumorigenesis*. Cancer Cell, 2003. **3**(6): p. 565-76.
55. Gilleron, J., et al., *A potential novel mechanism involving connexin 43 gap junction for control of sertoli cell proliferation by thyroid hormones*. J Cell Physiol, 2006. **209**(1): p. 153-61.
56. Ferrando, A.A. and A.T. Look, *Clinical implications of recurring chromosomal and associated molecular abnormalities in acute lymphoblastic leukemia*. Semin Hematol, 2000. **37**(4): p. 381-95.
57. Weng, A.P. and J.C. Aster, *Multiple niches for Notch in cancer: context is everything*. Curr Opin Genet Dev, 2004. **14**(1): p. 48-54.
58. Weng, A.P., et al., *Activating mutations of NOTCH1 in human T cell acute lymphoblastic leukemia*. Science, 2004. **306**(5694): p. 269-71.
59. Hayashi, T., et al., *Not all NOTCH Is Created Equal: The Oncogenic Role of NOTCH2 in Bladder Cancer and Its Implications for Targeted Therapy*. Clin Cancer Res, 2016. **22**(12): p. 2981-92.
60. Xing, F., et al., *Hypoxia-induced Jagged2 promotes breast cancer metastasis and self-renewal of cancer stem-like cells*. Oncogene, 2011. **30**(39): p. 4075-86.
61. Giachino, C., et al., *A Tumor Suppressor Function for Notch Signaling in Forebrain Tumor Subtypes*. Cancer Cell, 2015. **28**(6): p. 730-742.
62. Chu, D., et al., *Notch1 and Notch2 have opposite prognostic effects on patients with colorectal cancer*. Ann Oncol, 2011. **22**(11): p. 2440-7.
63. Andersson, E.R. and U. Lendahl, *Therapeutic modulation of Notch signalling--are we there yet?* Nat Rev Drug Discov, 2014. **13**(5): p. 357-78.

64. Barten, D.M., et al., *Dynamics of {beta}-amyloid reductions in brain, cerebrospinal fluid, and plasma of {beta}-amyloid precursor protein transgenic mice treated with a {gamma}-secretase inhibitor*. J Pharmacol Exp Ther, 2005. **312**(2): p. 635-43.
65. Burton, C.R., et al., *The amyloid-beta rise and gamma-secretase inhibitor potency depend on the level of substrate expression*. J Biol Chem, 2008. **283**(34): p. 22992-3003.
66. Kumar, D., et al., *Secretase inhibitors for the treatment of Alzheimer's disease: Long road ahead*. Eur J Med Chem, 2018. **148**: p. 436-452.
67. Poellinger, L. and U. Lendahl, *Modulating Notch signaling by pathway-intrinsic and pathway-extrinsic mechanisms*. Curr Opin Genet Dev, 2008. **18**(5): p. 449-54.
68. Groth, C. and M.E. Fortini, *Therapeutic approaches to modulating Notch signaling: current challenges and future prospects*. Semin Cell Dev Biol, 2012. **23**(4): p. 465-72.
69. Delbruck, M., *The Burst Size Distribution in the Growth of Bacterial Viruses (Bacteriophages)*. J Bacteriol, 1945. **50**(2): p. 131-5.
70. Dreiseikermann, B., *Translocation of DNA across bacterial membranes*. Microbiol Rev, 1994. **58**(3): p. 293-316.
71. Barbas, C.B., D.; Silverman, G.; and Scott, J., *Phage Display: A Laboratory Manual*. 2001: Cold Spring Harbor Press.
72. Cabilly, S., *The basic structure of filamentous phage and its use in the display of combinatorial peptide libraries*. Mol Biotechnol, 1999. **12**(2): p. 143-8.
73. Rodi, D.J. and L. Makowski, *Phage-display technology--finding a needle in a vast molecular haystack*. Curr Opin Biotechnol, 1999. **10**(1): p. 87-93.
74. Smith, G.P. and J.K. Scott, *Libraries of peptides and proteins displayed on filamentous phage*. Methods Enzymol, 1993. **217**: p. 228-57.
75. Hoogenboom, H.R., et al., *Multi-subunit proteins on the surface of filamentous phage: methodologies for displaying antibody (Fab) heavy and light chains*. Nucleic Acids Res, 1991. **19**(15): p. 4133-7.
76. Sidhu, S.S., *Engineering M13 for phage display*. Biomol Eng, 2001. **18**(2): p. 57-63.
77. Ullman, C.G., L. Frigotto, and R.N. Cooley, *In vitro methods for peptide display and their applications*. Brief Funct Genomics, 2011. **10**(3): p. 125-34.
78. Smith, G.P. and V.A. Petrenko, *Phage Display*. Chem Rev, 1997. **97**(2): p. 391-410.
79. Winter, G., et al., *Making antibodies by phage display technology*. Annu Rev Immunol, 1994. **12**: p. 433-55.
80. Paschke, M., *Phage display systems and their applications*. Appl Microbiol Biotechnol, 2006. **70**(1): p. 2-11.
81. Hoogenboom, H.R., et al., *Antibody phage display technology and its applications*. Immunotechnology, 1998. **4**(1): p. 1-20.

82. O'Brien, R.J. and P.C. Wong, *Amyloid precursor protein processing and Alzheimer's disease*. Annu Rev Neurosci, 2011. **34**: p. 185-204.
83. Pearson, H.A. and C. Peers, *Physiological roles for amyloid beta peptides*. J Physiol, 2006. **575**(Pt 1): p. 5-10.
84. Masters, C.L., et al., *Neuronal origin of a cerebral amyloid: neurofibrillary tangles of Alzheimer's disease contain the same protein as the amyloid of plaque cores and blood vessels*. EMBO J, 1985. **4**(11): p. 2757-63.
85. Preece, P., et al., *Amyloid precursor protein mRNA levels in Alzheimer's disease brain*. Brain Res Mol Brain Res, 2004. **122**(1): p. 1-9.
86. Gu, Y., et al., *Distinct intramembrane cleavage of the beta-amyloid precursor protein family resembling gamma-secretase-like cleavage of Notch*. J Biol Chem, 2001. **276**(38): p. 35235-8.
87. Postuma, R.B., et al., *Substrate-bound beta-amyloid peptides inhibit cell adhesion and neurite outgrowth in primary neuronal cultures*. J Neurochem, 2000. **74**(3): p. 1122-30.
88. Selkoe, D.J., *The cell biology of beta-amyloid precursor protein and presenilin in Alzheimer's disease*. Trends Cell Biol, 1998. **8**(11): p. 447-53.
89. Selkoe, D.J., *Cell biology of protein misfolding: the examples of Alzheimer's and Parkinson's diseases*. Nat Cell Biol, 2004. **6**(11): p. 1054-61.
90. Selkoe, D.J., *Amyloid beta-protein and the genetics of Alzheimer's disease*. J Biol Chem, 1996. **271**(31): p. 18295-8.
91. Selkoe, D.J., *Cell biology of the beta-amyloid precursor protein and the genetics of Alzheimer's disease*. Cold Spring Harb Symp Quant Biol, 1996. **61**: p. 587-96.
92. Cai, H., et al., *BACE1 is the major beta-secretase for generation of Abeta peptides by neurons*. Nat Neurosci, 2001. **4**(3): p. 233-4.
93. Ohno, M., et al., *BACE1 gene deletion prevents neuron loss and memory deficits in 5XFAD APP/PS1 transgenic mice*. Neurobiol Dis, 2007. **26**(1): p. 134-45.
94. Chen, G.F., et al., *Amyloid beta: structure, biology and structure-based therapeutic development*. Acta Pharmacol Sin, 2017. **38**(9): p. 1205-1235.
95. Tabaton, M. and E. Tamagno, *The molecular link between beta- and gamma-secretase activity on the amyloid beta precursor protein*. Cell Mol Life Sci, 2007. **64**(17): p. 2211-8.
96. Murphy, M.P. and H. LeVine, 3rd, *Alzheimer's disease and the amyloid-beta peptide*. J Alzheimers Dis, 2010. **19**(1): p. 311-23.
97. Hsiao, K., et al., *Correlative memory deficits, Abeta elevation, and amyloid plaques in transgenic mice*. Science, 1996. **274**(5284): p. 99-102.

98. Parvathy, S., et al., *Correlation between Abeta<sub>40</sub>-, Abeta<sub>42</sub>-, and Abeta<sub>43</sub>-containing amyloid plaques and cognitive decline*. Arch Neurol, 2001. **58**(12): p. 2025-32.
99. Mucke, L., et al., *High-level neuronal expression of abeta 1-42 in wild-type human amyloid protein precursor transgenic mice: synaptotoxicity without plaque formation*. J Neurosci, 2000. **20**(11): p. 4050-8.
100. Oakley, H., et al., *Intraneuronal beta-amyloid aggregates, neurodegeneration, and neuron loss in transgenic mice with five familial Alzheimer's disease mutations: potential factors in amyloid plaque formation*. J Neurosci, 2006. **26**(40): p. 10129-40.
101. Hardy, J. and D.J. Selkoe, *The amyloid hypothesis of Alzheimer's disease: progress and problems on the road to therapeutics*. Science, 2002. **297**(5580): p. 353-6.
102. Selkoe, D.J., *Amyloid beta-peptide is produced by cultured cells during normal metabolism: a reprise*. J Alzheimers Dis, 2006. **9**(3 Suppl): p. 163-8.
103. Bolduc, D.M., et al., *The amyloid-beta forming tripeptide cleavage mechanism of gamma-secretase*. Elife, 2016. **5**.
104. Szaruga, M., et al., *Alzheimer's-Causing Mutations Shift Abeta Length by Destabilizing gamma-Secretase-Abetan Interactions*. Cell, 2017. **170**(3): p. 443-456 e14.
105. Takami, M., et al., *gamma-Secretase: successive tripeptide and tetrapeptide release from the transmembrane domain of beta-carboxyl terminal fragment*. J Neurosci, 2009. **29**(41): p. 13042-52.
106. Siemers, E.R., et al., *Effects of a gamma-secretase inhibitor in a randomized study of patients with Alzheimer disease*. Neurology, 2006. **66**(4): p. 602-4.
107. Pollack, S.J. and H. Lewis, *Secretase inhibitors for Alzheimer's disease: challenges of a promiscuous protease*. Curr Opin Investig Drugs, 2005. **6**(1): p. 35-47.
108. Wolfe, M.S., *gamma-Secretase inhibitors and modulators for Alzheimer's disease*. J Neurochem, 2012. **120 Suppl 1**: p. 89-98.
109. Tanzi, R.E., *The genetics of Alzheimer disease*. Cold Spring Harb Perspect Med, 2012. **2**(10).
110. Kumar-Singh, S., et al., *Mean age-of-onset of familial alzheimer disease caused by presenilin mutations correlates with both increased Abeta<sub>42</sub> and decreased Abeta<sub>40</sub>*. Hum Mutat, 2006. **27**(7): p. 686-95.
111. Kounnas, M.Z., et al., *Modulation of gamma-secretase reduces beta-amyloid deposition in a transgenic mouse model of Alzheimer's disease*. Neuron, 2010. **67**(5): p. 769-80.
112. Schroeder, H.W., Jr. and L. Cavacini, *Structure and function of immunoglobulins*. J Allergy Clin Immunol, 2010. **125**(2 Suppl 2): p. S41-52.
113. Padlan, E.A., *Anatomy of the antibody molecule*. Mol Immunol, 1994. **31**(3): p. 169-217.



114. Salfeld, J.G., *Isotype selection in antibody engineering*. Nat Biotechnol, 2007. **25**(12): p. 1369-72.
115. Vieira, P. and K. Rajewsky, *The half-lives of serum immunoglobulins in adult mice*. Eur J Immunol, 1988. **18**(2): p. 313-6.
116. Buss, N.A., et al., *Monoclonal antibody therapeutics: history and future*. Curr Opin Pharmacol, 2012. **12**(5): p. 615-22.
117. Wang, W., et al., *Antibody structure, instability, and formulation*. J Pharm Sci, 2007. **96**(1): p. 1-26.
118. Adams, D.O., et al., *Tumors undergoing rejection induced by monoclonal antibodies of the IgG2a isotype contain increased numbers of macrophages activated for a distinctive form of antibody-dependent cytotoxicity*. Proc Natl Acad Sci U S A, 1984. **81**(11): p. 3506-10.
119. Lai, E.C., *Notch signaling: control of cell communication and cell fate*. Development, 2004. **131**(5): p. 965-73.
120. Andersson, E.R., R. Sandberg, and U. Lendahl, *Notch signaling: simplicity in design, versatility in function*. Development, 2011. **138**(17): p. 3593-612.
121. Aster, J.C., W.S. Pear, and S.C. Blacklow, *The Varied Roles of Notch in Cancer*. Annu Rev Pathol, 2017. **12**: p. 245-275.
122. Bland, C.E., P. Kimberly, and M.D. Rand, *Notch-induced proteolysis and nuclear localization of the Delta ligand*. J Biol Chem, 2003. **278**(16): p. 13607-10.
123. Kraman, M. and B. McCright, *Functional conservation of Notch1 and Notch2 intracellular domains*. FASEB J, 2005. **19**(10): p. 1311-3.
124. Nandagopal, N., et al., *Dynamic Ligand Discrimination in the Notch Signaling Pathway*. Cell, 2018. **172**(4): p. 869-880 e19.
125. Gordon, W.R., K.L. Arnett, and S.C. Blacklow, *The molecular logic of Notch signaling--a structural and biochemical perspective*. J Cell Sci, 2008. **121**(Pt 19): p. 3109-19.
126. Ellisen, L.W., et al., *TAN-1, the human homolog of the Drosophila notch gene, is broken by chromosomal translocations in T lymphoblastic neoplasms*. Cell, 1991. **66**(4): p. 649-61.
127. Joutel, A., et al., *Notch3 mutations in CADASIL, a hereditary adult-onset condition causing stroke and dementia*. Nature, 1996. **383**(6602): p. 707-10.
128. McDaniell, R., et al., *NOTCH2 mutations cause Alagille syndrome, a heterogeneous disorder of the notch signaling pathway*. Am J Hum Genet, 2006. **79**(1): p. 169-73.
129. Masuda, S., *Notch1 and Notch2 have opposite prognostic effects on patients with colorectal cancer*. Ann Oncol, 2011. **22**(11): p. 2533-4; author reply 2534.
130. Greiner, J., H. Dohner, and M. Schmitt, *Cancer vaccines for patients with acute myeloid leukemia--definition of leukemia-associated antigens and current clinical protocols targeting these antigens*. Haematologica, 2006. **91**(12): p. 1653-61.

131. Wang, Z., et al., *Targeting Notch signaling pathway to overcome drug resistance for cancer therapy*. Biochim Biophys Acta, 2010. **1806**(2): p. 258-67.
132. Baumgart, A., et al., *Opposing role of Notch1 and Notch2 in a Kras(G12D)-driven murine non-small cell lung cancer model*. Oncogene, 2015. **34**(5): p. 578-88.
133. Chillakuri, C.R., et al., *Notch receptor-ligand binding and activation: insights from molecular studies*. Semin Cell Dev Biol, 2012. **23**(4): p. 421-8.
134. Cordle, J., et al., *Localization of the delta-like-1-binding site in human Notch-1 and its modulation by calcium affinity*. J Biol Chem, 2008. **283**(17): p. 11785-93.
135. Takeuchi, H. and R.S. Haltiwanger, *Significance of glycosylation in Notch signaling*. Biochem Biophys Res Commun, 2014. **453**(2): p. 235-42.
136. Kovall, R.A., et al., *The Canonical Notch Signaling Pathway: Structural and Biochemical Insights into Shape, Sugar, and Force*. Dev Cell, 2017. **41**(3): p. 228-241.
137. Nowell, C.S. and F. Radtke, *Notch as a tumour suppressor*. Nature Reviews Cancer, 2017. **17**: p. 145.
138. Agrawal, N., et al., *Exome Sequencing of Head and Neck Squamous Cell Carcinoma Reveals Inactivating Mutations in *NOTCH1**. Science, 2011. **333**(6046): p. 1154-1157.
139. Pickering, C.R., et al., *Mutational Landscape of Aggressive Cutaneous Squamous Cell Carcinoma*. Clinical Cancer Research, 2014. **20**(24): p. 6582-6592.
140. Gao, Y.-B., et al., *Genetic landscape of esophageal squamous cell carcinoma*. Nature Genetics, 2014. **46**: p. 1097.
141. van Es, J.H., et al., *Notch/ $\gamma$ -secretase inhibition turns proliferative cells in intestinal crypts and adenomas into goblet cells*. Nature, 2005. **435**: p. 959.
142. Obexer, R., L.J. Walport, and H. Suga, *Exploring sequence space: harnessing chemical and biological diversity towards new peptide leads*. Curr Opin Chem Biol, 2017. **38**: p. 52-61.
143. Liu, H., et al., *Comparative analysis of Notch1 and Notch2 binding sites in the genome of BxPC3 pancreatic cancer cells*. J Cancer, 2017. **8**(1): p. 65-73.
144. Smith, G.P., *Surface presentation of protein epitopes using bacteriophage expression systems*. Curr Opin Biotechnol, 1991. **2**(5): p. 668-73.
145. Aujame, L., R. Sodoyer, and J.L. Teillaud, *Phage display and antibody engineering: a French overview*. Trends Biotechnol, 1997. **15**(5): p. 155-7.

146. Malecki, M.J., et al., *Leukemia-associated mutations within the NOTCH1 heterodimerization domain fall into at least two distinct mechanistic classes*. Mol Cell Biol, 2006. **26**(12): p. 4642-51.
147. Aste-Amezaga, M., et al., *Characterization of Notch1 antibodies that inhibit signaling of both normal and mutated Notch1 receptors*. PLoS One, 2010. **5**(2): p. e9094.
148. McConnell, S.J., et al., *Biopanning phage display libraries using magnetic beads vs. polystyrene plates*. Biotechniques, 1999. **26**(2): p. 208-10, 214.
149. Jaye, D.L., et al., *Direct fluorochrome labeling of phage display library clones for studying binding specificities: applications in flow cytometry and fluorescence microscopy*. J Immunol Methods, 2004. **295**(1-2): p. 119-27.
150. Wu, Y., et al., *Therapeutic antibody targeting of individual Notch receptors*. Nature, 2010. **464**(7291): p. 1052-7.
151. Amsen, D., et al., *Instruction of distinct CD4 T helper cell fates by different notch ligands on antigen-presenting cells*. Cell, 2004. **117**(4): p. 515-26.
152. Nandagopal, N.S., L.; & Elowitz Michael, *Cis-activation in the Notch signaling pathway*. BioRxiv, 2018.
153. Gao, Z., et al., *A dimeric Smac/diablo peptide directly relieves caspase-3 inhibition by XIAP. Dynamic and cooperative regulation of XIAP by Smac/Diablo*. J Biol Chem, 2007. **282**(42): p. 30718-27.
154. Alzheimer, A., *About a peculiar disease of the cerebral cortex*. By Alois Alzheimer, 1907 (Translated by L. Jarvik and H. Greenson). Alzheimer Dis Assoc Disord, 1987. **1**(1): p. 3-8.
155. Ballatore, C., V.M. Lee, and J.Q. Trojanowski, *Tau-mediated neurodegeneration in Alzheimer's disease and related disorders*. Nat Rev Neurosci, 2007. **8**(9): p. 663-72.
156. Schmechel, D.E., et al., *Increased amyloid beta-peptide deposition in cerebral cortex as a consequence of apolipoprotein E genotype in late-onset Alzheimer disease*. Proc Natl Acad Sci U S A, 1993. **90**(20): p. 9649-53.
157. Selkoe, D.J. and J. Hardy, *The amyloid hypothesis of Alzheimer's disease at 25 years*. EMBO Mol Med, 2016. **8**(6): p. 595-608.
158. Li, Y.M., et al., *Photoactivated gamma-secretase inhibitors directed to the active site covalently label presenilin 1*. Nature, 2000. **405**(6787): p. 689-94.
159. Li, Y.M., et al., *Presenilin 1 is linked with gamma-secretase activity in the detergent solubilized state*. Proc Natl Acad Sci U S A, 2000. **97**(11): p. 6138-43.
160. Vassar, R., et al., *Beta-secretase cleavage of Alzheimer's amyloid precursor protein by the transmembrane aspartic protease BACE*. Science, 1999. **286**(5440): p. 735-41.

161. Lammich, S., et al., *Constitutive and regulated alpha-secretase cleavage of Alzheimer's amyloid precursor protein by a disintegrin metalloprotease*. Proc Natl Acad Sci U S A, 1999. **96**(7): p. 3922-7.
162. Van Nostrand, W.E., et al., *Alzheimer's disease and hereditary cerebral hemorrhage with amyloidosis-Dutch type share a decrease in cerebrospinal fluid levels of amyloid beta-protein precursor*. Ann Neurol, 1992. **32**(2): p. 215-8.
163. Sturchler-Pierrat, C., et al., *Two amyloid precursor protein transgenic mouse models with Alzheimer disease-like pathology*. Proc Natl Acad Sci U S A, 1997. **94**(24): p. 13287-92.
164. Goedert, M., et al., *Multiple isoforms of human microtubule-associated protein tau: sequences and localization in neurofibrillary tangles of Alzheimer's disease*. Neuron, 1989. **3**(4): p. 519-26.
165. Binder, L.I., et al., *Tau, tangles, and Alzheimer's disease*. Biochim Biophys Acta, 2005. **1739**(2-3): p. 216-23.
166. Hardy, J., *Framing beta-amyloid*. Nat Genet, 1992. **1**(4): p. 233-4.
167. Hock, C., et al., *Antibodies against beta-amyloid slow cognitive decline in Alzheimer's disease*. Neuron, 2003. **38**(4): p. 547-54.
168. Sevigny, J., et al., *The antibody aducanumab reduces Abeta plaques in Alzheimer's disease*. Nature, 2016. **537**(7618): p. 50-6.
169. Mehta, D., et al., *Why do trials for Alzheimer's disease drugs keep failing? A discontinued drug perspective for 2010-2015*. Expert Opin Investig Drugs, 2017. **26**(6): p. 735-739.
170. Borchelt, D.R., et al., *Accelerated amyloid deposition in the brains of transgenic mice coexpressing mutant presenilin 1 and amyloid precursor proteins*. Neuron, 1997. **19**(4): p. 939-45.
171. Cruts, M. and C. Van Broeckhoven, *Molecular genetics of Alzheimer's disease*. Ann Med, 1998. **30**(6): p. 560-5.
172. Weiner, L.M., R. Surana, and S. Wang, *Monoclonal antibodies: versatile platforms for cancer immunotherapy*. Nat Rev Immunol, 2010. **10**(5): p. 317-27.
173. Bielefeld-Sevigny, M., *AlphaLISA immunoassay platform- the "no-wash" high-throughput alternative to ELISA*. Assay Drug Dev Technol, 2009. **7**(1): p. 90-2.
174. Cauchon, E., et al., *Development of a homogeneous immunoassay for the detection of angiotensin I in plasma using AlphaLISA acceptor beads technology*. Anal Biochem, 2009. **388**(1): p. 134-9.
175. Nelson, P.N., et al., *Monoclonal antibodies*. Mol Pathol, 2000. **53**(3): p. 111-7.
176. Stine, W.B., et al., *Preparing synthetic Abeta in different aggregation states*. Methods Mol Biol, 2011. **670**: p. 13-32.
177. Edbauer, D., et al., *Presenilin and nicastrin regulate each other and determine amyloid beta-peptide production via complex formation*. Proc Natl Acad Sci U S A, 2002. **99**(13): p. 8666-71.

178. Arumugam, T.V., et al., *Gamma secretase-mediated Notch signaling worsens brain damage and functional outcome in ischemic stroke*. Nat Med, 2006. **12**(6): p. 621-3.
179. Schor, N.F., *What the halted phase III gamma-secretase inhibitor trial may (or may not) be telling us*. Ann Neurol, 2011. **69**(2): p. 237-9.
180. Extnance, A., *Alzheimer's failure raises questions about disease-modifying strategies*. Nat Rev Drug Discov, 2010. **9**(10): p. 749-51.
181. Shelton, C.C., et al., *Modulation of gamma-secretase specificity using small molecule allosteric inhibitors*. Proc Natl Acad Sci U S A, 2009. **106**(48): p. 20228-33.
182. Uemura, K., et al., *Allosteric modulation of PS1/gamma-secretase conformation correlates with amyloid beta(42/40) ratio*. PLoS One, 2009. **4**(11): p. e7893.
183. He, G., et al., *Gamma-secretase activating protein is a therapeutic target for Alzheimer's disease*. Nature, 2010. **467**(7311): p. 95-8.
184. Gordon, W.R., et al., *Structural basis for autoinhibition of Notch*. Nat Struct Mol Biol, 2007. **14**(4): p. 295-300.
185. Sinz, A., *The advancement of chemical cross-linking and mass spectrometry for structural proteomics: from single proteins to protein interaction networks*. Expert Rev Proteomics, 2014. **11**(6): p. 733-43.
186. Sofou, S., et al., *Enhanced retention of the alpha-particle-emitting daughters of Actinium-225 by liposome carriers*. Bioconjug Chem, 2007. **18**(6): p. 2061-7.
187. Cummings, J.L., T. Morstorf, and K. Zhong, *Alzheimer's disease drug-development pipeline: few candidates, frequent failures*. Alzheimers Res Ther, 2014. **6**(4): p. 37.
188. Jones, D.T., et al., *Cascading network failure across the Alzheimer's disease spectrum*. Brain, 2016. **139**(Pt 2): p. 547-62.
189. Iqbal, K., F. Liu, and C.X. Gong, *Alzheimer disease therapeutics: focus on the disease and not just plaques and tangles*. Biochem Pharmacol, 2014. **88**(4): p. 631-9.
190. Godyn, J., et al., *Therapeutic strategies for Alzheimer's disease in clinical trials*. Pharmacol Rep, 2016. **68**(1): p. 127-38.